Department of Molecular and Clinical Pharmacology

Institute of Translational Medicine

University of Liverpool

Defining the effects of CD28 superagonist and TGF-β on T cell function and metabolism

Thesis submitted in accordance with the requirements of the University of Liverpool for the degree of Doctor in Philosophy

Thilipan Thaventhiran

October 2014

DECLARATION

This thesis is the result of my own work. The material contained within this thesis has not been presented, nor is currently being presented, either wholly or in part for any degree or other qualification.

Thilipan Thaventhiran

This research was carried out in the MRC Centre for Drug Safety Science,

Department of Pharmacology and Therapeutics,

The University of Liverpool

Table of contents

List of figures

1. Chapter ONE: Introduction

2. Chapter TWO: Methods and Materials

3. Chapter THREE: Failure to upregulate cell surface PD-1 is associated with dysregulated stimulation of T cells by TGN1412-like CD28 superagonist

4. Chapter FOUR: CD28 superagonist activation of T cells induces a cancer cell-like metabolic program

5. Chapter FIVE: Defining the role of oxidative stress in TGF-β-associated functional and metabolic alterations in antigen activated T cells

List of tables

Abstract

Immunomodulatory monoclonal antibodies (mAbs) indicated for the treatment of cancer, inflammatory and autoimmune diseases or to prevent organ transplant rejection, mostly target cell surface molecules expressed by immune cells including T cells. The presence of immunosuppressive molecules during disease progression can hinder the activity of immune cells. Tumour-induced immunosuppression enables disease progression and various strategies are being developed to enhance the anti-tumour responses of cytotoxic T cells. Activation of effective effector responses require resetting of metabolic activity to fit energy and anabolic needs. While the benefits of exploiting immunomodulatory mAbs for therapy are substantial, it is also clear that use of these biologics may be accompanied by adverse effects such as cytokine release, immunosuppression, infections and autoimmunity. Significant focus in recent times has been on assessing the potential of immunomodulatory mAbs to induce enhanced cytokine release but much less attention has been paid to other aspects of T cell biology including non-physiological activation phenotype/functions, migration characteristics and metabolism. An improved understanding of these parameters may assist in accurately predicting the propensity of new mAbs to induce serious adverse effects.

Superagonistic CD28-specific monoclonal antibody (CD28SA) is one such immunomodulatory monoclonal antibody which is a potent stimulator of T cells, originally intended for the management of B cell chronic lymphocytic leukaemia and rheumatoid arthritis. Human volunteers who received humanized CD28SA (TGN1412) as part of a first-in-man trial experienced life-threatening cytokine release syndrome. Follow-up studies revealed aberrant activation of effector memory T cells (T_{EM}) contributed towards the adverse reaction. The biopharmaceutical industry is actively pursuing development of T cell immunostimulatory mAbs and there is a significant need to improve the understanding of and accurately predict the propensity of a new mAb to drive excessive T cell activation. Therefore, one of the main aims of the study discussed

in this thesis was to determine mechanism/s underlying the hyperactive phenotype of CD28SA-activated T_{EM}. Observations in the current study revealed activation of T_{EM} by CD28SA upregulated the expression of activation markers such as CD137 and HLA-DR, but failed to express co-inhibitory receptor, PD-1. This led to the lack of PD-1-mediated regulation of aberrant T_{EM} activation. In addition, CD28SA-activated T_{EM} expressed elevated levels of LFA-1 and CCR5 receptors, and displayed increased migratory capacity. Subsequent studies highlighted increased metabolic demand of CD28SA-activated $T_{EM.}$ The hyperactive cells with increased proliferative capacity exhibited distinct metabolic profile characterized by increased glycolysis and lipogenesis. These findings have profound implications for strategies aiming at understanding and predicting the safety profile of immunostimulatory mAbs.

Deployment of immunosuppressive strategies, including TGF-β secretion by tumours to render immunostimulatory mAbs-mediated anti-tumour responses ineffective is well studied. The other study discussed in this thesis aimed to delineate the effects of oxidative stress in TGF-β-induced suppression of antigen-specific cytotoxic T cell responses. This study showed antigen-specific T cells exposed to TGF-β down regulate CD25 and LAG-3 (co-inhibitory T cell receptor) expression, secrete lower levels of IL-2 and IFN-γ, and reduced glycolysis. In addition, mitochondrial reactive oxygen species (MitoROS) scavenger rescued the effector functions such as proliferation and IFN-γ secretion of stimulated T cells that were inhibited by TGF-β. Our findings demonstrate that relief of TGF-β-induced oxidative stress restores the effector function of $CD8^+$ cytotoxic T cells. Based on the current findings it would be potentially beneficial to supplement immunotherapies with antioxidants to counteract the immunosuppressive effects of tumour-derived TGF-β to help restore $CD8^+$ T cell-mediated anti-tumour function. The findings presented in this thesis may help with defining key T cell biomarkers based of efficacy and hazard associated with immunomodulation.

Acknowledgments

Pursuing and completing this project was possible thanks to the help and support of several people. I would like to express my sincere gratitude to all of them.

First and foremost I would like to thank my primary supervisor and mentor, Dr Jean Sathish, for his support, advice and patience. His combination of guidance and freedom not only challenged me but also gave me scientific confidence. His valuable scholarly inputs and his genuine interest and passion for science kept me motivated.

I would like to thank Dr Swaminathan Sethu, for his timely support and encouragement. I am grateful for his great deal of scientific advice and technical assistance. His presence always created an enjoyable research environment.

I would like to thank my present and former lab colleagues: Han Aw Yeang, Junnat Hamdam, Laith Abbas Al-Huseini, Naif Alhumeed and Yulia Tingle for their help and great support during my time in the lab. I would also like to thank Ahmad Alghanem, Dammy Olayanju, Amy Chadwick, Wai Wong, Min Wei Wong, Mohammad Aljasir and Simeon Ramsey for their recent involvement in manuscript preparations.

I would like to acknowledge the Medical Research Council for funding my 4-year studentship. I would also like to thank the Biomedical services unit and the MRC Centre for Drug Safety Science, University of Liverpool.

Publications

Thaventhiran T, Alhumeed N, Xian Aw Yeang H, Sethu S, Downey J, Alghanem A, Olayanju A, Smith E, Cross M, Webb S, et al. Failure to upregulate cell surface PD-1 is associated with dysregulated stimulation of T cells by TGN1412-like CD28 superagonist. mAbs 2014; 6:12 - 21; http://dx.doi.org/10.4161/mabs.29758

Thaventhiran T, Sethu S, Xian Aw Yeang H, Al-Huseini L, Hamdam J, Sathish J. T cell co-inhibitory receptors - functions and signalling mechanisms. Journal of clinical and cellular Immunology 2012, S12:004. doi:10.4172/2155-9899.S12-004

Thaventhiran T, Wong W, Alghanem A, Olayanju A, Ramsey S, Webb S, Bristow A, Ball C, Stebbings R et al. CD28 superagonist activation of T cells induces a cancer cell-like metabolic program. EMBO Report To be submitted

Thaventhiran T, Alhumeed N, Wong M, Sethu S, Chadwick A, Webb S, Sathish J. Defining the role of oxidative stress in TGF-β-associated functional and metabolic alterations in antigen activated T cells. Manuscript in preparation

Abbreviations

ACC: Acetyl-CoA carboxylase

ACL: ATP citrate lyase

ADAM: A Disintegrin And Metalloproteinase

ADAP: Adhesion- and Degranulation-promoting Adapter Protein

ADP: Adenosine diphosphate

AKT: Protein Kinase B

AKT: RAC-alpha serine/threonine-protein kinase

AMPK: Adenosine monophosphate-activated protein kinase

ANOVA: Analysis of variance

AP-1: Activator protein 1

AP-1: Activator protein 1

APAP: N-acetyl-para-aminopheno

APC: Antigen presenting cell

ARE: Antioxidant response elements

ATM: Ataxia telangiectasia mutated

ATP: Adenosine triphosphate

BCA: Bicinchoninic Acid

BSA: Bovine serum albumin

BTLA: B- and T-lymphocyte attenuator

Ca^{2+}: Calcium ion

CCL: Chemokine (C-C motif) ligand

CCR: C-C chemokine receptor

CD: Cluster of differentiation

CD28SA: CD28 Superagonistic antibody

CDK: Cyclin-dependent kinases

cDNA: complementary DNA

CK2: Casein kinase 2

CoA: Coenzyme A

CPT1: Carnitine palmitoyltransferase I

CREB: cAMP responsive element binding protein

CTL: Cytotoxic T lymphocytes

CTLA-4: Cytotoxic T-lymphocyte-associated protein 4

Cys: Cysteine

DAG: Diacylglycerol

DC: Dendritic cell

DNA: Deoxyribonucleic acid

EDTA: Ethylenediaminetetraacetic acid

ELISA: Enzyme-linked immunosorbent assay

ELISpot: Enzyme-Linked ImmunoSpot

Erk: Extracellular signal-regulated kinases

FA: Fatty acids

$FADH_2$: Flavin adenine dinucleotide

FAO: Fatty acid oxidation

FAS: Fatty acid synthase

FBS: Fetal bovine serum

FCS: Fetal calf serum

FOXP3: Forkhead box P3

GADS: GRB2-related adaptor downstream of Shc

GAPDH: Glyceraldehyde-3-phosphate dehydrogenase

GITR: Glucocorticoid-induced tumour-necrosis-factor-receptor-related protein

GLUT1: Glucose transporters-1

H_2O: Water

H_2O_2: Hydrogen peroxide

HBSS: Hanks balanced salt solution

HDMEC: Human dermal microvascular endothelial cells

HEPES: 4-(2-hydroxyethl)-1-piperazineethanesulfonic acid

HLA: Human leukocyte antigen

Hr: Hour

HRP: horseradish peroxidase

ICAM-1: Intercellular Adhesion Molecule 1

IFN-γ: Interferon-γ

IL: Interleukin

IP: Inositol triphosphate

IS: immunological synapse

ITAM: Immunoreceptor tyrosine-based activation motif

ITIM: Immunoreceptor tyrosine-based inhibitory motif

Itk: Interleukin-2-inducible T-cell kinase

ITSM: Immunoreceptor tyrosine based Switch Motif

JNK: c-Jun N-terminal kinases

KO: Knock out

L: Litre

LAG-3: Lymphocyte-Activation Gene 3

LAIR-1: Leukocyte-Associated Immunoglobulin-like Receptor 1

LAT: Linker for Activation of T cells

Lck: lymphocyte-specific protein tyrosine kinase

LFA-1: Lymphocyte function-associated antigen 1

Lys: Lysine

m: Milli

M: Molar

MAPK: Mitogen-activated protein kinase

MEK: Mitogen-activated protein kinase kinase

MHC: Major histocompatibility complex

min: Minutes

MitoROS: Mitochondrial reactive oxygen species

MOPS: 3-(N-morpholino) propanesulfonic acid

MTOC: Microtubule-organising centre

mTOR: Mechanistic target of rapamycin

NADPH: Nicotinamide adenine dinucleotide phosphate

NF-Kb: Nuclear factor kappa-light-chain-enhancer of activated B cells

NK: Natural killer

OXPHOS: Oxidative phosphorylation

PBMC: Peripheral blood mononucleocytes

PBS: Phosphate-buffered saline

PCR: Polymerase chain reaction

PD-1: Programmed cell death protein 1

PD-L1: Programmed cell death 1 ligand 1

PI3K: Phosphatidylinositide 3-kinases

PKC: Protein kinase C

PTEN: Phosphatase and tensin homolog deleted on chromosome 10

PTK: Protein tyrosine kinase

RBC: Red blood cells

RIPA: Radioimmunoprecipitation assay

RNA: Ribonucleic acid

ROS: Reactive oxygen species

rpm: Revolutions per minute

RPMI: Roswell Park Memorial Institue-1640

SD: Standard deviation of the mean

SDS: Sodium dodecyl sulphate

Ser: Serine

SHP-1: Src homology region 2 domain-containing phosphatase-1

SLAM: signalling lymphocyte activation molecule

SLP-76: SH2 domain containing leukocyte protein of 76kDa

SMAD: Mothers against decapentaplegic homolog 3

SRC: Spare respiratory capacity

STAT: Signal Transducers and Activators of Transcription

TCA: Tricarboxylic acid

T_{CM}: Central memory T cells

TCR: T cell receptor

T_{EM}: Effector memory T cells

TGF-β: Transforming growth factor beta

T_H: Helper T cells

Thr: Threonine

TIGIT: T-cell immunoreceptor with immunoglobulin and ITIM domains

TIM-3: T cell immunoglobulin and mucin protein 3

TNF-α: Tumour necrosis factor alpha

TRIM: TCR-interacting molecule

v/v: volume/volume

WT: Wild type

ZAP70: Zeta-chain-associated protein kinase 70

α-KG: Alpha-ketoglutarate

µ: micro

2-ME: 2-mercaptoethanol

Chapter ONE

Introduction

1. Introduction

The immune system is a vast dynamic communication network of distinct populations of cells and chemical signals distributed in blood and tissue throughout the body to monitor tissue homeostasis, protect against invading pathogens and to eliminate damaged cells [1].

Cells of the immune system are categorised as innate or adaptive, based on their antigen specificity and timing of activation. Innate immune cells recognise and respond to invaders first, using generic germline-encoded receptors that recognize conserved patterns on different classes of pathogens. Among this first line defence of cells are natural killer (NK) cells, macrophages, neutrophils, basophils, eosinophils and mast cells, which secrete inflammatory mediators such as cytokines and chemokines, and engulf foreign antigens via phagocytosis [1]. Dendritic cells (DCs) and macrophages are termed antigen presenting cells (APCs) as they can take up antigens and migrate to lymphoid organs where they can present their antigens to adaptive immune cells. In contrast to innate cells, an individual adaptive immune cell specifically recognizes a unique antigen by using somatically generated antigen-specific receptors, which are formed as a consequence of random gene rearrangements. Among the adaptive immune cells are B lymphocytes, $CD4^+$ helper T lymphocytes and $CD8^+$ cytotoxic T lymphocytes (CTLs). Helper T lymphocytes provide necessary signals for B cells to proliferate and differentiate into either antibody-secreting effector cells or memory cells. Helper T lymphocytes also contribute to the activation of cytotoxic T cells by stimulating DCs to produce more costimulatory proteins [1]. Activated cytotoxic T cells utilize contact-dependent pathways such as the granule exocytosis pathway and the Fas-Fas ligand (FasL) pathway, and contact-independent pathways such as Interferon-γ (IFN-γ) secretion, to induce target cell killing [2].

The adaptive immune response is mediated mainly through B and T lymphocytes. T lymphocytes differentiate in the thymus and migrate to secondary lymphoid organs such as the lymph nodes and spleen. Here the T lymphocytes play a prominent role to sense, monitor and respond to the presence of foreign antigens that have been

previously engulfed by highly phagocytic immature DCs at sites of infection and brought in to the secondary lymphoid organs. Mature DCs display these foreign antigens as proteasome-processed peptides in the context of major histocompatibility complex (MHC) glycoproteins. In the secondary lymphoid tissues (e.g. lymph nodes, tonsils and spleen) mature DCs activate T cells when the peptide-MHC complex engages the T cell receptor complex (TCR) expressed by $CD8^+$ and $CD4^+$ T cell subsets. The TCR serve as highly variable receptor molecules that enable T cells to recognize and respond to foreign peptides [1]. Intracellular peptides (e.g. derived from viral proteins) bind to MHC class I molecules and are recognized by the $CD8^+$ T cell subtype, while extracellular peptides (e.g. derived from bacterial proteins) bind to MHC class II molecules and are recognized by $CD4^+$ T cells.

1.1. T cell subsets

The CD4 helper T cells (T_H) are more heterogeneous than the CD8 cytotoxic T cells (CTL) and can further differentiate into different phenotypes depending on the cytokines in the local environment. The different T_H subsets have a defined signature cytokine profile and distinct transcription factors that regulate their development (figure 1.1). T_H1 cells produce IFN-γ and Interleukin (IL)-2 and express the transcription factor T-bet. T_H2 cells produce IL-4, IL-5 and IL-13 and express GATA3. Th17 cells produce IL-17 and IL-22 and express ROR-γ t. Treg can be divided into different subsets based on the expression of FoxP3 and/or the production of IL-10, transforming growth factor-β (TGF-β) and IL-35 [3].

Following activation all T cells differentiate into different subsets of memory cells categorized based on their homing capacities and effector functions, namely central memory cells (T_{CM}) and effector memory cells (T_{EM}) (figure 1.2). T_{CM} express CCR7 and secrete IL-2 but lack the capacity to produce IFN-γ. T_{EM} lack CCR7 and express characteristic sets of chemokine receptors and adhesion molecules that enable homing to inflamed tissues. T_{EM} secrete less IL-2 but produce high levels of IFN-γ [4].

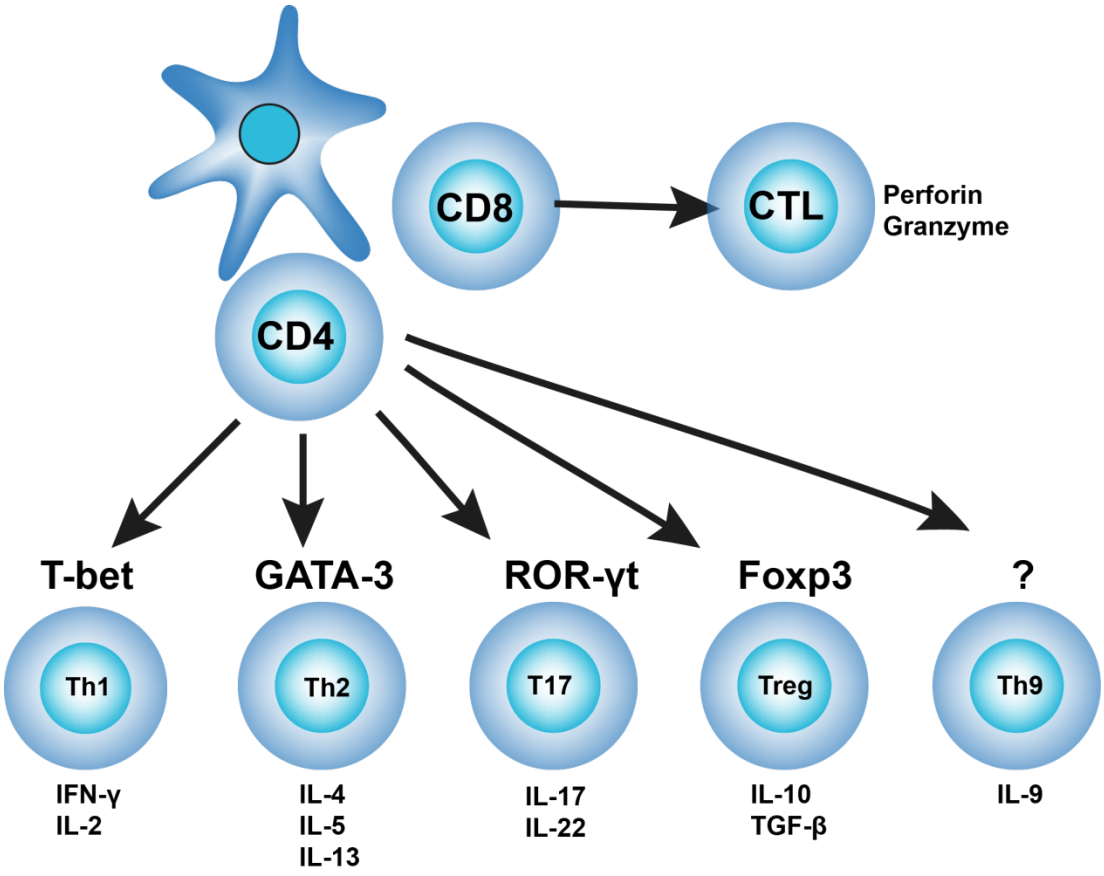

Figure 1.1: CD4 and CD8 T cell subtypes

Mature DCs activate T cells when the peptide-MHC complex engages the TCR expressed by $CD8^+$ and $CD4^+$ T cell subsets. These subsets differentiate into different phenotypes depending on the cytokine milieu and can be characterized by their cytokine profile and by transcription factors. (Adapted from Broere et al., 2011 [5]).

$CD8^+$ cytotoxic T cells are regarded as the main mediators of anti-tumour immune response. Among the cytotoxic effector functions, the secretion of IFN-γ is considered the most successful in T cell-mediated tumour rejection [6]. The anti-tumour activities of IFN-γ include the induction of MHC expression and antigen presentation, the induction of additional inflammatory cytokine production, and inhibit tumour angiogenesis [6]. However, tumour-specific $CD8^+$ T cell responses tend to be weak and susceptible to suppression in the tumour-promoting microenvironment. Mechanism utilised by tumour cells to inactivate immune responses include the secretion of inhibitory cytokines such as TGF-β. Tumour-

derived TGF-β suppresses $CD8^+$ cytotoxic function through an anti-cytotoxic program of transcriptional repression [7].

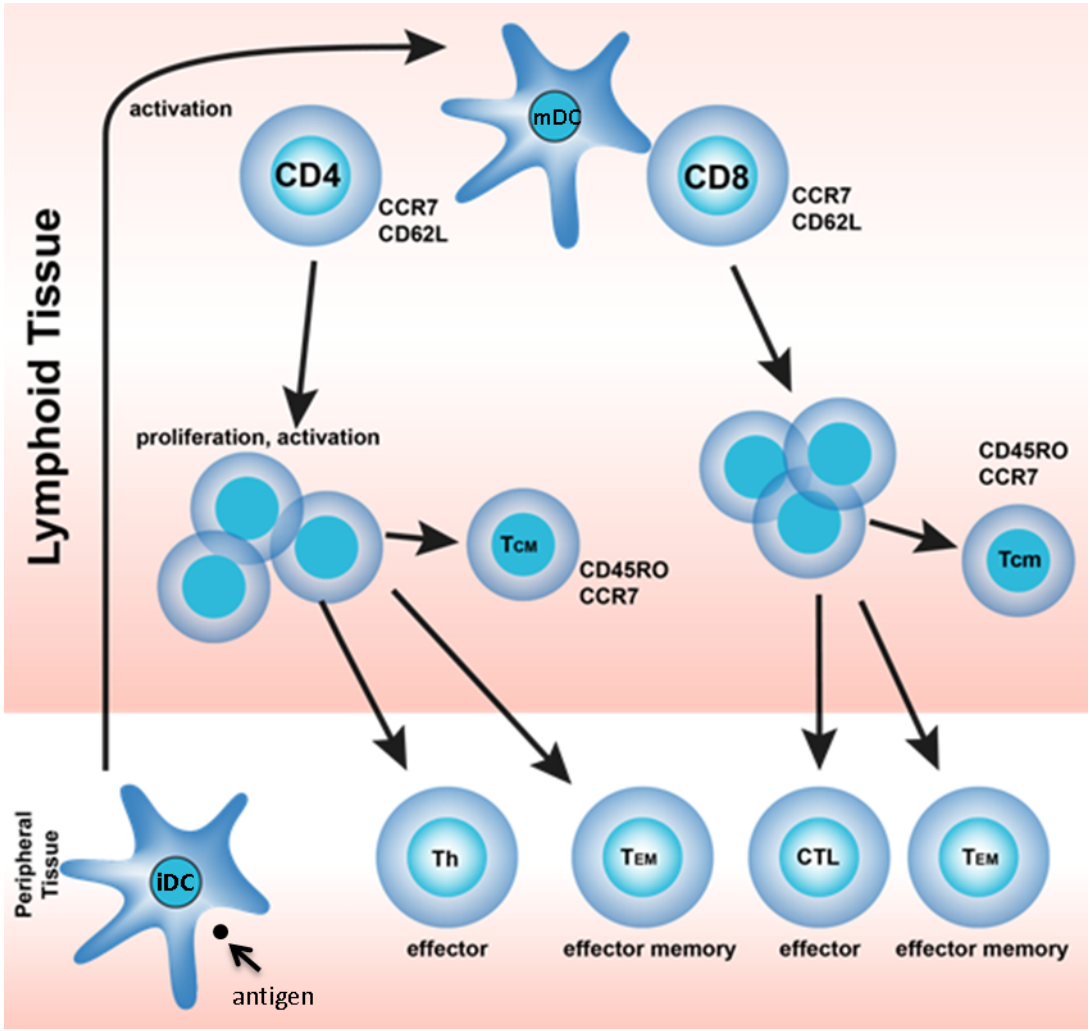

Figure 1.2: CD4 and CD8 T cell subtypes based on function

Immature DCs (iDC) take up foreign peptides/antigens in peripheral tissue and migrate to secondary lymphoid tissues. Here as matured DCs (mDC), the processed peptide in the context of an MHC molecule is presented to naïve T cells. Upon activation naïve T cells proliferate and differentiate into effector or memory T cells, and will migrate to peripheral tissue to exert their effector functions. Memory T cells can develop into effector (Th: $CD4^+/CCR7^-CD45RO^-$, CTL: $CD8^+/ CCR7^-CD45RO^-$) and effector memory cells (T_{EM}: $CCR7^- CD45RO^+$) that will migrate to peripheral tissues or central memory T cells (T_{CM}: $CCR7^+ CD45RO^+$). CCR7 is a chemokine receptor, CD62L (L-selectin) is an adhesion receptor, while CD45RO is a marker of memory T cells. (Adapted from Broere et al., 2011 [5]).

To study antigen-specific T cell responses, TCR transgenic mice are one of the most useful tools. In TCR transgenic mice the majority of T cells that develop express TCRs with known antigen specificity and can thus be used to study antigen-specific

immune responses. In this thesis we used a TCR transgenic mouse model wherein the TCR (F5-TCR) of the $CD8^+$ T cells can specifically be activated by an antigenic peptide, NP68.

1.2. T cell activation

The binding of the peptide-MHC complex to the TCR initiates the formation of microclusters at distinct contact areas between the T cell and the APC. These microclusters represent essential membrane-associated platforms where TCR-mediated signalling is initiated and maintained, before the formation of the immunological synapse (IS) [8]. TCR engagement is translated into changes in the TCR-associated CD3 subunits that allow tyrosines within their immunoreceptor tyrosine-based activation motifs (ITAMs) to be phosphorylated by CD4- and CD8-p56 Lck complexes. This event represents the start of assembly of the TCR signalling machinery or TCR signalosome which consists of a complex modular architecture made up of three independent signalling modules whose connectivity and inter-regulation are increased upon TCR stimulation. These are the src-family protein tyrosine kinase (PTK) regulation module, the signal triggering module which consist of the ITAM motifs associated with the TCR complex and the PTK ZAP70, and the signal diversification and regulation module that includes components such as ITK and Vav1 [9]. Following the phosphorylation of CD3 ITAMs by the src-family PTK Lck, ZAP 70 is recruited. Activated ZAP70 in turn phosphorylates the adaptor protein LAT which then nucleates the assembly of a multiprotein complex that bridges T cell-specific signalling events to the general signalling pathways that are involved in T cell development and function. Phosphorylation of LAT creates binding sites for PLC-γ (leads to the generation of diacylglycerol (DAG) and inositol triphosphate (IP_3) which activate the nucleotide exchange factor RasGRP1 and trigger Ca^{2+} flux, respectively), Gads (binds SLP-76 which when phosphorylated interacts with the cytosolic adaptor protein Nck and with the nucleotide exchange factor Vav1, to induce cytoskeletal reorganization, and also increases cell adhesion by interacting with the adaptor protein ADAP) and Grb2 (binds Sos and leads to Ras activation and subsequent activation of MAPKs, Rac, and ultimately several transcription factors)

[10]. These signalling events lead to effector functions such as cell migration, cytokine synthesis and cell division.

1.3. Regulation of T cell activation

The process of T cell activation consists of an orchestration of various functional modules such as actin polymerization, cell surface receptor patterning, calcium fluxing, immunological synapse formation, enhanced adhesion and gene transcription. These modules are mediated by a number of signalling proteins through inducible phosphorylation, enzyme activation and protein-protein & protein-lipid interactions. This complex and dynamic interplay of signalling events governs the decisions the T cell makes in terms of gene expression, proliferation, differentiation, survival and migration. These outcomes are influenced by the magnitude, duration and context of the activation signals [11]. Additional cell surface glycoproteins provide contextual information that influence TCR-mediated activation signals and can be classified as either co-stimulatory or co-inhibitory. The overall balance between these positive and negative signals directs the magnitude of the T cell response. TCR signalling is modulated by four different families of costimulatory and coinhibitory molecules: (1) B7-CD28 family including CD28, CTLA-4, PD-1 and BTLA; (2) CD2/signalling lymphocyte activation molecule (SLAM) family including SLAM (CD150), 2B4 (CD244), and CD48; (3) Ig family including TIM-3, CD160 and LAG-3; and (4) TNF-receptor superfamily including CD137, GITR and CD27. In addition to costimulatory and coinhibitory receptors, the cytokine milieu plays an important role in the promotion of activation, differentiation, proliferation, or cell death of T cells. The major stimulatory cytokine for T cells is IL-2, while the major inhibitory cytokine is TGF-β.

1.3.1. CD28 co-stimulatory receptor

The primary TCR signal provides the minimal scaffold for the recruitment of essential signalling molecules that then form nexus points to other major signalling pathways such as the MAPK/Erk pathways. Signalling molecules recruited by co-stimulatory receptors such as CD28 add to this central scaffold and act as amplifiers, enabling signalling thresholds to be overcome when TCR occupancy is low or to

maximize amplitude of T cell activation when TCRs are fully occupied [12]. CD28 is expressed by T cells and binds to ligands B7.1 (CD80) and B7.2 (CD86) expressed by professional APCs such as DCs. Upon receptor triggering, signal transduction cascades are initiated when signalling proteins associate with the cytoplasmic tail of CD28. Within the cytoplasmic tail, the proximal YMNM motif binds to the p85 subunit of PI3K and Grb2 or GADS. The distal proline-rich motifs PRRP and PYAP bind to the proteins Itk and Grb2/filamin A/Lck, respectively (figure 1.3) [13].

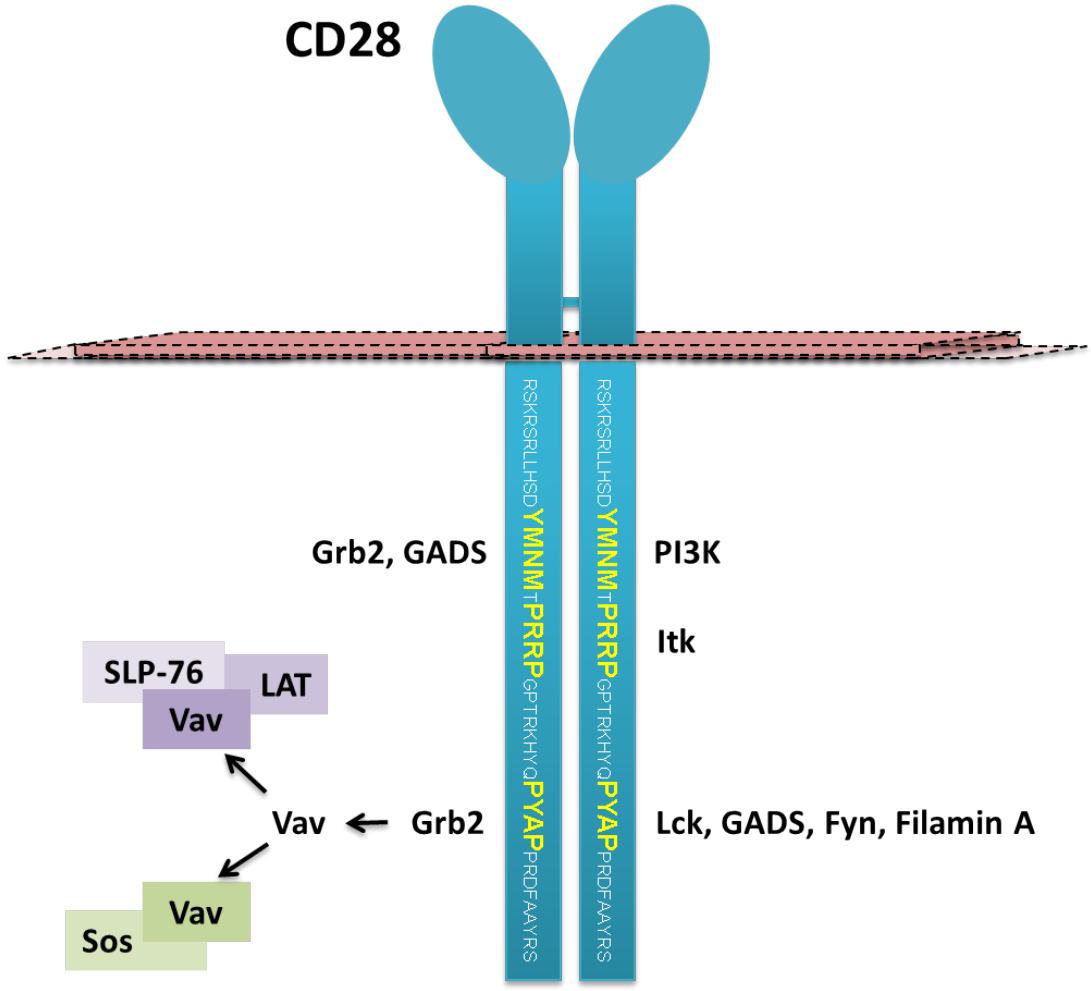

Figure 1.3: The CD28 co-stimulatory receptor

CD28 lacks intrinsic catalytic activity and delivers signals via three potential protein-protein interaction motifs (shown in yellow) found within the cytoplasmic tail.

The PI3K signal pathway ultimately leads to increased NF-κB transcriptional activity and increased survival. Binding of Grb2 to the distal motif initiates the formation of

two signalling complexes. The vav-Sos complex leads to cytoskeletal rearrangement and formation of the AP1 transcriptional complex via JNK activation, while the SLP-76-LAT complex leads to NF-κB transcriptional activation and enhanced transcription of NFAT-dependent genes including IL-2 [13].

Under physiological conditions, T cell activation requires two stimulatory signals. Signal 1 mediated by the engagement of the TCR with the peptide-MHC complex and signal 2 is mediated by the CD28 receptor engaging its natural ligands, CD80 and CD86, expressed on mature DCs. Conventional CD28 mAbs can mimic the second signal and lead to a signal1-dependent T cell activation. Superagonistic CD28 mAbs (CD28SA) however can provide both stimulatory signals and achieve full T cell activation independent of TCR engagement [14]. The signalling events generated by CD28SA are strictly dependent on the expression of functional TCR, the downstream syk family kinase ZAP-70 and the transmembrane adaptor LAT [15]. The activation of the SLP76 signalosome (SLP76-Vav-Itk-PLCγ) is also essential for inducing the sustained transmembranous calcium flux required for CD28SA-mediated production of IL-2 and IFNγ[14]. Furthermore, PI3K or its downstream effector AKT is mandatory for CD28SA-mediated IL-2 and IFNγ production [16].

1.3.2. Co-inhibitory receptors

TCR signaling can be controlled by various mechanisms that differ in their time of action and/or target molecule. Negative regulatory mechanisms are in place to act before T cell activation to maintain its quiescent state. These range from the sequestration of ITAM motifs in the lipid bilayers [17] to the autoinhibitory domain of phosphatase calcineurin, the action of IkB and its transcriptional activators Foxj and Foxo3a [18]. Rapidly after activation of the TCR signalosome, immediate feedback is provided by the protein tyrosine phosphatase SHP-1, miR-181a and DOK adaptor proteins. Delayed feedback is conducted by the HPK1-SLP76-14-3-3 pathway and STS proteins. Hours after T cell activation, modulation of TCR signaling is conducted by additional inhibitory signals downstream of immune checkpoint proteins impart a degree of control over the direction and magnitude of the primary signal, keeping the immune response tuned and amenable to baseline tonic signaling [19]. Inhibitory receptors (figure 1.4) attenuate and counterbalance

activation signals initiated by stimulatory receptors. The subsequent outcomes on T cell function can range from temporary inhibition to permanent inactivation and cell death [20].

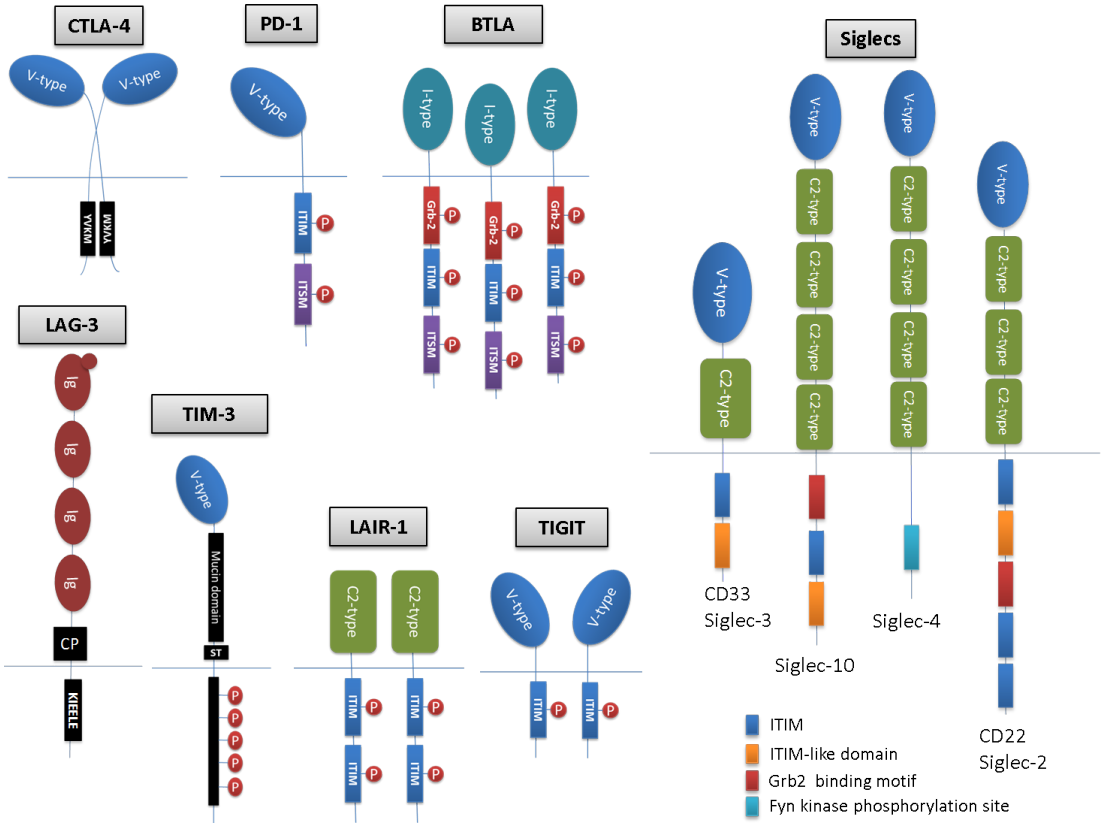

Figure 1.4: Schematic structure of T cell co-inhibitory receptors

The domain structures of the following co-inhibitory receptors are schematically depicted: B- and T-lymphocyte attenuator (BTLA), Cytotoxic T-Lymphocyte Antigen 4 (CTLA-4), Lymphocyte-activation gene 3 (LAG-3), Leukocyte-associated immunoglobulin-like receptor 1 (LAIR-1), Programmed Death 1 (PD-1) sialic acid binding Ig-like lectins (Siglecs), T-cell immunoreceptor with immunoglobulin and ITIM domains (TIGIT), T cell immunoglobulin mucin-3 (TIM-3). Extracellular immunoglobulin domains of co-inhibitory receptors include Ig-like (Ig), V-type, C2-type and I-type. ITIM- immunoreceptor tyrosine-based inhibition motif, ITSM-immunoreceptor tyrosine-based switch motif. (Table adapted from Thaventhiran et al., 2012 [11])

1.3.2.1. Mechanisms of co-inhibitory receptors

The majority of T cell co-inhibitory receptors belong to the immunoglobulin (Ig) superfamily (table 1) [21].

Table 1: T cell co-inhibitory receptors

Receptor (Ligand)	Intracellular motif	Mechanism of Action	Receptor distribution	Ligand distribution	Disease
CTLA-4 (CD80, CD86)	YxxM	[1]Use of intracellular mediators – SHP-2, PI3K [3]Ectodomain competition – with counter receptor (CD28); interference of lipid-raft and microcluster formation	Activated T cells	B cells, Mo, DCs, T cells, inducible in some somatic tissues	RA, MS, LN, Melanoma
PD-1 (PD-L1, PD-L2)	ITIM, ITSM	[1]Use of intracellular mediators – recruitment of SHP-1, SHP-2; suppression of transcription factor SKP2 [2]Inducing genes that negatively regulate T cell signalling – BATF	Activated T cells, B cells, DCs, NKT cells, Mo	B cells, T cells, inducible in Mo, DCs, some somatic tissues	Melanoma, RCC, HIV
BTLA (HVEM)	ITIM, ITSM	[1]Use of intracellular mediators – SHP-1, SHP-2 [3]Ectodomain competition with counter receptor (LIGHT)	T cells, B cells, DCs, Myeloid cells	naive T cells, B cells, DCs, NK cells, myeloid cells, inducible in somatic tissues	GVHD, Autoimmune diabetes
LAG-3 (MHC II)	KIEELE	[3]Ectodomain competition with counter receptor (CD4)	T cells, B cells, NK cells	DCs, MΦ, B cells, Mo, thymic epithelial cells	Melanoma, RCC
TIM-3 (Galectin-9, PS)	Y235, Y242	[1]Use of intracellular mediators – Lck, Fyn, p85 PI3K, Bat3 (repressor of TIM-3 signalling)	T cells, B cells, NK cells, NKT cells, DCs, MΦ	T cells, eosinophils, endothelial cells, DCs, MΦ	MS, colitis, HIV, HCV
LAIR-1 (Collagen)	2 x ITIM	[1]Use of intracellular mediators – SHP-1, SHP-2, Csk	T cells, B cells, NK cells, DCs, Mo, eosinophils, Basophils, Mast cells	Extracellular matrix components	RA
TIGIT (CD155)	2 x ITIM	[3]Ectodomain competition with the counter receptor (CD266)	T cells, NK cells	T cells, B cells, DCs	MS
Siglecs (sialylated glycoconjugates)	variable number of ITIM, Grb2 and ITIM-like domains	[1]Use of intracellular mediators – SHP-1, SHP-2, PI3K [3]Ectodomain competition with the counter receptor (cis/trans-ligand binding)	T cells, B cells, DCs, pDCs, MΦ, Mo, Neutrophils, NK cells, eosinophils	widespread on cell surfaces, proteins, pathogens	Leukaemia, SLE, B cell-NHL

Abbreviations: [1-3] three general types of distinct mechanisms of action; B cell-NHL: B cell non-Hodgkin's Lymphomas; Bat3- Human Leukocyte Antigen B (HLA-B)-associated Transcript 3; BATF: Basic Leucine Zipper Transcription Factor, ATF-like; BTLA: B- and T-lymphocyte Attenuator; Csk: COOH-terminal; CTLA-4: Cytotoxic T-Lymphocyte Antigen 4; DC: Dendritic Cells; Fyn: a Src family tyrosine-protein kinase; Grb2: Growth factor receptor-bound protein 2; GVDH: Graft Versus Host Disease; HCV: Hepatitis C Virus; HIV: Human Immunodeficiency Virus; HVEM: Herpes Virus Entry Mediator; ITIM- Immunoreceptor Tyrosine-based Inhibition n Motif; ITSM: Immunoreceptor Tyrosine based Switch Motif; LAG-3: Lymphocyte-Activation Gene 3; LAIR-1: Leukocyte-Associated Immunoglobulin-like Receptor 1; Lck: Lymphocyte-specific protein tyrosine kinase; LIGHT: Lymphotoxin-like, exhibits inducible expression, and competes with herpes simplex virus glycoprotein D for HVEM, a receptor expressed by T lymphocytes; LN: Lupus Nephritis; MHC II: Major Histocompatibility Complex II; Mo: Monocyte; MS: Multiple Sclerosis; MΦ: Macrophage; N/A: Not

Applicable; NK: Natural Killer cells; NKT: Natural Killer T cells; PD-1: Programmed cell death protein 1; pDC: plasmacytoid dendritic cell; PD-L1: Programmed cell death 1 ligand 1; PI3K: Phosphoinositide 3-kinase; PS: Phosphatidyl Serine; RA: Rheumatoid Arthritis; RCC: Renal Cell Carcinoma; SHP-1/2/: Src homology 2-containing tyrosine phosphatase 1/2/; Siglecs: Sialic acid binding Ig-like lectins; SLE: Systemic Lupus erythematous, Srk kinase; SKP2: S-phase Kinase-associated Protein 2; TIGIT: T-cell immunoreceptor with immunoglobulin and ITIM domains; TIM-3: T cell Immunoglobulin Mucin-3 (Table adapted from Thaventhiran et al., 2012 [11]).

There are three major mechanisms that are utilized by membrane bound inhibitory receptors in T cells (Figure 1.5). The first mechanism involves the sequestration of the ligands for costimulatory receptors, depriving the T cell from receiving activation signals necessary for complete activation. The second mechanism involves the recruitment of intracellular phosphatases by an immunoreceptor tyrosine-based inhibition motif (ITIM) and/or an immunoreceptor tyrosine-based switch motif (ITSM) that make up the cytoplasmic tail of certain inhibitory receptors, which dephosphorylate signalling molecules downstream of the TCR and costimulatory pathways, leading to a quantitative reduction in activation-induced gene expression. The third mechanism involves the upregulation (or downregulation) of genes that code for proteins involved in the inhibition of immune functions [21]. A co-inhibitory receptor could use a combination of the above and possibly other yet to be discovered mechanisms to regulate T cell signalling. A large number of co-inhibitory receptors recruit intracellular phosphatases to their cytoplasmic domains in order to dephosphorylate signaling molecules downstream of the TCR and co-stimulatory pathways.

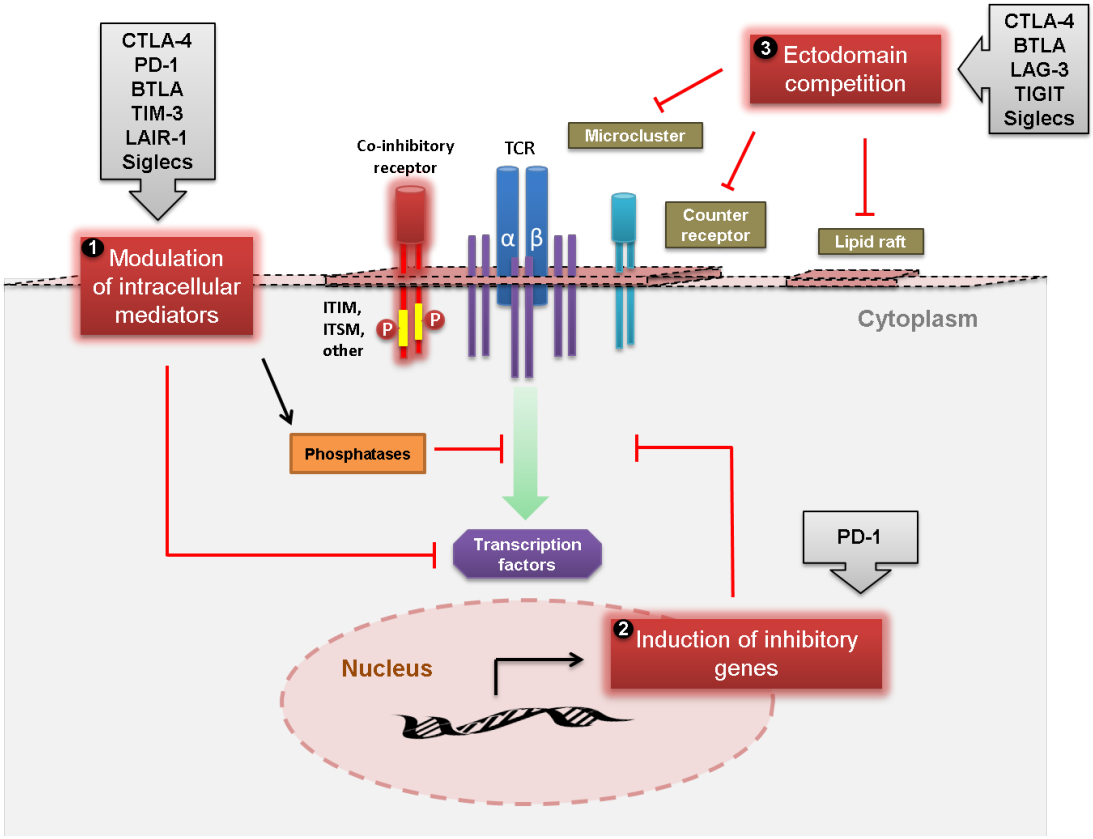

Figure 1.5: Mechanisms through which co-inhibitory receptors regulate T cell signaling

Upon ligand engagement the cytoplasmic signaling motifs of co-inhibitory receptors such as ITIM or ITSM are phosphorylated and bind intracellular mediators such as the phosphatases SHP-1 and SHP-2, which then dephosphorylate key signaling molecules downstream of the T cell receptor. The suppression of transcription factors can also be classified under mechanism 1. Co-inhibitory receptors that use this mechanism are CTLA-4, PD-1, BTLA, TIM-3, LAIR-1and Siglecs. Mechanism 2 is used by co-inhibitory receptors such as PD-1 and involves upregulating a program of genes that inhibit T cell function. Mechanism 3 involves ectodomain competition. Here the co-inhibitory receptors (CTLA-4, BTLA, LAG-3, TIGIT and Siglecs) prevents optimal signal transduction at the cell membrane by sequestering counter receptors/ligands and/or preventing the formation of microclusters and lipid rafts which are necessary for immunological synapse formation and T cell activation. (Figure adapted from Thaventhiran et al., 2012 [11]).

Most of these co-inhibitory receptors contain one or several ITIMs within the cytoplasmic domain (figure 1.4) which recruit Src homology 2 (SH2) domain-containing phosphatases. ITIMs are structurally defined as a six-amino acid consensus sequence (I/V/L)xYxx(L/V), containing a single tyrosine (Y), a hydrophobic residue (I, V or L) at the C-terminal position Y+3 and a less conserved hydrophobic

residue at the N-terminal position Y-2 [22, 23]. The motif is highly conserved except for the amino acids surrounding the single tyrosine residue, where x denotes any amino acid.

Despite the large number of different ITIM-bearing receptors on a single cell type, each co-inhibitory receptor has a crucial and non-redundant role in immunoregulation. The ITIM-bearing co-inhibitory receptors vary in their expression patterns, level of inhibition and the type of signal delivered. Upon T cell activation ITIM-bearing receptors translocate to the immunological synapse with activating receptors that brings them in close proximity to a kinase, which in the majority of cases is a Src family kinase (e.g. Lck). The kinase phosphorylates the tyrosine residue within the ITIM motif and leads to the recruitment of SH2 domain-containing phosphatases SHP-1 and/or SHP-2, SHIP, which then dephosphorylate several key molecules that are involved in the initial steps of the T cell signalling pathway (figure 1.6). SHIP1 and SHIP2 are lipid phosphatases while SHP-1 and SHP-2 are tyrosine phosphatases [24]. The way in which activating signals are modified depends on the phosphatase recruited to the ITIM motif.

A variant of the ITIM termed immune receptor tyrosine-based switch motif (ITSM) is found in some co-inhibitory receptors. Programmed cell death protein 1 (PD-1), B- and T-lymphocyte attenuator (BTLA) contain both an ITIM and an ITSM within their cytoplasmic domain. The ITSM motif has a consensus sequence (T)xYxx(V/I) and binds to an adaptor protein called SH2 domain-containing molecule 1A, which influences the activating signals by regulating the recruitment of SHP-1 and SHP-2 [25]. Inhibition can also be executed by a co-inhibitory receptor in the absence of an intracellular ITIM motif. For example, CTLA-4 does not have ITIMs but does contain two tyrosine residues that could act as potential SH2-domain binding sites (figure 1.6).

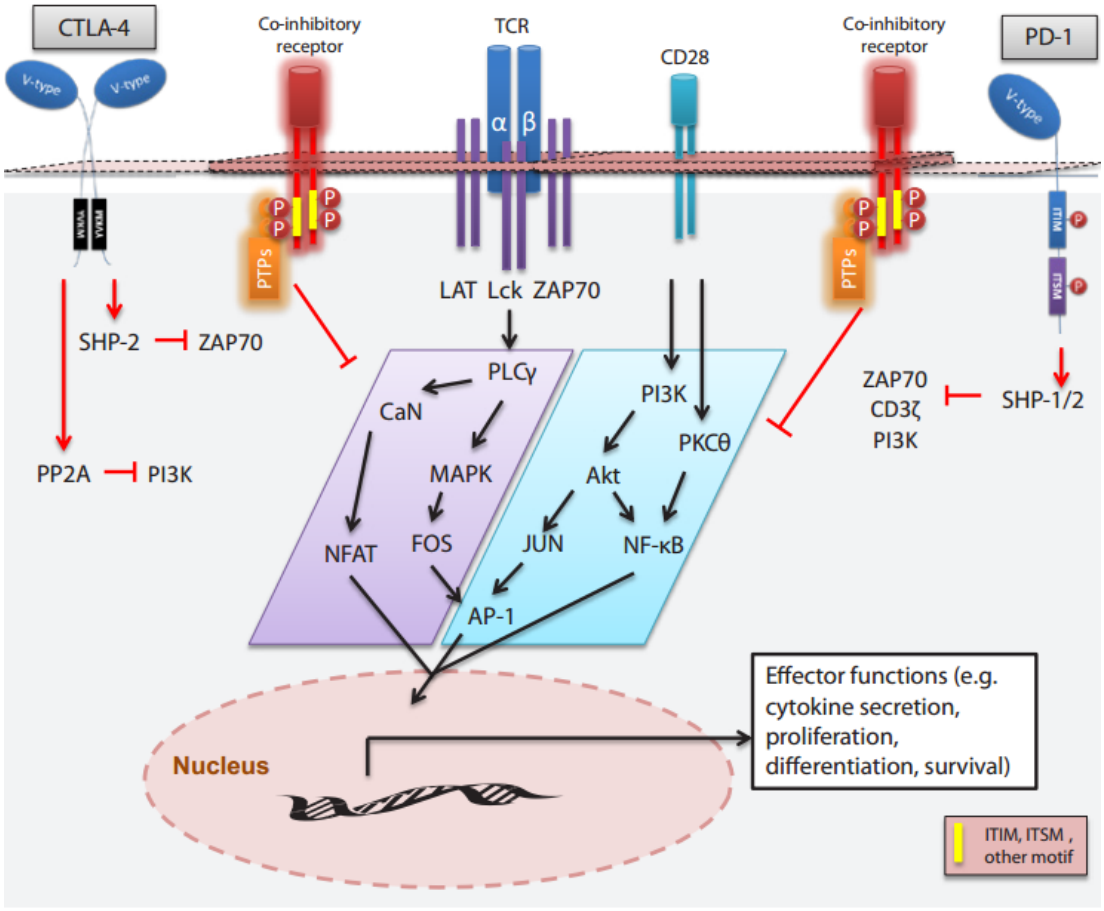

Figure 1.6: Activation of protein tyrosine phosphatases (PTP) and regulation of TCR signalling

TCR triggering activates a number of signalling pathways that include calcium, MAPK and NFκB. Co-inhibitory receptors recruit SH2-domain containing protein tyrosine phosphatases, SHP-1 & SHP-2 through binding of the PTP SH2 domains to phosphorylated ITIMs in their cytoplasmic domains. Engagement of PTP SH2 domains leads to activation of the PTPs which dephosphorylate key substrates that lie within the TCR signalling pathways. CTLA-4 and PD-1 are shown as specific examples with the PTPs that are recruited and the substrates that are dephosphorylated. In addition to PTPs, CTLA has been shown to associate with the protein phosphatase PP2A and negatively regulate PI3K. CTLA-4-Cytotoxic T-Lymphocyte Antigen 4, ITIM-immunoreceptor tyrosine-based inhibition motif, ITSM-immunoreceptor tyrosine-based switch motif, PD-1-Programmed cell death protein 1 SHP-1/2-Src homology 2-containing tyrosine phosphatase 1/2, Siglecs-sialic acid binding Ig-like lectins, PP2A–protein phosphatase 2A. (Figure adapted from Thaventhiran et al., 2012 [11]).

1.3.2.2. PD-1 and LAG-3 co-inhibitory receptors

PD-1 belongs to the Ig superfamily (IgSF) of surface proteins (Table 1). PD-1 is made up of one Ig domain, a ~20 amino acid stalk region, a transmembrane domain and an intracellular domain containing both an ITIM and an ITSM (figure 1.4). PD-1 is inducibly expressed on the surface of T cells within 24hours of activation, although its functional effects on for e.g. IFN-γ, TNF-α and IL-2 production are observable within a few hours [26]. PD-1 normally exhibits a uniform cell surface expression but redistributes itself close to the site of TCR engagement within microclusters for successful interaction with its ligands PD-L1 (constitutively expressed on T cells, B cells, DCs, macrophages, mesenchymal stem cells and bone marrow derived mast cells) and PD-L2 (inducibly expressed on DCs, macrophages and bone marrow derived mast cells) [27].

Upon PD-1 ligation, both of the cytoplasmic ITIM and ITSM tyrosine motifs are phosphorylated possibly by Lck and/or C-terminal Src kinase with a consequent recruitment of SHP2. This reduces the TCR-triggered phosphorylation of CD3ζ, ZAP70 and PKCθ, while also blocking the CD28-mediated activation of PI3K and Akt [28]. TCR stimulation induces the activation and upregulation of casein kinase 2 (CK2), which phosphorylates PTEN (phosphatase and tensin homolog deleted on chromosome 10) in the Ser380-Thr382-Thr383 cluster within the C-terminal regulatory domain and inhibits its phosphatase activity, allowing sustained activation of the PI3K/Akt pathway to support glucose uptake, survival and expansion. PD-1 inhibits the TCR-induced CK2-mediated stabilizing phosphorylation of PTEN, which results in ubiquitin-dependent degradation and diminished abundance of PTEN protein but increased PTEN phosphatase activity [29]. PTEN acts predominantly as a lipid phosphatase by dephosphorylating PI(3,4,5)P3 to generate PI(4,5)P2 and thus directly opposes PI3K activation by limiting its substrate availability (figure 1.7).

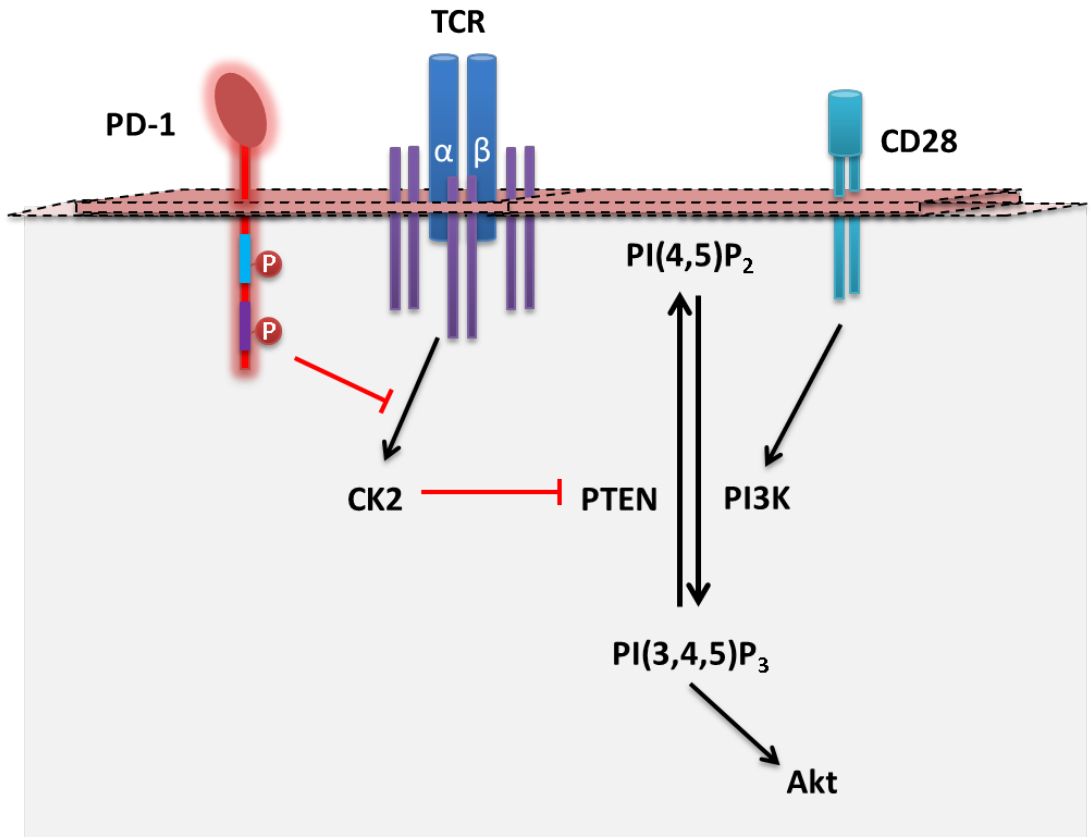

Figure 1.7: PD-1-mediated regulation of PTEN activity via CK2

TCR activation induces CK2 activation and subsequent phosphorylation of the PTEN C-terminal serine-threonine cluster S380-T382-T383, which inhibits the PTEN phosphatase activity and allows activation of the PI3K/Akt pathway. PD-1 suppresses CK2 and prevents the stabilizing phosphorylation of the PTEN C-terminal serine-threonine cluster S380-T382-T383. This results in increased PTEN phosphatase activity and inhibition of PI3K/Akt.

The inhibitory signal mediated by PD-1 depends on the strength of the TCR signal with much stronger phosphorylation of PD-1 and association with SHP2 observed at high levels of TCR stimulation. Even in the absence of TCR engagement, a basal level of PD-1 phosphorylation and SHP2 recruitment is detectable [30].

PD-1 ligation interferes with the induction of the cell survival factor Bcl-xL [25] and the expression of transcription factors associated with effector cell function such as GATA-3, T-bet and Eomes [26]. PD-1 ligation can also block cell cycle progression and proliferation of T cells by interfering with multiple regulators of the cell cycle via a mechanism that utilises the suppression of transcription factors in order to downregulate genes that code for proteins involved in cell cycle control. The

standard cell cycle is traditionally subdivided into the G_1, S, G_2 and M phases with a G_0 resting state. Cyclin-dependent kinases (CDK) are key regulatory proteins that are activated at specific checkpoints during the cell cycle to influence downstream processes by phosphorylating specific proteins. There are five active CDKs during the cell cycle; during G1 (CDK4, CDK6 and CDK2), S (CDK2), G2 and M (CDK1), and different cyclins are needed at different phases to provide enzymatic activity to the cyclin-Cdk holoenzyme complexes which can be inhibited by Cdk inhibitors (CKI) of the Cip/Kip family such as p21 (Waf1, Cip1), p27 (kip1) and p57 (Kip2). Cdc25 are dual-specificity phosphatases that target CDKs and control the entry and progression through the cell cycle phases [31].

A recent study demonstrated that PD-1 ligation blocks cell cycle progression through the G1 phase by suppressing the transcription of *SKP2*, a gene that encodes components of a $p27^{kip1}$degrading ubiquitin ligase called SCF^{Skp2}, via inhibition of PI3K–Akt and Ras–MEK-ERK signalling pathway. These result in the accumulation of $p27^{kip1}$and suppression of cyclin E-Cdk2 activity. Consequent impairment in phosphorylation of the transcription factor retinoblastoma (Rb) and the anti-proliferative signal transducer Smad3, increase Smad3 transactivation due to the inhibition of E2F-regulated gene expression. This results in the suppression of the gene encoding Cdc25A with concomitant increase in ubiquitin-dependent proteosomal degradation of the Cdc25A protein, increased p15 abundance and finally more suppression of *SKP2* expression [32]. In addition to influencing cell cycle genes, PD-1 can cause T cell exhaustion by upregulating a program of genes including that of the basic leucine transcription factor, ATF-like (BATF) which functions as a negative regulator of AP-1 activity [33].

Continued interaction between PD-1 and its ligand PD-L1 suppress TCR-driven stop signals and prevent recruitment of key signalling molecules to initiate T cell activation. The inability to form stable immunological synapses with allogeneic APCs causes a long-term maintenance of the anergic state that seems to depend on PD-1-PD-L1 interaction [34]. The expression of PD-1 also modulates the threshold of antigen density required to activate cognate T cells which has an impact on antigen recognition in peripheral tissues especially in the context of tolerance [35].

Another co-inhibitory molecule that plays an important role in regulating T cell activation is the Lymphocyte activation gene-3 (LAG-3; CD223), a CD4-related transmembrane protein. LAG-3 binds to MHC class II molecules found on the surface of APCs but with a much higher affinity than CD4 and at a different site from CD4 endowing it with a possible role as a negative competitor for CD4 (Table 1). LAG-3 is mainly retained intracellularly near the microtubule-organising centre (MTOC) and is found co-localised with Rab11b, a monomeric G-protein that regulates endosomal recycling of transferrin (Tfn) receptors to the plasma membrane [36]. Upon T cell activation LAG-3 is rapidly translocated to the plasma membrane. LAG-3 is first detectable 24hrs following activation and peak expression is observed at around day 2 followed by a gradual decline in expression by day 8 [37]. LAG-3 expressed on the surface can be cleaved within the transmembrane domain at the connecting peptide (CP) by two members of the TNFα converting enzyme (TACE) family of metalloproteases known as ADAM 10 and ADAM 17 [38], to release soluble LAG-3 (sLAG-3) which may contribute to the regulatory function of LAG-3. Although the mechanism of how LAG-3 associates with the TCR-CD3 complex and negatively regulates TCR-induced signal transduction is not completely understood, a single lysine residue 468 within a conserved KIEELE motif in the cytoplasmic domain of LAG-3 has been shown to be indispensable in executing the inhibitory effect on CD4-dependent T cell function [39, 40]. Similar to the protein kinase C binding site in the CD4 molecule, the cytoplasmic tail of LAG-3 contains a region with a potential serine phosphorylation site. Another motif that has been identified in the intracytoplasmic region of LAG-3 is an unusual 'EP' (glutamic acid-proline) repeat that binds a protein termed LAP (LAG-3-associated protein) and is predicted to be important in the anchorage of the IS to the microtubule network following TCR engagement [41]. These properties suggest that the LAG-3 cytoplasmic domain mediates intracellular signal transduction and/or molecular aggregation [40]. LAG-3 inhibits T cell expansion by blocking entry of activated T cells into the growth phase of the cell cycle and results in the accumulation of cells in the S-phase. LAG-3 is involved in limiting the expansion of activated T cells and controlling the size of the memory T cell pool [42]. LAG-3 is also thought to play a role in modulating DC function and also in enhancing the suppressive activity of

$CD4^+CD25^+$ regulatory T cells (Treg). LAG-3 can negatively regulate T cell homeostasis by Treg-dependent and independent mechanisms.

1.3.2.3. Other key co-inhibitory receptors

In addition to PD-1 and LAG-3 other T cell co-inhibitory receptors include CTLA-4, BTLA, TIM-3, LAIR-1, TIGIT and Siglecs (figure 1.4 and table 1).

CTLA-4 has an essential role in negative regulation and maintenance of T cell homeostasis. The expression of CTLA-4 on T cells controls the thresholds of T cell activation following TCR ligation [43]. CTLA-4 is a type I transmembrane glycoprotein of the Ig superfamily found at low levels as a non-functional covalent homodimer on the surface of T cells 24-48 hours following TCR stimulation and binds to the homodimeric ligand CD80 (B7-1) and CD86 (B7-2) expressed by APCs (Table 1). These ligands also bind to the more abundant CD28 receptor, although with a lower affinity. Naive and memory T cells have a large pool of CTLA-4 localized to intracellular vesicles (TGN, endosomes and lysosomes) which can be mobilised to accumulate at the IS and partitioned to lipid rafts upon T cell activation. The amount of CTLA-4 transported depends on the strength of the TCR signal and calcium influx, and is facilitated by the chaperone adaptor TCR-interacting molecule (TRIM) [44]. CTLA-4 uses a mechanism of signal initiation that does not fit with the current paradigm for receptor-medicated signalling where ligand-induced conformational changes or ligand-induced dimerization take place [44]. Several models have been proposed to explain how CTLA-4 can influence TCR signalling. These include competitive antagonism of CD28, direct engagement of negative signalling molecules and the inhibition of lipid-raft and microcluster formation (Figure 1.5 & 1.6). Studies have shown that CTLA-4 can bind negative signalling molecules such as SHP2 and PP2A (a serine/threonine phosphatase) which can then dissociate upon CTLA-4 ligation and dephosphorylate certain proximal TCR signalling proteins such as TCR-ζ and LAT [45].

B and T lymphocyte associated (BTLA) belongs to the IgSF of co-inhibitory receptors and binds to the herpes virus entry mediator (HVEM) which belongs to the TNF superfamily of costimulatory molecules (Table 1). Surface expression levels of BTLA

is low on naive $CD4^+$ T cells but is rapidly upregulated following TCR activation with peak surface expression after 48 hours [46].

BTLA functions via the recruitment of tyrosine phosphatases (SHP-1 and SHP-2) and interaction with lipid raft components in order to attenuate TCR downstream signalling pathways [47].

T cell immunoglobulin-3 (Tim-3) is a type I glycoprotein receptor with a membrane distal immunoglobulin variable (IgV) domain and a membrane proximal mucin domain and is mainly expressed on IFN-γ-producing $CD4^+$ T helper 1 (Th1) and $CD8^+$ CTLs. TIM-3 is recognized by galectin-9, a member of carbohydrate-binding proteins that belong to a group of S-type lectins (Table 1) [48].

Unlike the inhibitory receptors which are expressed after T cell activation, LAIR-1 is expressed in very high and relatively homogenous levels in naive T cells but in lower and more heterogeneous levels in memory T cells [49]. LAIR-1 has been shown to exist in a basally tyrosine phosphorylated state that constitutively recruits and activates SHP-1, which can then dephosphorylate downstream TCR signalling components and influence the basal threshold of T cell activation [50, 51]. LAIR-1 expression levels might contribute to the higher threshold for TCR stimulation observed in naive cells compared to effector and memory cells.

T cell Ig and ITIM domain (TIGIT) is a more recently identified inhibitory receptor that is expressed on activated T cells. TIGIT is an immunoglobulin protein of the CD28 family [52]. TIGIT binds to surface CD155 (poliovirus receptor) molecules on DCs (Table 1). TIGIT-CD155 interaction can indirectly inhibit T cell responses by driving DCs to a more IL-10 producing-tolerogenic phenotype [53].

Sialic acid-binding Ig-like lectins (Siglecs) are type I transmembrane proteins of the IgSF and have the unique ability to transmit signals into immune cells upon binding to sialylated glycans [54]. Several Siglecs contain inhibitory signalling motifs within their cytoplasmic domains and are thought to be important contributors of negative signals that dampen the immune response [55].

1.3.3. Cytokines regulate T cell function

Regulation of T cell activation can also be mediated by the binding of cytokines to specific cell-surface receptors. IL-2 is a potent T-cell growth factor and plays a central role in controlling the magnitude of clonal expansion, the development of effector cells and the subsequent contraction of the antigen-specific T cells [56]. The secretion of IL-2 as a consequence of signalling through the TCR is accompanied by the expression of a high affinity receptor consisting of three subunits, IL-2Rα (CD25), IL-2Rβ (CD122), and γc (CD132). IL-2 is directionally secreted within the immunological synapse. IL-2 is first captured by CD25 and the resulting binary complex leads to conformational changes within IL-2 that promote interactions with the other subunits, forming a stable quaternary high-affinity IL-2R, which then drives clonal expansion [57]. Upon signal transduction the IL-2/IL-2R complex is rapidly internalized. IL-2, CD122 and CD132 components of the complex are rapidly degraded, while CD25 is recycled to the cell surface. Thus, the clonal expansion of T cells requires a continuous source of IL-2 to engage IL-2R and form additional IL-2/IL-2R complexes to sustain signalling [57].

IFN-γ is a major pro-inflammatory effector and regulatory cytokine produced by activated T cells and NK cells. In addition to suppressing tumour development and promoting tumour rejection, IFN-γ orchestrates the trafficking of T cells to sites of inflammation by up-regulating the expression of adhesion molecules (ICAM-1) and chemokines (RANTES/CCL5) [58].

TGF-β is a key immunosuppressive cytokine that enforces T cell tolerance by limiting T-cell activation signals. TGF-β binds to type I and type II transmembrane serine/threonine kinase receptors which signal to the nucleus via phosphorylation and subsequent nuclear localization of intracellular Smad proteins, culminating in the transcriptional regulation of target genes [59]. TGF-β is usually found at high concentrations in the immediate tumour microenvironment, where it can regulate tumour initiation, progression and metastasis. TGF-β inhibits both the clonal expansion and cytotoxicity of $CD8^+$ T cells via repression of the cytotoxic gene program, which ultimately favours tumour progression [7]. Furthermore, TGF-β triggers apoptosis as well as oxidative stress in immune cells [60].

1.3.4. Membrane lipids and Integrins in T cell activation

The efficiency of T cell signalling is increased by spatial organisation of receptors and signalling mediators. In particular, the triggered receptors and their downstream signalling proteins are spatially organised into cholesterol- and sphingolipid-rich plasma membrane microdomains termed lipid rafts [61]. In addition apical sorting, lipid rafts facilitate cell migration, association of signalling molecules and crosstalk between cell types. Upon T cell activation there is an increase in the synthesis fatty acids for the biogenesis of new membrane domains prior to cell division. In addition fatty acids are also a source of energy and functions as signalling molecules.

Apart from influencing TCR stimulation, co-stimulatory and co-inhibitory receptors play a role in trafficking of effector memory T cells by regulating their migration to non-lymphoid tissue. T cell migration involves four different adhesion steps; tethering, rolling, activation and arrest. CD28 enhances integrin-mediated T cell adhesion and cytoskeletal rearrangements via the Rho family GTPase Rac1, while CTLA-4 enhances integrin-mediated adhesion via a Rap1-mediated pathway [62]. CD28 and CTLA-4 enhance integrin-mediated T cell adhesion in vitro but exert opposite effects on T cell motility in vivo, through unknown mechanisms.

Sustained T cell signalling requires prolonged T cell-APC interactions. Integrins such as lymphocyte function-associated antigen 1 (LFA1) constitute a family of proteins that are capable of inside-out signalling, mediate T cell-APC adhesion and are essential for IS formation [63]. The principle ligand of LFA-1 is the intercellular adhesion molecule-1 (ICAM-1). LFA-1 integrates into TCR-linked cytoskeletal-regulated signalling events, inducing T cell migration [64]. LFA-1 engagement also lowers TCR activation thresholds and increases sensitivity to CD28 costimulation, accelerating several aspects T cell maturation [65]. In addition to integrins, the expression of chemokines receptors by T cells enables migration in response to chemoattractant gradients provided by chemokines. These directional cues are critical for T cell trafficking and migration into inflammatory sites. CCR5 and CXCR4 are structurally related chemokine receptors which bind to RANTES/CCL5 and SDF-1/CXCL12, respectively [66].

1.4. T cell metabolism underpins activation

Upon activation naïve T cells undergo a rapid burst in proliferation and differentiate towards an effector phenotype depending on the stimulatory cues and cytokines present during the priming event [67]. The pro-stimulatory immune cell response involves epigenetic changes, elevated production of inflammatory cytokines, transmigration through tissues and cellular division. Activated dynamic T cells need to adopt a metabolic program that would satisfy the bioenergetic and biosynthetic demands of sustaining rapid cell proliferation, adapting to changes in microenvironment and performing the necessary effector functions [68]. In addition to being regulated by inhibitory receptors, the metabolic commitment of an immune cell following activation enforces its fate and effector function [69].

Adenosine triphosphate (ATP) shuttles chemical energy within the cell to fuel anabolic functions. ATP is produced in both quiescent and activated cells via glycolysis and/or mitochondrial oxidative phosphorylation (OXPHOS). AMPK functions as a sensor of cellular adenylates [ATP, adeonsine diphosphate (ADP), and AMP], where an elevated AMP to ATP ratio leads to increased phosphorylation of AMPK at Thr172 on its activation loop by the kinases LKB1, TAK1, or CaMKKβ. AMP binds and activates AMPK when ATP levels drop [70]. This promotes ATP production and blocks its consumption, until ATP homeostasis is re-established whereupon increased binding of ATP to AMPK inhibits its kinase activity. Activation of AMPK leads to the inhibition of mRNA translation through inhibition of mTORC1 activity [70].

1.4.1. Glycolysis

TCR stimulation induces cell surface expression of glucose transporters-1 (Glut1) which mediates the transport of glucose into T cells. Glycolysis refers to the metabolic pathway that converts glucose into pyruvate through a sequence of ten enzyme-catalysed reactions. Glyceraldehyde-3-phosphate dehydrogenase (GAPDH) is a bifunctional enzyme involved in both glucose metabolism and gene regulation. The RNA binding function of the enzyme is influenced by the metabolic state of the cell. GAPDH dampens the posttranscriptional production of proinflammatory

cytokines such as IFNγ and IL-2, by binding to AU-rich regions in the 3' untranslated region (UTR) of the cytokine mRNAs [71]. Upon T cell activation and a rise in glycolysis, GAPDH switches from an RNA binding protein to function as a metabolic enzyme. Thus supporting T cell proliferation and facilitating full effector cytokine production.

TCR-mediated glucose uptake requires CD28-mediated Akt-dependent regulation of Glut1 trafficking and glucose uptake and Akt-independent regulation of Glut1 expression [72], to allow maximal glucose uptake for T cell activation and proliferation. CD28-mediated increase glycolytic flux is required for T cells to meet the energetic and biosynthetic demands associated with a sustained proliferation and effector functions [73]. TCR-mediated upregulation of Glut1 facilitates the uptake of glucose. Each glucose molecule is broken down in the cytosol by anaerobic glycolysis into two molecules of pyruvate, two reduced nicotinamide adenine dinucleotide (NADH) molecules and two net ATP molecules. Depending on the state of T cell activation pyruvate has two alternate fates. Metabolically quiescent naïve cells adopt a basal level of nutrient uptake and primarily channel glucose-derived pyruvate to be fully oxidized in the tricarboxylic acid (TCA) cycle [69]. This generates NADH and reduced flavin adenine dinucleotide ($FADH_2$) to fuel oxygen-dependent OXPHOS, which will generate up to 36 molecules of ATP per glucose. Metabolically active cells adopt an increased level of nutrient uptake and preferentially use glycolysis over OXPHOS for ATP production. Here glucose-derived pyruvate is primarily transformed into lactate to regenerate NAD^+ for use in glycolysis [69]. The intermediates of the glycolytic pathway provide entry points for glycolysis and also form building blocks for macromolecular synthesis. The intermediates of the glycolytic pathway provide entry points for glycolysis and also provide precursors for chemical constituents (e.g. nucleotides, amino acids and lipids) required for macromolecular synthesis via anabolic pathways essential for constructing new daughter cells.

1.4.2. Tricarboxylic acid cycle (TCA) and OXPHOS

In the TCA cycle, named after the three carboxyl groups of citric acid, citrate is both the first product and the final reagent. During aerobic glycolysis pyruvate is decarboxylated by pyruvate dehydrogenase to acetyl-CoA with the release of CO_2 and NADH. The high-energy acetyl-CoA molecule is combined with oxaloacetate to form citrate, which undergoes further reactions catalysed by a series of seven enzymes into two molecules of CO_2, together with three equivalents of NADH from NAD^+ and one equivalent of $FADH_2$ from FAD. The NADH and $FADH_2$ generated by the citric acid cycle are in turn oxidized by the electron transport chain (ETC) in the inner mitochondrial membrane [1]. Here, electrons are transported from higher energy NADH/$FADH_2$ to lower energy O_2 through a chain of four protein complexes (I, II, III and IV), with a lipid soluble cofactor ubiquinone (coenzyme Q) and a water soluble protein cytochrome c shuttling between the protein complexes (figure 1.8). During electron transport, the accompanying protons are released and pumped out of the mitochondrial matrix. This creates a pH gradient across the inner mitochondrial membrane due to the uneven distribution of protons and results in electrochemical potential energy which returns the protons to mitochondrial matrix through an integral membrane protein known as ATP synthase. The released energy is used to phosphorylate ADP. The coupling of ATP synthesis to NADH/$FADH_2$ oxidation is termed oxidative phosphorylation (OXPHOS) [1]. The mitochondrial ETC "leaks" electrons which react with oxygen to produce superoxide (O_2^-), which in turn gets converted to hydrogen peroxide (H_2O_2) by Mn-superoxide dismutase (MnSOD). TCR-induced calcium flux can permeate into the mitochondria and stimulate the activity of the TCA cycle enzymes, and increase the electron "leak". Thus the greater the calcium flux, the greater the rise in mitochondrial respiration to meet metabolic demands, and the more O_2^- is produced. These mitochondrial reactive oxygen species (mitoROS) permeate membranes and represent the major redox signal originating from the mitochondria. MitoROS can influence cell signaling by redox modification of protein phosphatases which reduces their function and in turn enhances kinase signaling cascades [74].

1.4.3. Lipogenesis and glutaminolysis

Carbon enters the TCA cycle primarily at (i) the condensation of glucose-derived acetyl CoA with oxaloacetate (OAA) to generate citrate and at (ii) the conversion of glutamine to alpha-ketoglutarate (α-KG) via glutaminolysis. Both entry points contribute to the mitochondrial citrate pools. A key metabolic intermediate and precursor for lipid biosynthesis is the cytosolic pool of acetyl-CoA, formed from glucose derived-mitochondrial citrate via ATP citrate lyase (ACL). The acetyl-CoA is then converted to malonyl-CoA [69]. This irreversible reaction is the committed step in fatty acid synthesis and is catalysed by the enzyme acetyl-CoA carboxylase (ACC). Acetyl-CoA and malonyl-CoA are then coupled to the substrate entry and condensation domain of the multifunctional fatty acid synthase (FAS) enzyme [75]. Repeated condensations and reduction generate a palmitoyl (C16) chain on the condensing domain, which is hydrolyzed to palmitate by the thioesterase on one of the two other catalytic domains within the FAS enzyme. Newly synthesized fatty acids (FA) can be converted into diacylglycerides (DAGs) and triacylglycerides (TAGs). DAGs and TAGs are formed when fatty acids are esterified to a glycolysis-derived glycerol backbone. TAGs are mainly used for energy storage in the form of lipid droplets. Intermediates of this pathway can also be converted into different phosphoglycerides, including phosphatidylcholine (PC), phosphatidylethanolamine (PE), phosphatidylglycerol (PG) and phosphatidylserine (PS), which build the major structural components of biological membranes [75].

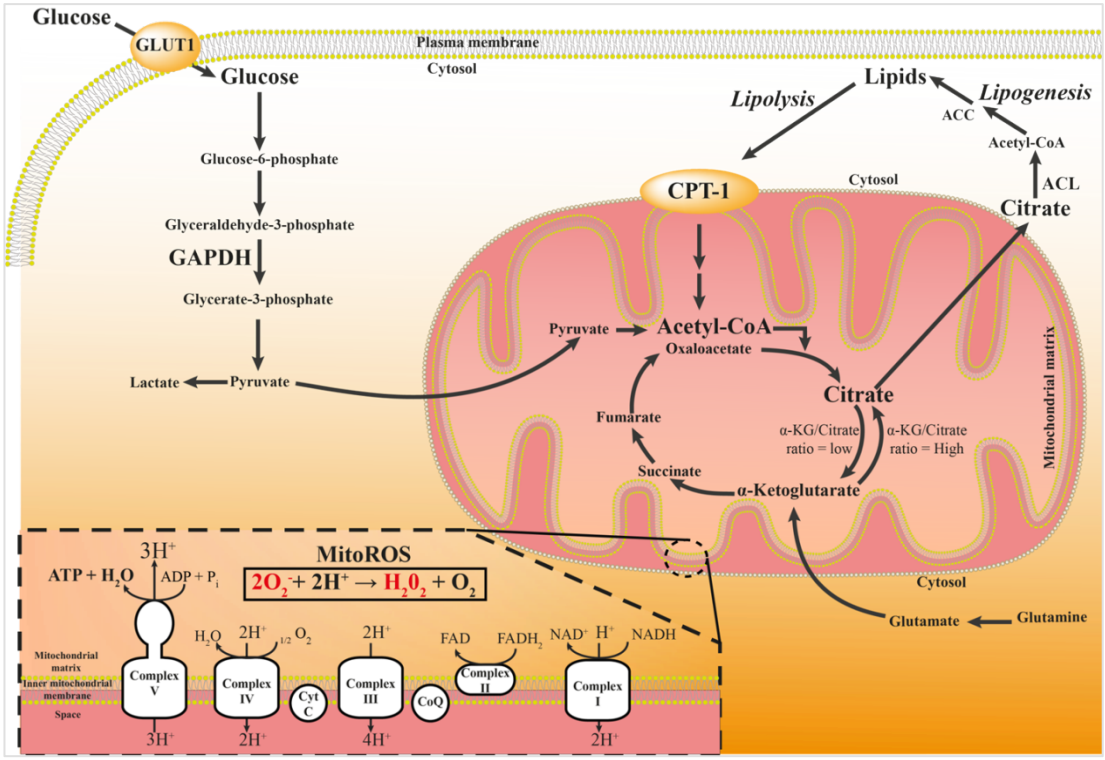

Figure 1.8: A schematic of glycolysis and de novo lipogenesis pathway

Glucose is transported into the cell via glucose transporter 1 (Glut1). Pyruvate is the end product of glycolysis and is used either to produce lactate or is shuttled into the mitochondria. Inside the mitochondria, pyruvate is either oxidized to AcCoA or converted to oxaloacetic acid (OAA) (anaplerosis). AcCoA and OAA together give rise to citrate, which enters the Krebs cycle. Citrate either continues with the next step in the Krebs cycle or leaves the mitochondria and is used by ATP-citrate lyase (ACL) in the cytosol to produce AcCoA and OAA. In the cytosol, AcCoA is carboxylated to malonyl-CoA by acetyl-CoA carboxylase (ACC) which subsequently results in lipid synthesis. Fatty acids can become available from the lipolysis of lipid droplets, converted to acyl-carnitine for transport into the mitochondria via the carnitine shuttle and used as fuel for β-oxidation. The Krebs cycle also generates NADH and FADH2, which donate electrons to the mitochondrial electron transport chain, which produces ROS. Abbreviations for the components of the schematic are ATP-citrate lyase; ACL, acetyl-CoA carboxylase; ACC, glucose transporter 1; GLUT1, Glyceraldehyde 3-phosphate dehydrogenase; GAPDH, Carnitine palmitoyltransferase I; CPT1, mitochondrial reactive oxygen species; mitoROS.

Glucose-dependent fluctuations in the acetyl-CoA pool availability for histone acetylation reactions influences epigenetic regulation of T cell fate and function. To prevent the depletion of the TCA cycle intermediates and disruption of mitochondrial function, rapidly proliferating cells utilise anaplerosis (the process of replenishing supplies of metabolic intermediates) to generate TCA cycle

intermediates to replace the carboxylic acids withdrawn for other synthetic routes. A key anaplerotic pathway is glutaminolysis; a metabolic shunt that converts glutamine into α-KG [76]. In addition to being a precursor for amino acid and nucleotide biosynthesis, glutamine is a key metabolite for supporting T cell function.

1.4.4. T cell activation-induced metabolic switch

TCR engagement induces a change in the expression of metabolic genes in order for cellular metabolism to meet the bioenergetic and biosynthetic needs of T cell activation. Cytokine receptors that are upregulated upon T cell activation further fine-tune the flux through the metabolic pathways that are integral for T cell effector functions [68].

Quiescent cells catabolize nutrients to generate ATP for anabolic reactions that maintain homeostasis and cell survival. Activated dynamic T cells uptake nutrients such as glucose and glutamine for ATP production and convert glucose-derived pyruvate into metabolite precursors for macromolecular biosynthesis required for cell division. In rapidly proliferating T cells the rates of glycolysis and mitochondrial OXPHOS are increased to satisfy the high anabolic demands [77].

The bias towards glycolysis over OXPHOS depends on the differentiation state of the T cell. Effector cells (Th1, Th2 and Th17) rely more on glycolysis whereas regulatory cells (Tregs) equally utilise glycolysis, fatty acid oxidation (FAO) and OXPHOS. Although glycolysis is the major energy generating pathway in activated effector T cells, mitochondrial OXPHOS is also required for *de novo* ATP production and to generate mitochondrial-derived reactive oxygen species (mitoROS). MitoROS is thought to function as “bioenergetic” second messengers and essential for T cell activation-induced IL-2 production [78].

1.4.5. Role of autophagy in T cell metabolism

Autophagy has been shown to be vital for the maintenance of cellular bioenergetics and sustained T cell viability following activation. Autophagy refers to the catabolic process that recycles cytoplasmic components such as cytosolic proteins and organelles, which get sequestered inside double-membrane vesicles called autophagosomes. These vesicles dock and fuse with lysosomes to generate

metabolites that can be used either as an energy source or as building blocks for macromolecular biosynthesis [79].

Autophagy initiation and progression requires the phosphorylation of Beclin-1 by UNC51-like kinase 1 (ULK1), which then activates the class III phosphoinositide 3-kinase VPS34 [80]. Beclin-1 and VPS34 together with p150, ATG14L, UVRAG and Rubicon form the class III phosphatidylinositol 3-kinase (PI(3)KC3) complex [81]. The activity of the PI(3)KC3 is vital for autophagy initiation and is tightly regulated. One of the modulators of autophagy is mTOR complex 1 (mTORC1) [81]. The activation of mTOR1 by anabolic inputs inhibits the activity of the ULK1 complex through direct phosphorylation, and autophagy is repressed. Conversely, ULK1 is directly phosphorylated by the AMP-activated protein kinase (AMPK) in response to energy restriction. Activated AMPK triggers autophagy by both inducing ULK1 and inhibiting mTOR [82]. In tumour cells, Akt activity can inhibit autophagy via mTORC1 activation. Akt can also directly phosphorylate Beclin-1 and increase its interactions with 14-3-3 regulatory proteins which then sequesters Beclin-1 from other core autophagy proteins and suppress autophagy [83].

During autophagy, a protein called Microtubule-associated protein 1A/1B-light chain 3 (LC3) is conjugated to phosphatidylethanolamine (PE) through two consecutive ubiquitylation-like reactions catalyzed by the E1-like enzyme Atg7 and the E2-like enzyme Atg3 to form LC3-II, which is recruited to the autophagosomal membrane. When the autophagosomes fuse with lysosomes, the intra-autophagosomal LC3-II is also degraded by lysosomal proteases [84]. Since changes in cellular LC3-II are proportional to the dynamic turnover of LC3-II via the lysosome, LC3-II is a marker for autophagy [85].

1.5. Targeting T cells for therapy

T cells play an important role in disease initiation and propagation through the secretion of a myriad of pro-inflammatory cytokines. The targeting of T-cell co-stimulatory/co-inhibitory receptors in the treatment of immune disorders (e.g. cancer, autoimmunity and infections) is a promising avenue. These therapies are largely based on T cell Immunomodulatory monoclonal antibodies (mAbs) that are either direct agonists or relieve T cell inhibitory signals [86]. At the same time, however, these mAbs can be associated with a risk of serious adverse effects, which include systemic induction of proinflammatory cytokines (cytokine release syndrome) and organ-specific autoimmunity, which arise from dysregulated activation of the T cells. These T-cell engaging biologics potentially alter cellular metabolism and the expression of stimulatory/inhibitory receptors. A detailed understanding of these altered parameters would be highly beneficial and aid our understanding of the safety profile of T cell modulatory mAbs in general.

1.5.1. Immunomodulatory monoclonal antibodies

The exquisite specificity and high avidity towards a target antigen has made antibody based therapeutic agents the most rapidly expanding class of biotherapeutics undergoing clinical evaluation and development for the treatment of cancers, autoimmune and inflammatory disorders. Antibodies, in addition to inducing immune mechanisms can act through multiple mechanisms of action such as inhibition of angiogenesis, blockage of receptors and signalling perturbations, restricts tumour growth e.g. EGF-R blocking antibodies, initiates G1 arrest and induces p27. Antibody therapy has revolutionized treatment for major disease indications e.g. leukaemia, lymphoma, colorectal cancer, breast cancer, melanoma, asthma, rheumatoid arthritis, psoriasis, multiple sclerosis, Crohn's disease, systemic lupus erythematosus and several other autoimmune diseases [87].

Antibodies (immunoglobulins, Ig) are protein molecules secreted by mature B lymphocytes which are vital mediators of the humoral immunity branch of the adaptive immune system. Antibodies produced by a single B cell clone are called monoclonal antibodies (mAbs) and have the ability to bind to a unique target antigen with high specificity and affinity. Antibodies function as nature’s pro-drugs,

being inactive in the soluble form but become activators of effector systems upon target antigen recognition. Antibodies are made up of different domains each with a particular function. The Fab portion of antibodies determine target specificity while the Fc portion binds to membrane Fc receptors (FcR) and is responsible for effector function [88]. Antibodies have key properties relevant to therapy and are different from conventional small molecule drugs in their unique biological activities, restricted tissues distribution and a common structural format. The clinical efficacy of therapeutic mAbs is generally attributed to the target-specific mechanisms resulting from (1) binding to soluble ligands such as cytokines and growth factors, (2) receptor antagonist activity by blocking dimerization, (3) triggering downstream signalling to reduce proliferation and apoptosis, and (4) target cell depletion through the induction of apoptosis or the activation of immune mediated effector functions such as antibody-dependent cell-mediated cytotoxicity (ADCC), antibody-dependent cellular phagocytosis (ADCP) and complement-dependent cytotoxicity (CDC) via interactions involving the Fc domain. Some therapeutic antibodies utilise a combination of several mechanisms of action [89].

1.5.2. Co-inhibitory receptors as mAb targets: PD-1 and LAG-3

T cell co-inhibitory receptors are dysregulated by the tumour microenvironment leading to a reduction in endogenous anti-tumour immunity. Antagonists of inhibitory signals can result in the amplification of antigen-specific T cell responses and increase anti-tumour immune responses. PD-1 is being considered as a viable target for therapeutic immunomodulation. $CD8^+$ T cell dysfunction brought about by chronic antigen stimulation (e.g. during lymphocytic choriomeningitis virus LCMV infection or tumours) has been shown in animal models to be partially reversed by blockage of the PD-1/PD-L1 pathway [90]. LAG-3 is also overexpressed in $CD8^+$ T cell exhaustion and the blockade of the LAG-3/MHC II interactions using LAG-3 Ig fusion protein enhances anti-tumour immunity and is being evaluated in a number of clinical trials. In addition to inducing T-cell co-inhibitory receptor expression, tumour cells secrete TGF-β into the microenvironment to render T cells hyporesponsive by inhibiting their effector functions. TGF-β antagonists can

significantly suppress tumorigenesis and greatly improves the efficacy of immunomodulatory chemotherapy in preclinical models [91].

1.5.3. Co-stimulatory receptor as mAb targets: CD28

TGN1412 was a humanised IgG4 anti-CD28 superagonistic mAb (CD28SA) withdrawn from development after a disastrous first-in-man trial in 2006. CD28SA is associated with a risk of serious adverse effects, which include systemic induction of proinflammatory cytokines (cytokine release syndrome) and organ-specific autoimmunity, which arise from dysregulated activation of the T cells [92]. Significant focus in recent times has been on assessing the potential of immunostimulatory mAbs to induce enhanced cytokine release, but much less attention has been paid to other aspects of T cell biology including non-physiological activation phenotype/functions and migration characteristics. In this thesis we study the activation parameters, migration capacity, degree of regulation, and metabolic profiles of CD28SA-activated T cells.

1.6. Rationale, hypothesis, strategy and aims

Rationale

Physiological activation of T cells is associated with downregulation of cell surface TCR, expression of adhesion molecules such as LFA-1, expression of chemokine receptors such as CCR5, synthesis of IL-2, T cell proliferation and expression of death receptors such as CD95, that help in contraction of the T cell immune response. The activation of T cells is regulated by the expression and function of co-inhibitory receptors such PD-1 and LAG-3, and by the presence of TGF-β in the microenvironment, which prevent excessive T cell activation by attenuating the activation signals initiated by T cell stimulatory receptors. Dysregulation in any of these parameters can result in substantial T cell proliferation and extravasation of T cells, and highly elevated secretion of a number of pro-inflammatory cytokines. Since specific effector functions require specific metabolic pathways to provide energy and biosynthetic precursors, dysregulated effector functions stem from metabolic dysregulation.

Aims

1. To elucidate the underlying cellular and molecular events that result in aberrant activation of human T cells by CD28SA.
2. To determine the metabolic program of CD28SA-activated and anti-CD3-activated human T cells
3. To define the role of oxidative stress in TGF-β-associated functional and metabolic alterations in TCR-activated mouse T cells

Hypotheses tested in this study

1. Activation of T cells with TGN1412-like CD28SA results in a hyperactive phenotype with uninhibited effector functions. ***We hypothesised that CD28SA-activated T cells acquire a proactivatory phenotypic profile with increased functional activities and deficiency in inhibitory inputs.***

   Experimental strategy: We used a humanized CD28-specific superagonistic (CD28SA) mAb called NIB1412 to stimulate human $CD4^+$ T cells and compared this to activation with conventional anti-CD3 mAbs.
2. CD28SA activation results in dramatic hyperactivation and proliferation, which requires an altered metabolic program to satisfy the energy demands. ***We postulated that the phenotypic and functional characteristics of T cells activated with CD28SA are associated with a distinct metabolic profile.***

   Experimental strategy: We used NIB1412 and conventional anti-CD3 mAbs to stimulate human $CD4^+$ T cells, and compared their metabolic parameters following activation.
3. Antigen-specific activation of T cells in the presence of TGF-β results in deficient proliferation and reduced effector functions. Since studies have found that TGF-β triggers ROS, ***we hypothesised that antioxidant supplementation following T cell activation restores the phenotypic and functional activities, and the metabolic profile of T cells that are exposed to inhibitory inputs by TGF-β.***

   Experimental strategy: We used an ex vivo antigen-specific $CD8^+$ T cell mouse model (transgenic F5-TCR mouse model) to examine effector of TGF-β-exposed antigen-activated T cells.

Chapter TWO

Methods and Materials

2. Methods and Materials

2.1. Reagents

All reagents were obtained from Sigma-Aldrich unless otherwise stated.

2.2. Complete medium

Roswell Park Memorial Institute-1640 (RPMI-1640) medium was supplemented with 10% FBS, 50 µM 2-ME, 2 mM HEPES buffer, 1 mM sodium pyruvate, 2 mM L-glutamine, 100 IU/ ml streptomycin and 100 µg/ ml penicillin

2.3. Human T cell isolation

Ethical approval for the use of human peripheral blood mononuclear cells (PBMCs) from healthy donors was approved by the local ethical committee and all subjects provided informed consent. PBMCs were isolated from heparinised venous blood by density gradient separation using Lymphoprep as described by Böyum [93] (Axis-Shield, cat # O7811). The effector memory $CD4^+$ T cell (T_{EM}) isolation kit (Miltenyi Biotec, cat # 130-094-125) was used to purify T_{EMs} from PBMCs according to manufacturer's instructions.

2.4. Mouse T cells and dendritic cells

C57BL/6 mice homozygous for the H-2Db-restricted TCR-αβ transgene, F5, which recognises NP-68 [94], a nonameric peptide derived from influenza virus A/NT/60/68 nucleoprotein were a kind gift from Dr James Matthews [Cardiff; Wales]. Mice were housed under controlled conditions (temperature of between 19°C - 23°C under 12 h light/dark cycles, with free access to food and water) at the Biomedical Services Unit, University of Liverpool. All animals were bred under pathogen free conditions. Protocols described herein were undertaken in accordance with criteria outlined in licenses granted under the Animals (Scientific Procedures) Act 1986 (PPL 40/2937 and PPL 40/2544) and approved by the Animal Ethics Committee of the University of Liverpool. The NP68 peptide (^{366}ASNENMDAM^{374}) used to stimulate F5 CD8 T cells was synthesised by Peptide Protein Research Ltd [Hampshire, UK].

For the generation of mature DCs, bone marrow cells were flushed from femora of wild type mice. Cells were washed and cultured at a density of 3x 10^6 cells/microbiological petri dish in complete medium supplemented with 20ng/ml GM-CSF and kept in a fully humidified incubator at 37°C under 5% CO_2. Media was then replenished on day 3 supplemented with 20ng/ml GM-CSF and differentiated DCs were used between days 6 or 7. Spleens were isolated from F5 TCR transgenic mice and homogenised using Jencons Uniform Grade B-24 Tissue Homogeniser [Jencons Scientific Ltd., Leighton Buzzard, UK] and then filtered through 40 µm gauge Nylon Cell Strainers [Falcon, UK]. Splenocytes were washed in HBSS and centrifuged at 300 g for 5 minutes. Pelleted cells were treated with red blood cell (RBC) lysis buffer (8.3 g/L ammonium chloride in 0.01 M Tris-HCl buffer) for 6 minutes at room temperature to remove red blood cells. Following a final wash/centrifugation cycle lymphocytes were re-suspended in complete medium.

F5-TCR T cells were activated according to the scheme below (figure 2.1).

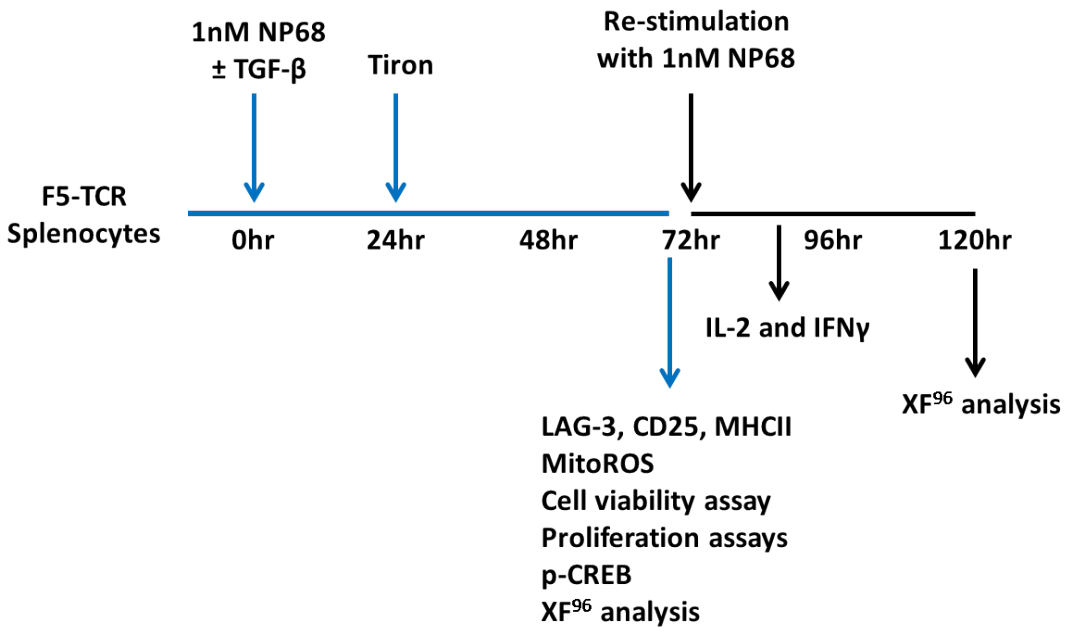

Figure 2.1: schematic outline of the experimental procedures used in Chapter 5

Splenocytes derived from F5-TCR mice were subjected to primary stimulation with NP68 ± TGF-β. Tiron (Sigma, cat# 89460) was added 24hrs later as mitoROS produced upon TCR stimulation is essential for T cell expansion. At 72hrs cells were either re-stimulated with 1nM NP68 (DCs pre-pulsed with NP68 was used for IFN-γ ELISpot) or harvested for the respective assays. Re-stimulated cells were used for three assays: staining with fluorochrome-conjugated IL-2/ IFN-γ after 6 hours followed by flow cytometric analysis, IFN-γ producing cells were measured by ELISpot after 16h stimulation with NP68-pulsed DCs ± anti-LAG-3, and metabolic measurements after 48hrs using Seahorse XF analyzer.

2.5. Human endothelial cell culture

Human dermal microvascular endothelial cells (HDMEC) were purchased from Promocell and were cultured in endothelial cell basal media (EBM) MV2 growth media (C-22221; Promocell), supplemented with 5% (v/v) fetal calf serum (FCS) and EGF (5 ng/ml), VEGF (0.5 ng/ml), FGF-2 (10 ng/ml), long R3 insulin growth factor-1 (20 ng/ml), hydrocortisone (0.2 µg/ml) and ascorbic acid (1 µg/ml) (supplement pack C-39221; Promocell).

2.6. Stimulating antibodies and recombinant proteins

Humanized superagonistic anti-CD28 antibody NIB1412, a human IgG4 sharing the H chain V region and L chain sequences of TGN1412 [95], was generated at the

National Institute for Biological Standards and Control (NIBSC). Murine anti-human CD3 (clone: UCHT1, cat # 16-0038-85) antibody was purchased from eBioscience. The cross-linking goat anti-human IgG (Fc) secondary antibody was purchased from AbD Serotec (cat # 5211-8004). Recombinant PD-L1 was purchased from R&D Systems (cat # 156-B7-100). For mouse F5-TCR work, anti-LAG-3 blocking antibody (C9B7W, cat# 16-2231-85) was purchased from eBioscience Ltd, and recombinant TGF-β (HEK293 derived, cat# 100-21) and IL-2 (E.coli derived, cat# 200-02) were purchased from Peprotech EC Ltd.

2.7. T cell proliferation assays

96-well round-bottom non-tissue culture treated plates were coated with stimulating antibodies at 37°C for 2 hours. Plates were washed twice to remove unbound antibody before addition of T cells. Where NIB1412 was used, the wells were pre-coated with cross-linking goat anti-human IgG (Fc) mAb anti-IgG mAb (20μg/ml). For the F5 CD8 T cell proliferation assay, isolated splenocytes from F5-TCR mice were plated out in quadruplicate at a density of 1 x 10^5 cells/ well in 96-well round-bottom microtitre plates and activated with NP68 or DCs pre-pulsed with NP68 (In a 20:1, T-cell to DC ratio).

T cells were cultured in complete media (RPMI 1640 supplemented with 15% foetal calf serum (Life Technologies), 2 mM L-glutamine, 50 U ml^{-1} penicillin and 0.05 mg ml^{-1} streptomycin) for 72 h (at 37 °C) in either normoxic (20% O_2) or hypoxic (5% O_2) conditions, and 18 hours before the end of the time point, the cells were pulsed with tritiated thymidine ([^{3}H]-TdR, 0.5 μCi/well). Incorporation of [^{3}H]-TdR in T cells was determined using a β-scintillation counter (MicroBetaTrilux; PerkinElmer Life Sciences,). Data obtained are presented as mean counts per minute (cpm).

2.8. Cell viability assay

Briefly, $CD4^+$ T_{EM} were plated in base media with L-glutamine ± glucose at a density of 5 × 10^4 cells/well in 96-well plates pre-coated with anti-CD3 mAbs or NIB1412.

For the mouse F5-TCR CD8 T cell viability assay, cells were activated with NP68 ± TGF-β at a density of 5 × 10^4 cells/well in 96-well plates. Following overnight incubation at 37°C, each sample was collected and assayed for cell viability using

trypan blue exclusion. Percentage viability was determined by the Countess™ automated cell counter.

2.9. Flow cytometric analysis

T cells were stained for 20 minutes at 4°C. The following fluorochrome conjugated antibodies (eBioscience Ltd,) diluted to the optimal concentration were used for human work: anti–CD4 PerCP-Cyanine5.5 (RPA-T4, cat # 45-0049-42), anti–PD-1-PE (J105, cat # 12-2799-42), anti–CD11a-FITC (HI111, cat # 11-0119-42), anti-CCR5-PE (NP-6G4, cat # 12-1956-42), anti–TCR-APC (IP26, cat # 17-9986-42), anti-CD28-APC (CD28.2, cat# 17-0289-41), anti-CXCR4-APC (12G5, cat# 17-9999-41), anti-CD137-FITC (4B4, cat# 11-1379-42), anti-GITR-PE (eBioAITR, cat# 12-5875-41), anti-CD27-FITC (O323, cat# 11-0279-41), anti-CD80-FITC (2D10.4, cat# 11-0809-41), anti-HLA-DR-FITC (LN3, cat# 11-9956-42) and anti–IFNγ-APC (4S.B3, cat # 17-7319-82). For mouse T cells cell surface staining was done with the following fluorochrome conjugated antibodies: TRI-COLOUR® conjugated anti-mouse CD8 (5H10, cat# MCD0806) and Alexa Fluor® 488 conjugated anti-mouse CD25 (PC61 5.3, cat# RM6020) were purchased from Invitrogen [Paisley, UK], PE-conjugated anti-mouse I-A/I-E (M5/114.15.2, cat# 562010), FITC-conjugated anti-mouse IL-2 (JES6-5H4, cat# 554427) and FITC-conjugated anti-mouse IFN-γ (XMG1.2, cat# 554411) were purchased from BD Bioscience Ltd, and anti-LAG-3-PE (C9B7W, cat# 12-2231-83) was purchased from eBioscience Ltd. For intracellular staining, surface markers were stained first, followed by permeabilization using Cytofix/Cytoperm (BD Pharmingen, cat # 555028) and stained with anti–IFNγ-APC or anti–PD-1-PE for human cells, and for mouse cells with anti-IL-2 FITC or anti- IFN-γ-FITC. To quantify mitochondrial superoxide production, cells were incubated with MitoSOX Red (Invitrogen, cat# M36008) at 37°C for 10 minutes, washed and fixed in 2% paraformaldehyde. MitoSOX Red was excited at 488 nm and fluorescence emission at 575 nm was measured. Fluorescent signals from cells were acquired on BD FACS Canto II flow cytometer and data were analysed using Cyflogic software v. 1.2.1.

2.10. IFNγ ELISpot assay

Mouse IFN-γ ELISpot kit (MABTECH, cat# 3321-2A) was used to enumerate IFN-γ-secreting cells according to manufacturer's instructions. Briefly, ELISpot plates were

washed and coated overnight at 4˚C with IFN-γ capture antibody (15µg/ml). The following day, wells were washed five times with 200µl sterile PBS and blocked with complete medium for 30mins at room temperature. Medium was removed and F5-TCR mouse T cells ($2x10^4$, 100µl) were added to the wells with DCs pre-pulsed with 1nM NP68 as APCs ($1x10^3$, 50µl) in the presence or absence of LAG-3 blocking antibody (5µg/ml, 50µl). Plates were incubated at 37˚C in 5% CO2 for 48hours, after which cells were discarded and wells washed five times with 200µl PBS. Biotin-labelled detection antibody was diluted to 1µg/ml in PBS containing 0.5% FBS and added to the wells (100µl), and incubated at room temperature for 2 hours. Wells were then washed five times with PBS and 100µl of Streptavidin-ALP (diluted 1:1000 in PBS containing 0.5% FBS) was added and incubated at room temperature for 1hour. Wells were washed five times with PBS (200µl) and spots were visualised by the addition of 100µl BCIP/NBT substrate. Dried plates were counted on an AID ELISpot reader (Cadama Medical, Stourbridge,UK).

2.11. Re-stimulation assay using rPD-L1

Isolated T cells were stimulated and cultured as described above for 48 hours and re-stimulated in a 96-well round-bottom non-tissue culture treated plate pre-coated with 1 µg/ml anti-CD3, 10 µg/ml rPD-L1 and the combination of 1 µg/ml anti-CD3 + 10 µg/ml rPD-L1. Cells were incubated at 37°C for one hour after which Golgi plug was added and incubated for another 5 hours (figure 2.2). Intracellular IFNγ staining was then performed and cells were analysed using flow cytometry as described above.

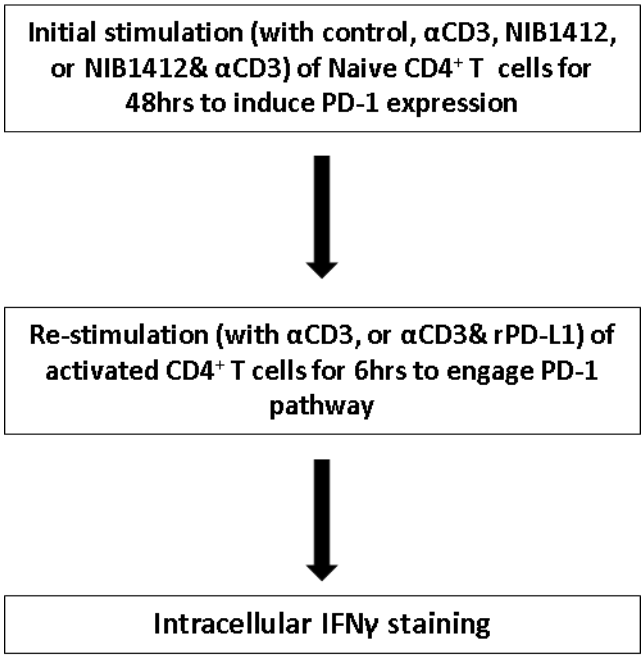

Figure 2.2: Schematic of the protocol used to investigate the functional significance of PD-1 pathway on NIB1412-activated $CD4^+$ T cells.

2.12. Cell cycle analysis

Cells stimulated and cultured as described above were collected at the end of each time point, fixed in ice-cold 70% ethanol and kept at 4°C until analysis. Fixed cells were washed and treated with RNase for 20 minutes. Subsequently, 5 μg/mL of propidium iodide and 0.1% Triton-X were added for 15 mins and analysed by flow cytometry.

2.13. Measurement of IL-2

IL-2 levels in culture supernatants were determined by enzyme-linked immunosorbent assay (ELISA) using the Human Ready-SET-Go! ELISA kit from eBioscience Ltd (cat # 88-7025-22) following manufacturer's instructions.

2.14. Gel Electrophoresis and Western Immunoblotting

Cells were lysed with RIPA buffer (150 mM NaCl, 1.0% IGEPAL® CA-630, 0.5% sodium deoxycholate, 0.1% SDS, and 50 mM Tris, pH 8.0) with 1 mM PMSF and protease inhibitor cocktail. 10-20 μg of protein lysate were mixed with 5 μL loading buffer (70% (v/v) NuPAGE sample loading buffer, 30% (v/v) NuPAGE reducing agent) and denatured by incubating at 90°C for 5mins. Samples and PrecisionPlus protein Kaleidoscope standards were loaded onto NuPAGE Novex bis-tris polyacrylamide

gels and resolved by electrophoresis in a XCell Surelock mini-cell (Invitrogen), using a 3-(N-morpholino) propanesulphonic acid (MOPS) running buffer (50 mM MOPS, 50 mM Tris base, 3.5 mM sodium dodecyl sulphate, 1mM EDTA, 0.25% (v/v) NuPAGE antioxidant), at 90 Volts for 10 minutes, followed by 60 minutes at 170 Volts. The resolved proteins were transferred to polyvinylidene difluoride (PVDF) membranes (BioRad) at at 200 mA for 90 minutes. PVDF membranes were then blocked with tris-buffered saline (TBS; 150 mM NaCl, 50 mM Tris base, pH 7.6) containing 0.1% (v/v) Tween-20 and 10% (weight/volume; w/v) non-fat dry milk at room temperature for 1hour. Washing steps between were done with TBS-0.1% Tween-20. Membranes were probed overnight at 4°C with the following primary antibodies (at 1:1000): anti-pPTEN (phospho S380+ T382+T383) antibody (Abcam, cat # ab131107) and anti-casein kinase IIα (1AD9) (Santa Cruz Biotechnology, cat # sc-12738), or anti-LC3 (MBL, cat# M152-3), anti-CREB (phospho Ser133) (CST, #9198), anti-ATP-Citrate Lyase (phospho S455) (CST; #4331) and anti-Acetyl Coenzyme A Carboxylase (phospho S79) (Abcam; ab68191), diluted at optimal concentrations in TBS-0.1% Tween-20 containing 2% (w/v) BSA, and followed by appropriate horseradish peroxidase-conjugated secondary antibodies (1:20000) (CST, UK). Immunoblots were visualized using the ECL system (PerkinElmer Life Sciences, UK).

Densitometry was performed using a GS-710 calibrated imaging densitometer (BioRad) and quantification of immunoreactive bands using TotalLab 100 software, normalised to total protein.

2.15. Real-time RT-PCR

Total RNA was extracted from cells and purified using RNeasy Mini Kit from QIAGEN kit, according to the manufacturer's instructions. cDNA was synthesized using ImProm-II^{Tm} Reverse Transcription System Promega kit according to the manufacturer's instructions. Primers were designed to amplify the entire coding sequence of CTLA-4: 5'-ATGGCTTGCCTTGGATTTCAGCGGCACAAGG-3' and 5'-TCAATTGATGGGAATAAAATAAGGCTGAAATTGC-3', and PD-1: 5'-CTCAGGGTGACAGAGAGAAG-3' and 5'-GACACCAACCACCAGGGTTT-3'. Real-time quantitative PCR (qRT-PCR) analysis of PD1, CTLA-4 and GAPDH genes were

performed on an ABI PRISM 7000 real-time PCR instrument using Applied Biosystems (UK) SYBR green PCR master mix. The GAPDH level was used as a normalization control.

2.16. Static adhesion and transendothelial migration of T_{EMs}

Isolated T_{EMs} were stimulated with 5 µg/ml anti-CD3, 10µg/ml NIB1412 and the CD3+NIB1412 as described above and harvested after 48hours. Cells were then centrifuged and after the supernatant was discarded, cells were treated with pre-warmed CellTracker™ Green CMFDA (Molecular Probes) working solution (1 µM). Following an incubation period at 37°C for 30mins, cells were centrifuged and the CellTracker™ working solution was discarded. Labelled cells were re-suspended in complete media and added to the HDMEC layer as described below.

For the adhesion assay HDMECs were seeded on gelatin-coated 96-well tissue culture plates (Nunc) in endothelial cell media for 48 hours, while for the transendothelial migration assay HDMECs were seeded on gelatin-coated Transwell inserts [6.5mm diameter, 3.0µm polyester membrane; Corning Costar; Pittston, PA, USA]. Media was then changed to 1% (v/v) FCS containing media for 24 hours. For the adhesion assay the CMFDA-labelled T_{EMs} (0.2 mL, 5×10^5 cells/mL) were added to the confluent HDMECs and incubated for 30 minutes. After washing three times with PBS (0.2 mL), adherent cells in three randomly selected optical fields per well were visualized and counted. For immunofluorescence imaging, samples were fixed in 4% formaldehyde for 30 min and following a washing step stained with rhodamine phalloidin and DAPI (Molecular Probes) overnight at 4°C and subsequently washed three times with PBS. Images were acquired using a Axio Observer Zeiss microscope with objective LD "Plan-Neofluar" 20x/0.4 Corr Ph2 M27, and analysed with ZEN Pro 2012 software.

For the transendothelial cell migration assay, CMFDA-labelled T_{Ems} (1×10^5 cells/insert) were added to the confluent HDMECs and incubated for 12 hours. Cells in the lower compartment were collected and fluorescence was quantified using a Varioskan™ Flash Multimode Plate Reader (Thermo Scientific, Waltham, MA).

2.17. Bioenergetics of T cells

$CD4^+$ T_{EM} were stimulated with plate-bound anti-CD3 mAb or NIB1412 for 48 h in complete media, while mouse F5-TCR CD8 T cells were activated with NP68 for 72h. Cells were then re-suspended in serum-free base media (Seahorse Bioscience; 102353-100) with 2 mM L-glutamine ± 1mM sodium pyruvate ± 25 mM glucose. Subsequently cells were seeded in pre-coated Poly-D Lysine (50 µg/ml) XF 96-well microplates (Seahorse Bioscience) at 3×10^5 cells per well, spun down, and inoculated at 37°C for 30mins. Bioenergetics of $CD4^+$ T_{EM} and F5-TCR $CD8^+$ T cells were determined using the XF Cell Mito Stress Test Kit (Seahorse Bioscience; 103015-100) (figure 2.3), XF Glycolysis Stress Test Kit (Seahorse Bioscience; 102194-100) (figure 2.4) and a XFe^{96} Analyzer (Seahorse Bioscience). For the XF Cell Mito Stress Test Kit the drug injections ports of the XF96 Assay Cartridge were loaded with 1 µM Oligomycin in port A, 160 µM 2,4-DNP in port B, and 1 µM of both Antimycin A and Rotenone in port C. For the XF Glycolysis Stress Test Kit, the culture media was replaced with glucose-free media and all ports were loaded with 10mM of glucose in port A, 1 µM Oligomycin in port B and 100mM of 2-deoxy-D-glucose (2-DG) in port C. Seahorse experiments were done using the following assay conditions: (2 min MIX TIME, 2 min WAIT TIME and 4 to 5 min MEASURE TIME).

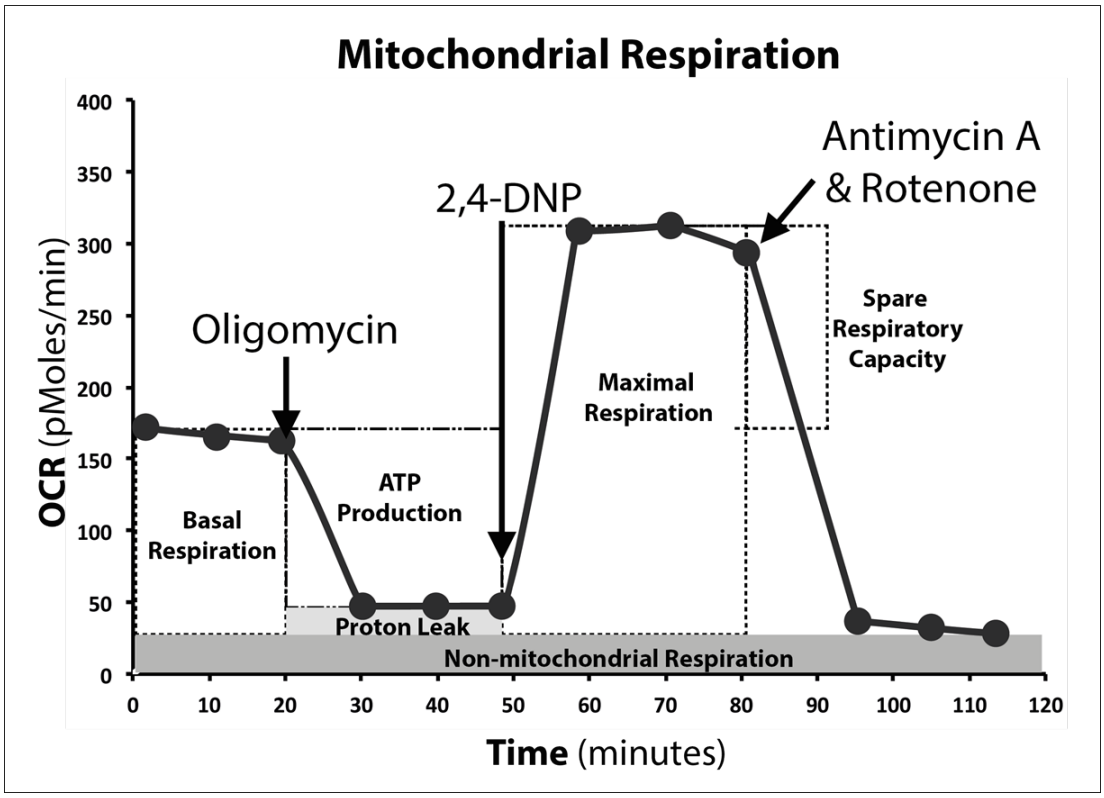

Figure 2.3: Changes in oxygen consumption rates (OCR) during the sequential delivery of drugs

Following the measurement of basal respiration, Oligomycin was injected to inhibit ATP-synthase in order to measure the oxygen consumed for ATP production during mitochondrial respiration-coupled oxidative phosphorylation of ADP. The addition of the uncoupling agent 2, 4-DNP enabled measurement of the maximal respiratory capacity of the cells. The final injection of rotenone and antimycin A (R&A) blocked the electron transport chain leaving non-mitochondrial oxygen consumption.

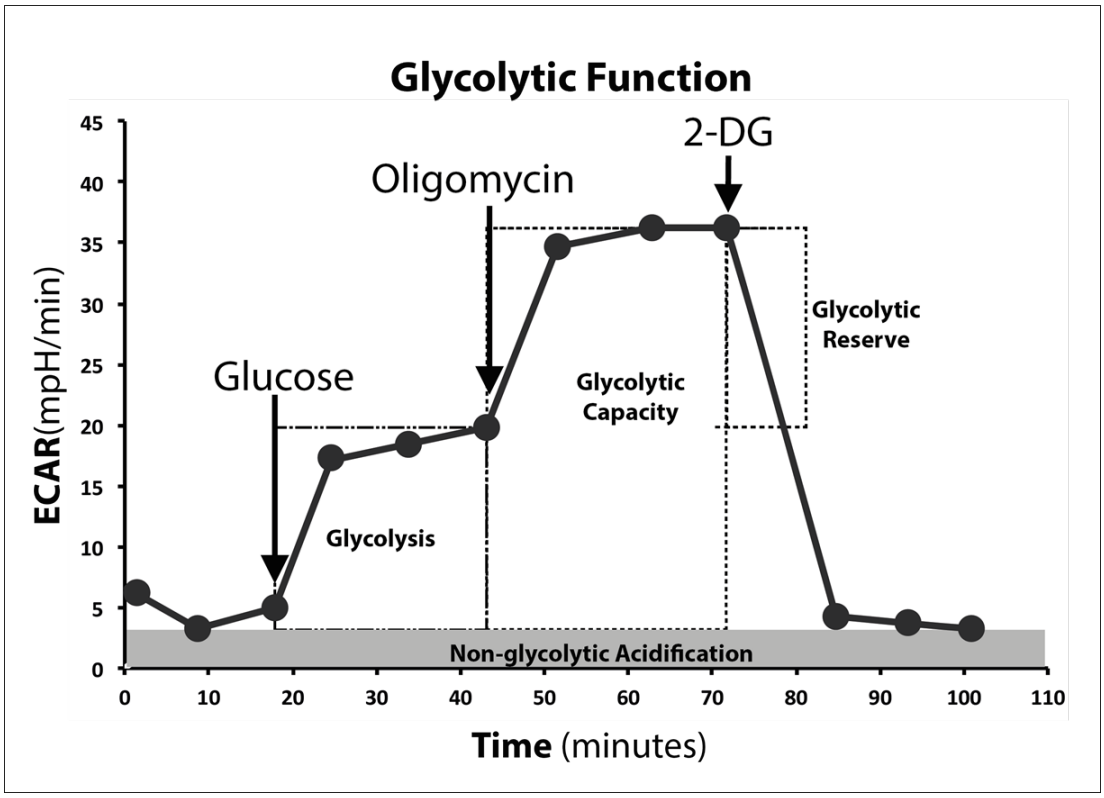

Figure 2.4: Changes in extracellular acidification rate (ECAR) during the sequential delivery of drugs

Glycolysis and the glycolytic reserve of cells were measured by the sequential addition of glucose, Oligomycin and 2-D-glucose (2-DG). The ECAR after glucose injection is the basal rate of glycolysis, while the addition of Oligomycin inhibits mitochondrial ATP production and shifts energy production predominantly to the glycolytic pathway, revealing the maximum glycolytic capacity of the cells. The difference between the glycolytic capacity and the glycolytic rate revealed the glycolytic reserve.

2.18. Acetyl-CoA measurement

Concentration of acetyl-CoA in whole-cell lysates (lysed in RIPA buffer) from pre-activated $CD4^+$ T_{EM} was measured by fluorescence assay using a commercial kit according to the manufacturer's instructions (Abcam; PicoProbe Acetyl CoA Assay kit: ab87546). Fluorescence was quantified using a Varioskan™ Flash Multimode Plate Reader (Thermo Scientific, UK).

2.19. Citrate and alpha-ketoglutarate measurement

Concentration of Citrate and α-ketoglutarate in whole-cell lysates (lysed in RIPA buffer) from pre-activated $CD4^+$ T_{EM} was measured by fluorescence assay using a commercial kit according to the manufacturer's instructions (Abcam; Citrate assay kit: ab83396, Alpha Ketoglutarate (alpha KG) Assay Kit: ab83431). Relative

fluorescence units / intenstiy were quantified using a Varioskan™ Flash Multimode Plate Reader (Thermo Scientific, UK).

2.20. Statistical analysis

Unpaired t-test was used to analyse proliferation, adhesion, transendothelial migration, phospho-PTEN and Ck2 densitometric data and results presented as mean ± SD/SEM. Two-way ANOVA followed by Bonferroni test was used to analyse IL-2 ELISA data using GraphPad Prism 5 (GraphPad Software Inc, San Diego, CA). p values of <0.05 were considered to be statistically significant.

Chapter THREE

Failure to upregulate cell surface PD-1 is associated with dysregulated stimulation of T cells by TGN1412-like CD28 superagonist

3. Failure to upregulate cell surface PD-1 is associated with dysregulated stimulation of T cells by TGN1412-like CD28 superagonist

3.1. Abstract

The CD28 superagonist (CD28SA), TGN1412 was administered to humans as an agent that can selectively activate and expand regulatory T cells but resulted in uncontrolled T cell activation accompanied by cytokine storm. The molecular mechanisms that underlie this uncontrolled T cell activation are unclear. Physiological activation of T cells leads to upregulation of not only activation molecules but also inhibitory receptors such as PD-1. The uncontrolled activation of CD28SA-stimulated T cells was hypothesised to be caused by both the enhanced expression of activation molecules and the lack of or reduced inhibitory signals. In this study, anti-CD3 antibody-stimulated human T cells were shown to undergo time-limited controlled DNA synthesis, proliferation and interleukin-2 secretion, accompanied by PD-1 expression. In contrast, CD28SA activated T cells demonstrate uncontrolled activation parameters including enhanced expression of LFA-1 and CCR5 but fail to express PD-1. The functional relevance of the lack of PD-1 mediated regulatory mechanism in CD28SA-stimulated T cells was demonstrated. The findings provide a molecular explanation for the dysregulated activation of CD28SA-stimulated T cells and also highlight the potential for the use of differential expression of PD-1 as a biomarker of safety for T cell immunostimulatory biologics.

3.2. Introduction

Immunostimulatory antibodies are in clinical trials for a variety of indications, [86] particularly in eliciting anti-tumour responses but they come with a risk of serious adverse effects such as systemic induction of pro-inflammatory cytokines (cytokine storm) and organ-specific autoimmunity [96]. In 2006, a phase I first-in-man dose-escalation trial of TGN1412, a humanized CD28-specific superagonistic mAb originally intended for the treatment of B cell chronic lymphocytic leukaemia and rheumatoid arthritis, caused severe immune-mediated toxicity in a cohort of healthy volunteers [92]. The unforeseen biological action in humans included

substantial proliferation and extravasation of T cells, and a life-threatening cytokine storm with highly elevated levels of various pro-inflammatory cytokines [97].

Physiological T cell activation occurs when the T cell receptor (TCR) is engaged by an antigen-bearing MHC molecule on the surface of antigen presenting cells (APCs) and this represents the first signal for T cell activation. Co-stimulatory receptors such as CD28 can act as secondary signals to amplify this first signal. In general, CD28 ligation in the absence of TCR engagement has no functional effect on T cells; however, CD28SA antibodies can activate T cells without concomitant TCR engagement [16].

Activation of T cells through TCR triggering and CD28 engagement leads to downregulation of cell surface TCR, expression of molecules such as lymphocyte function-associated antigen-1 (LFA-1) and C-C chemokine receptor type 5 (CCR5), synthesis of interleukin (IL)-2 and T cell proliferation. Importantly, the activation of T cells is regulated by the expression and function of co-inhibitory receptors such as PD-1, TIM-3, LAG-3 and CTLA-4 [11]. These co-inhibitory receptors prevent excessive T cell activation by attenuating the activation signals initiated by T cell stimulatory receptors [98]. The PD-1 co-inhibitory receptor has been shown to be a powerful negative regulator of activated T cells [26]. In the absence of PD-1-mediated signals, there is an increased propensity for T cells to expand with stronger accompanying inflammatory cascades [99]. It remains unknown whether the excessive T cell activation observed with CD28SA-stimulated T cells is a result of dysregulated inhibitory inputs to these T cells. We hypothesized that a lack of inhibitory inputs from the PD-1 pathway could contribute to the uncontrolled proliferation and cytokine release of CD28SA-activated T cells. In this study, we characterized the dysregulated T cell phenotype and function of CD28SA activated T cells.

3.3. Results

3.3.1. Dysregulated T cell function induced by CD28SA stimulation

Ligation of the TCR/CD3 complex activates T cells and co-engagement of CD28 with TCR/CD3 enhances this response, while in general, ligation of CD28 in isolation with conventional monoclonal antibodies does not stimulate T cells. To assess the effects of CD28SA-mediated T cell stimulation, we activated human T cells with either NIB1412 (CD28SA), or anti-CD3.

Previous studies have identified $CD4^+$ effector memory T cells (T_{EMs}) as the primary responders to CD28SA stimulation, [100] [101] and therefore we mainly focussed on T_{EMs} for phenotypic and functional assessments. Phosphorylation of the TCR/CD3 complex upon T cell activation results in a rapid downregulation of the complex, [102] to allow for the desensitization of the stimulated cell. We have shown that NIB1412-activated T_{EMs} maintain elevated TCR expression levels of up to 80%, similar to that of unstimulated cells, while anti-CD3 stimulated T_{EMs} rapidly reduce TCR expression upon activation and maintain negligible surface expression throughout day 1 to 4 (Figure 3.1).

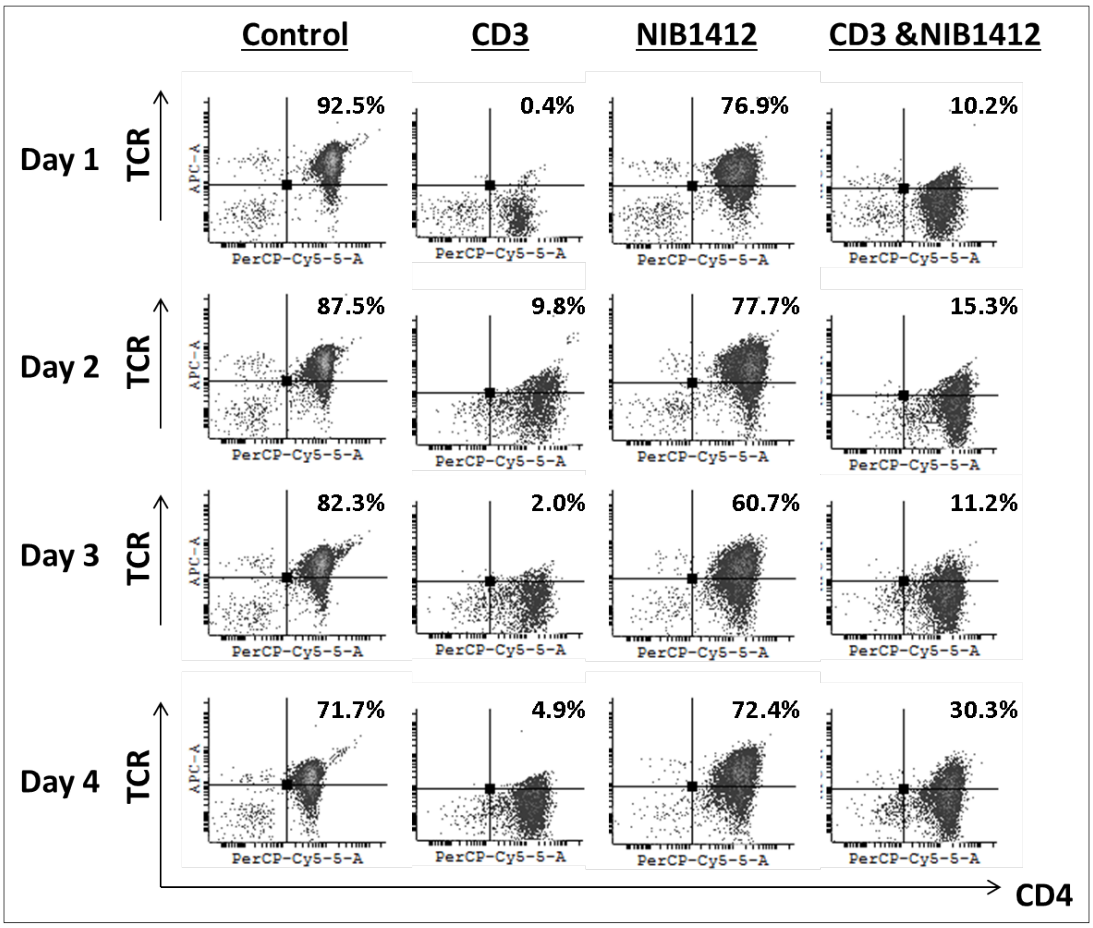

Figure 3.1: Elevated TCR expression in NIB1412-activared T_{EMS}

Human $CD4^+$ T_{EM} were stimulated for 1 to 4 days with plate-bound anti-CD3 mAb (CD3, 5 µg/ml); NIB1412 (NIB1412, 10 µg/ml); anti-CD3 mAb and NIB1412 (CD3 & NIB1412); control category included cells without any treatment (Control). Cells were harvested at indicated time points and stained with fluorochrome-conjugated anti-CD4 and anti-TCR antibodies followed by flow cytometric analysis. Populations of $CD4^+TCR^+$ cells are shown in the upper right quadrant as percentages of total T cells. Results are representative of four independent experiments.

Our results also show that NIB1412-stimulated T_{EM} cells showed greater proliferation at antibody concentrations of 2.5. 5 and 10 µg/ml and displayed a higher maximum proliferative capacity compared to anti-CD3-stimulated T cells (figure 3.2), and also express lower levels of the prototypical death receptor Fas (CD95) (Figure 3.3).

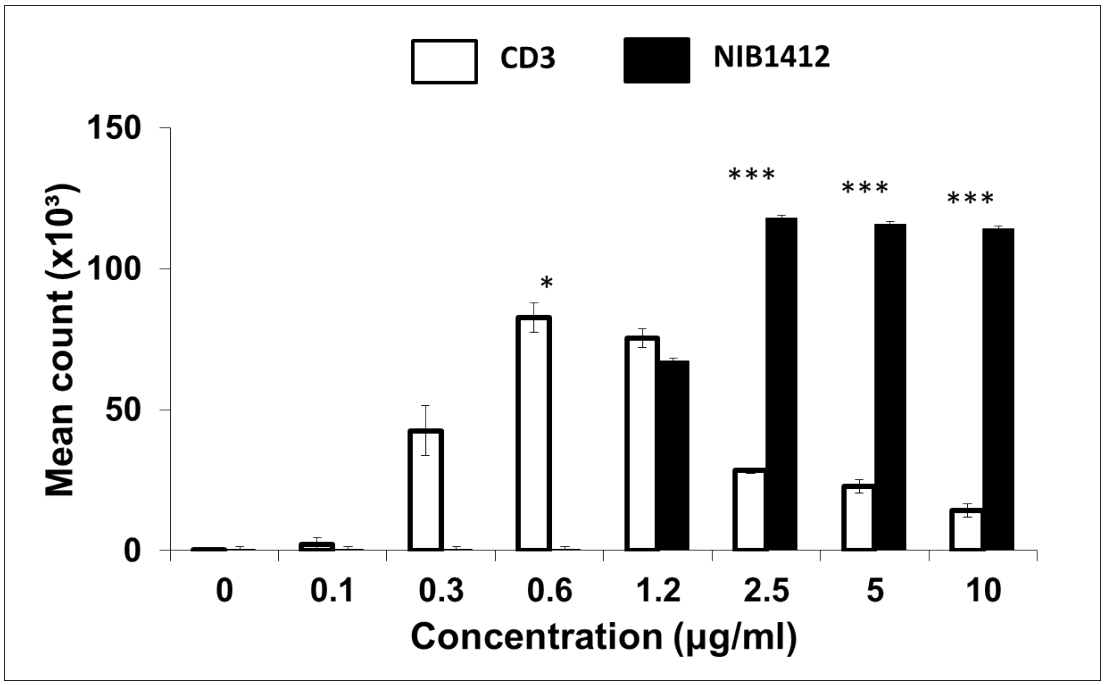

Figure 3.2: Higher proliferative capacity of NIB1412-stimulated T_{EMS}

Human $CD4^+$ T_{EM} cells were stimulated with the indicated concentrations of plate-bound antibodies and proliferation was measured three days post-activation by ^3H-labeled thymidine incorporation. The vertical axis represents mean cpm ± SD from triplicate wells. The data are representative of four independent experiments, (*$p < 0.05$, ***$p < 0.001$; unpaired t-test).

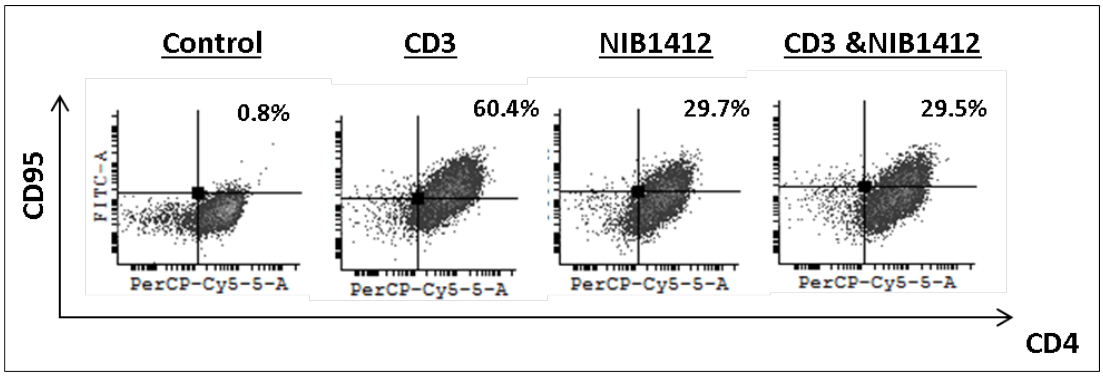

Figure 3.3: Reduced CD95 receptor expression on NIB1412-stimulated T_{EMS}

Cell surface staining of human $CD4^+$ T_{EM} stimulated for 4days with 5µg/ml of plate-bound anti-CD3 mAb and/or 10µg/ml of NIB1412. The percentages of the $CD4^+$ $CD95^+$ cells are shown in the upper right quadrant. Results are representative of three independent experiments

To better understand the proliferative activity of stimulated T_{EMs}, we determined the percentage of cells in S-phase of the cell cycle (figure 3.4).

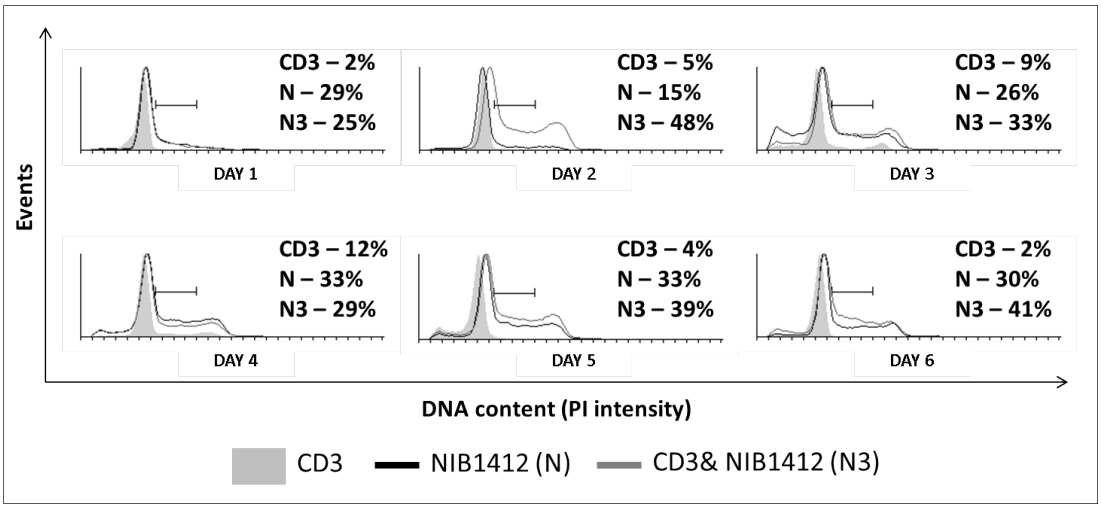

Figure 3.4: A higher percentage of NIB1412-stimulated T_{EMS} remain in S-phase

Human $CD4^+$ T_{EM} were stimulated for 1 to 6 days, fixed with ice cold 70% ethanol, stained with propidium iodide and cells in S-phase were quantified by flow cytometry. Results are representative of at least four independent experiments.

A higher percentage of NIB1412-stimulated T_{EMs} were in S-phase throughout the measured six days. The proportion of anti-CD3-stimulated T_{EMs} in S-phase was highest on day 4 with percentages of up to 12%, which then reduced in numbers while the proportion of NIB1412-stimulated T_{EMs} in S-phase remained high at around 30%. Following day 4, the percentage of cells in S-phase remained stable in NIB1412-stimulated T_{EMs} (Figure 3.4). When NIB1412 was combined with anti-CD3, the percentage of cells in S-phase peaked earlier (at day 2) and was significantly higher than the cells stimulated with either of the antibodies on their own. This result shows that NIB1412-stimulated T_{EMs} remain in S-phase for a much longer period of time than anti-CD3-stimulated T cells.

IL-2 is a prerequisite growth factor for the long term proliferation and survival of activated T cells [103]. *In vitro* studies of TGN1412 have shown high levels of IL-2 cytokine release [104]. In the current study, NIB1412-stimulated T_{EMs} displayed prolonged and higher IL-2 secretion of up to 25,000pg/ml, compared to ~ 5,000 pg/ml of IL-2 secretion for anti-CD3-stimuated T_{EMs}. The anti-CD3 and NIB1412 combination-stimulated T_{EM} population also displayed high IL-2 secretion (Figure 3.5).

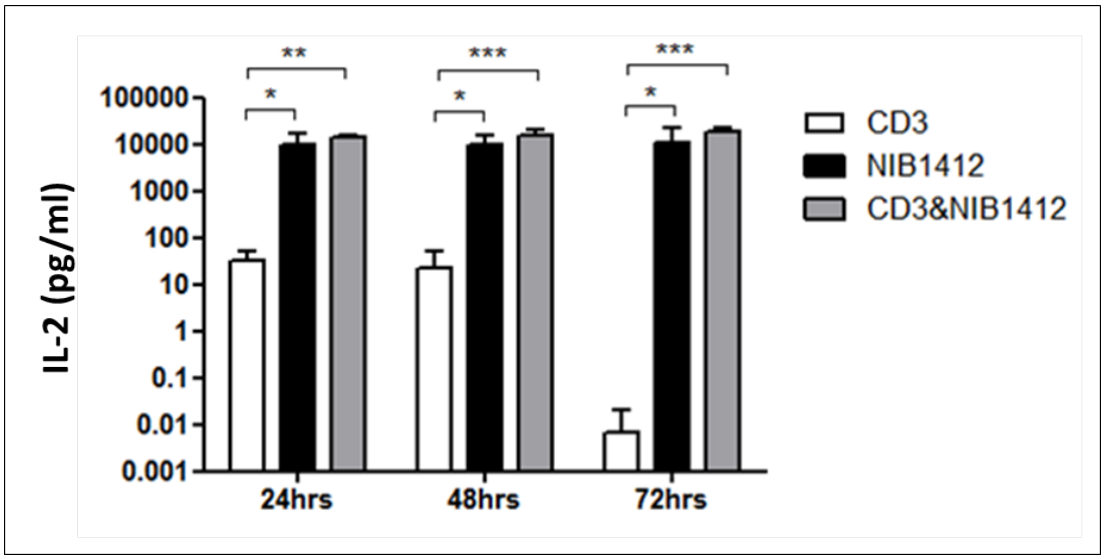

Figure 3.5: NIB1412-stimulated T_{EMS} secrete more IL-2

IL-2 concentrations in the supernatants from human $CD4^+$ T_{EM} stimulated for 24, 48 and 72hrs were determined by two-site enzyme-linked immunosorbent assay (ELISA). The IL-2 titres from four independent experiments (mean ± SD of replicate samples) are expressed as picograms per mL on a $\log_{10}$ scale. (*$p < 0.05$, **$p < 0.01$, ***$p < 0.001$; two-way ANOVA)

Our results show elevated IL-2 release by T_{EMs} when stimulated with NIB1412, which may contribute to the prolonged S-phase observed in the NIB1412-stimulated conditions.

3.3.2. Dysregulated expression of co-stimulatory receptors on CD28SA-activated $CD4^+$ effector memory T cells

Studies have shown that CD28 superagonists induce a sustained activation of downstream signalling events [16]. Flow cytometric analysis of the CD28 receptor revealed that anti-CD3 mAb stimulated T_{EMs} have no CD28 expression at 24hrs after TCR activation but re-express the receptor back to levels similar of unstimulated control cells from day 2 onwards. In contrast, NIB1412-activated T_{EMs} do not reduce CD28 expression at 24hrs post-activation. Instead the CD28 receptor fluctuates in expression levels as shown in Figure 3.6.

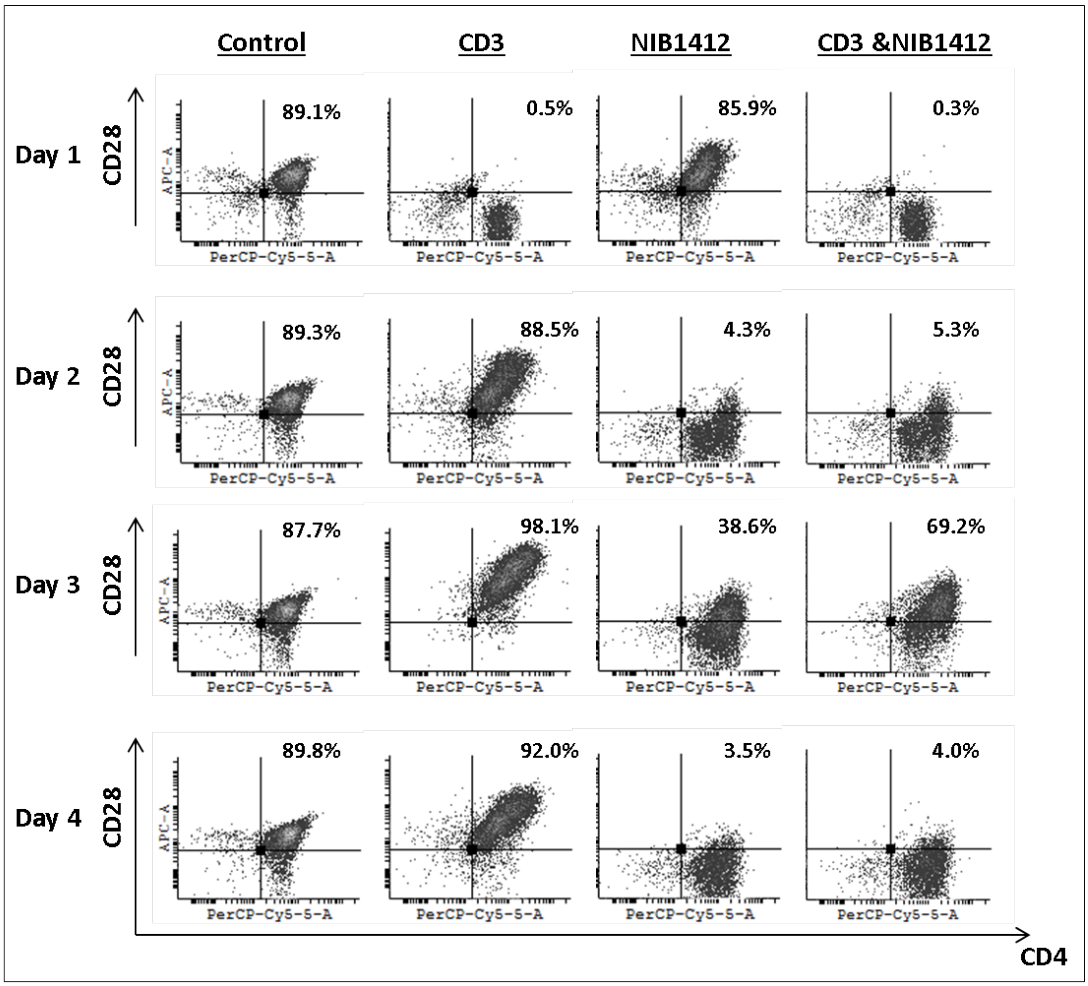

Figure 3.6: CD28 receptor expression levels fluctuate in NIB1412-stimulated T_{EMS}

Human $CD4^+$ T_{EM} were stimulated for 1 to 4 days with plate-bound anti-CD3 mAb (CD3, 5 µg/ml); NIB1412 (NIB1412, 10 µg/ml); anti-CD3 mAb and NIB1412 (CD3 & NIB1412); control category included cells without any treatment (Control). Cells were harvested at indicated time points and stained with fluorochrome-conjugated anti-CD4 and anti-CD28 antibodies followed by flow cytometric analysis. Populations of $CD4^+CD28^+$ cells are shown in the upper right quadrant as percentages of total T cells. Results are representative of four independent experiments.

We also examined the expression of other co-stimulatory receptors: CD137, GITR and CD27 (figure 3.7). Both CD137 and GITR were found to be expressed at a much higher percentage on NIB1412-activated T_{EMs} compared to T_{EMs} that were activated with anti-CD3 mAb. Interestingly, the CD27 receptor was only induced in anti-CD3 mAbs-stimulated T_{EMs} and was absent in both unstimulated and on NIB1412-activated T_{EMs} (figure 3.7).

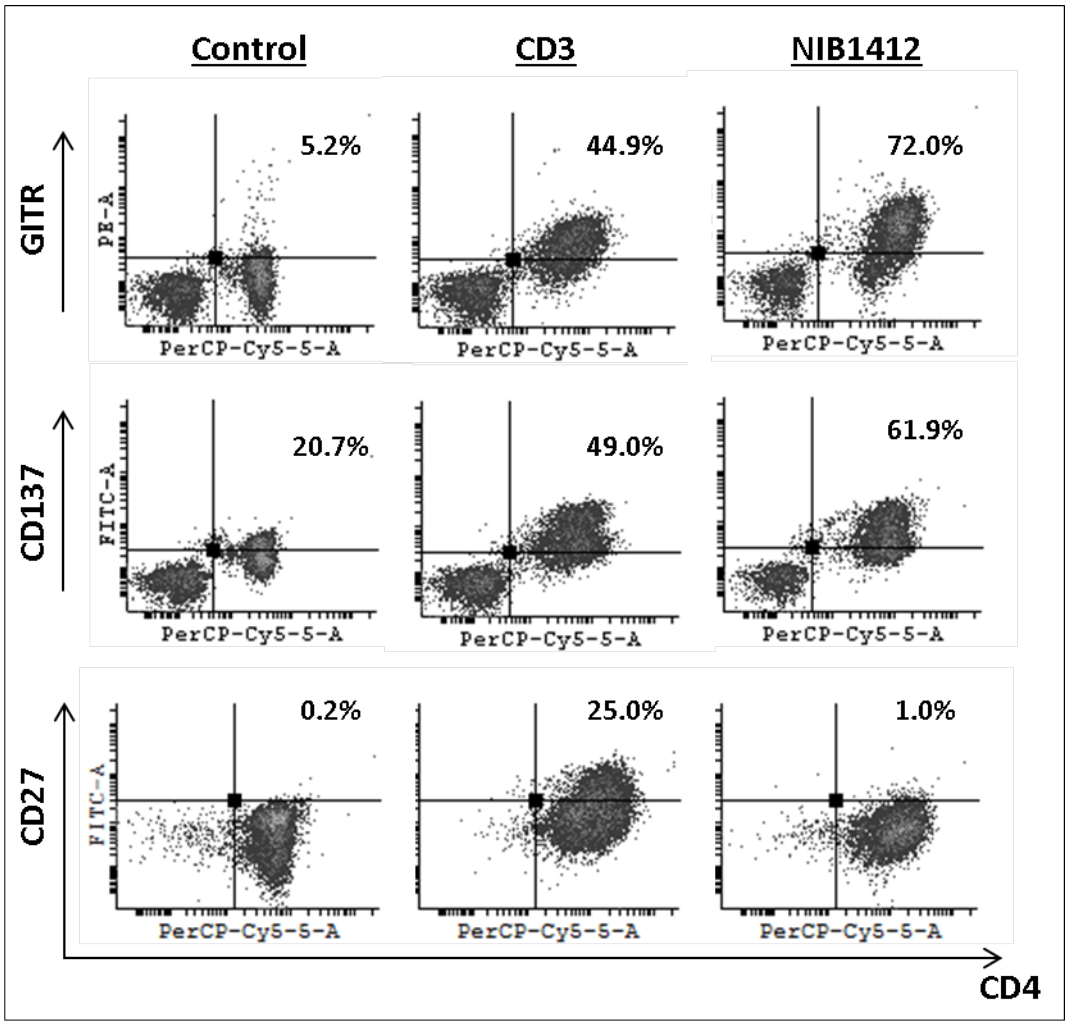

Figure 3.7: NIB1412-stimulated T_{EMS} express high levels of GITR and CD137 but not CD27

Human $CD4^+$ T_{EM} were stimulated for 3 days with plate-bound anti-CD3 mAb (CD3, 5 µg/ml); NIB1412 (NIB1412, 10 µg/ml); control category included cells without any treatment (Control). Cells were harvested and stained with fluorochrome-conjugated anti-CD4 and anti-GITR, anti-CD137, or anti-CD27 antibodies followed by flow cytometric analysis. Populations of double positive cells are shown in the upper right quadrant as percentages of total T cells. Results are representative of four independent experiments.

3.3.3. CD28SA-activated $CD4^+$ effector memory T cells express markers associated with antigen presentation

In addition to the co-stimulatory receptors CD137 and GITR, we also found that HLA-DR and CD80 were expressed at a much higher percentage on NIB1412-activated T_{EMs} compared to anti-CD3 mAb-activated T_{EMs} (figure 3.8). HLA-DR and CD80 are known to be markers associated with antigen presentation [105].

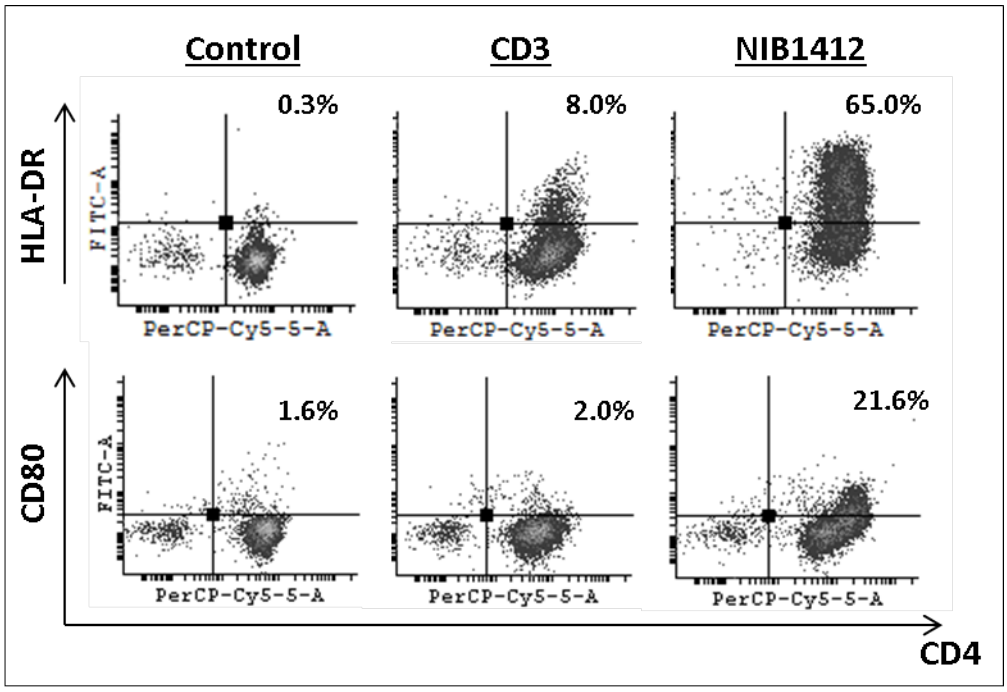

Figure 3.8: NIB1412-stimulated T_{EMS} express high levels of HLA-DR and CD80

Human $CD4^+$ T_{EM} were stimulated for 3 days with plate-bound anti-CD3 mAb (CD3, 5 µg/ml); NIB1412 (NIB1412, 10 µg/ml); control category included cells without any treatment (Control). Cells were harvested and stained with fluorochrome-conjugated anti-CD4 and anti-HLA-DR, or anti-CD80 antibodies followed by flow cytometric analysis. Populations of double positive cells are shown in the upper right quadrant as percentages of total T cells. Results are representative of four independent experiments.

3.3.4. Enhanced expression of LFA-1 and CCR5 on CD28SA-activated $CD4^+$ effector memory T cells

Following the TGN1412 clinical study, it was found that the lymphocytes migrated from the blood stream into organs causing significant tissue damage [92, 106]. The capability of superagonists to upregulate chemokine and adhesion receptors has not been investigated. In this study, flow cytometric analysis of the cell surface expression of LFA-1 and CCR5 revealed that a much higher percentage of NIB1412-activated T_{EMs} express LFA-1 (up to 3-fold higher) and CCR5 (up to 8-fold higher) compared to T_{EMs} that were activated with anti-CD3 mAb (Figure 3.9 and 3.10).

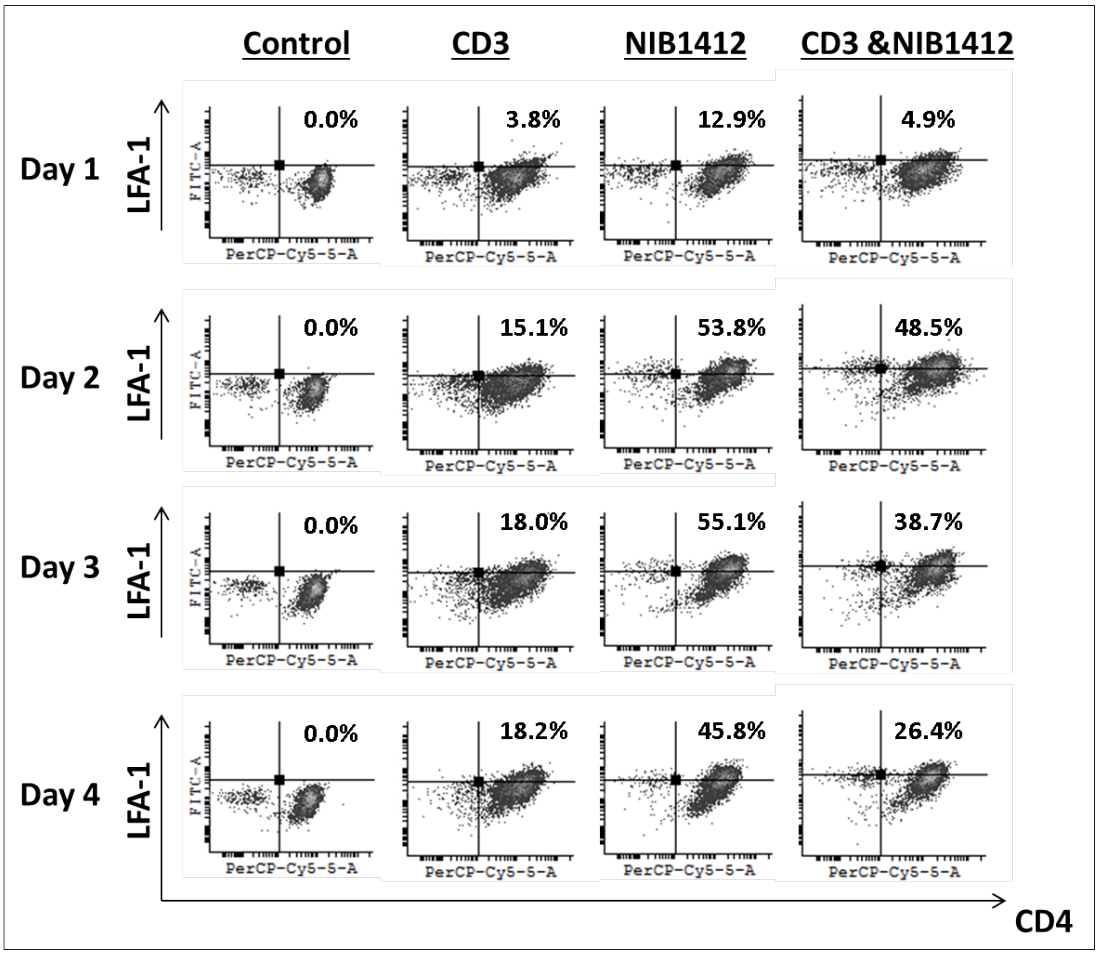

Figure 3.9: NIB1412-stimulated T_{EMS} express high levels of LFA-1

Human $CD4^+$ T_{EM} were stimulated for 1 to 4 days with plate-bound anti-CD3 mAb (CD3, 5 µg/ml); NIB1412 (NIB1412, 10 µg/ml); anti-CD3 mAb and NIB1412 (CD3 & NIB1412); control category included cells without any treatment (Control). Cells were harvested at indicated time points and stained with fluorochrome-conjugated anti-CD4 and anti-LFA-1 antibodies followed by flow cytometric analysis. Populations of $CD4^+LFA\text{-}1^+$ cells are shown in the upper right quadrant as percentages of total T cells. Results are representative of four independent experiments.

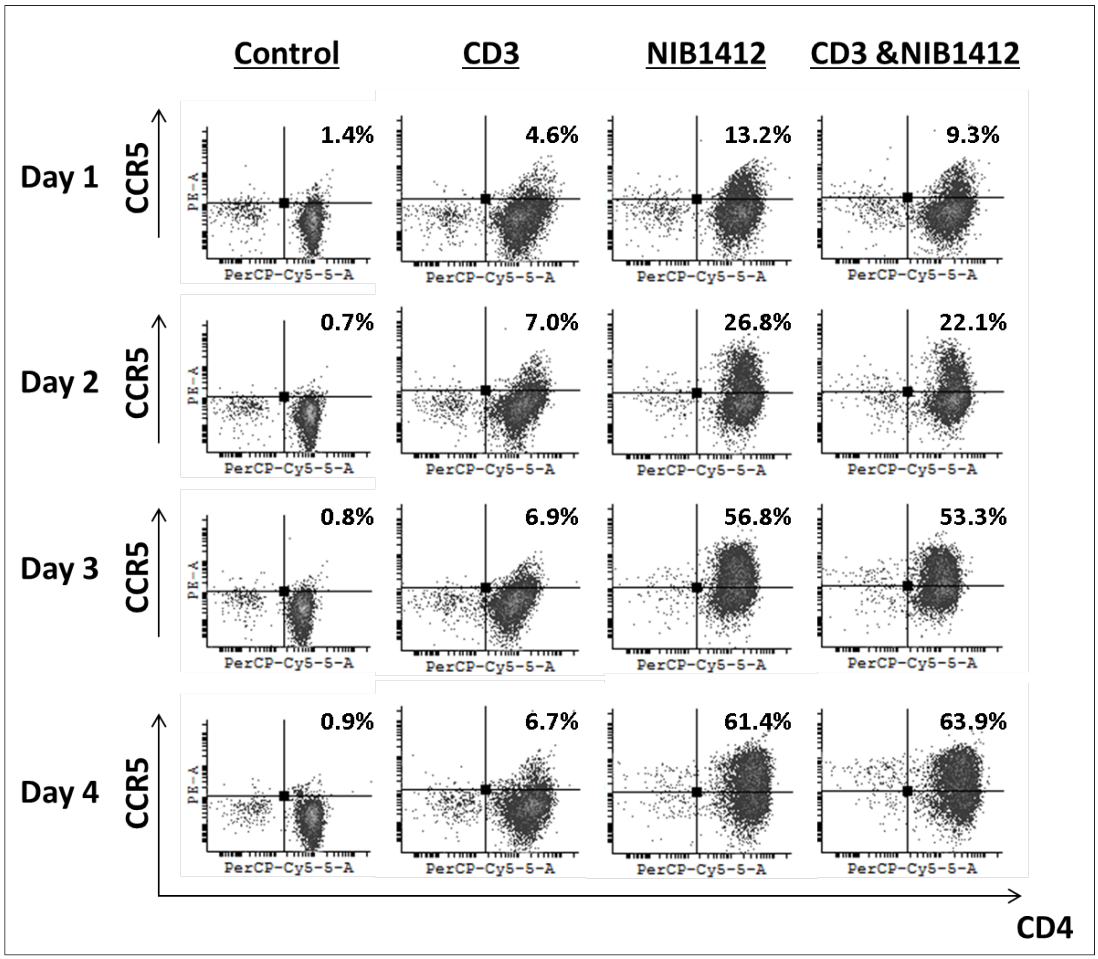

Figure 3.10: NIB1412-stimulated T_{EMS} express high levels of CCR5

Human $CD4^+$ T_{EM} were stimulated for 1 to 4 days with plate-bound anti-CD3 mAb (CD3, 5 µg/ml); NIB1412 (NIB1412, 10 µg/ml); anti-CD3 mAb and NIB1412 (CD3 & NIB1412); control category included cells without any treatment (Control). Cells were harvested at indicated time points and stained with fluorochrome-conjugated anti-CD4 and anti-CCR5 antibodies followed by flow cytometric analysis. Populations of $CD4^+CCR5^+$ cells are shown in the upper right quadrant as percentages of total T cells. Results are representative of four independent experiments.

Combined anti-CD3 and NIB1412-stimulated T_{EMs} displayed an LFA-1 expression level intermediate to that of either agonist alone, while CCR5 expression was similar to that of NIB1412-stimulated T_{EMs}. In addition to elevated CCR5 expression, NIB1412-stimulated T_{EMs} also expressed CXCR4 at low albeit detectable levels (figure 3.11).

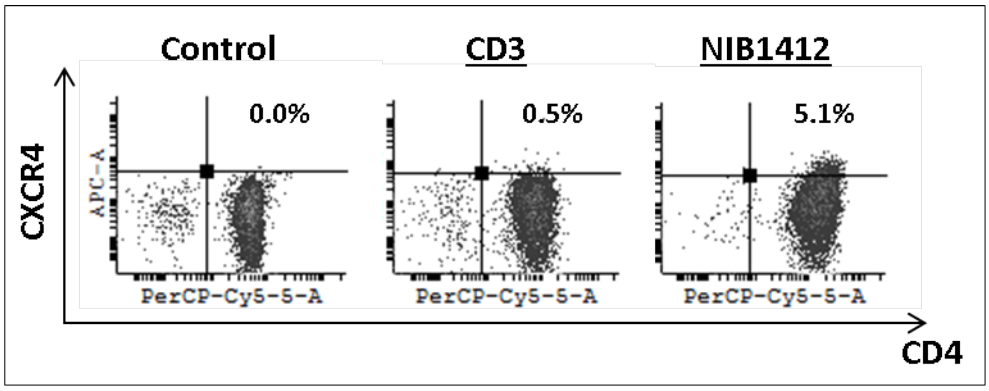

Figure 3.11: NIB1412-stimulated T_{EMS} express CXCR4

Human $CD4^+$ T_{EM} were stimulated for 3 days with plate-bound anti-CD3 mAb (CD3, 5 µg/ml); NIB1412 (NIB1412, 10 µg/ml); control category included cells without any treatment (Control). Cells were harvested and stained with fluorochrome-conjugated anti-CD4 and anti-CXCR4 antibodies followed by flow cytometric analysis. Populations of $CD4^+CXCR4^+$ cells are shown in the upper right quadrant as percentages of total T cells. Results are representative of four independent experiments.

3.3.5. Enhanced adhesion and migration of CD28SA-activated $CD4^+$ effector memory T cells

The ability of T cells to adhere and migrate along endothelial surfaces is dependent on the binding of LFA-1 on T cells to the intercellular adhesion molecule-1 (ICAM-1) expressed on endothelial cells [107]. Since our data showed elevated LFA-1 expression on NIB1412-stimulated T_{EMs}, we investigated their attachment and migratory capabilities. We show that NIB1412-stimulated T_{EMs} adhere to (Figure 3.12 and 3.13) and migrate (Figure 3.14) across endothelial cell layers in significantly greater numbers than anti-CD3-stimulated T_{EMs}.

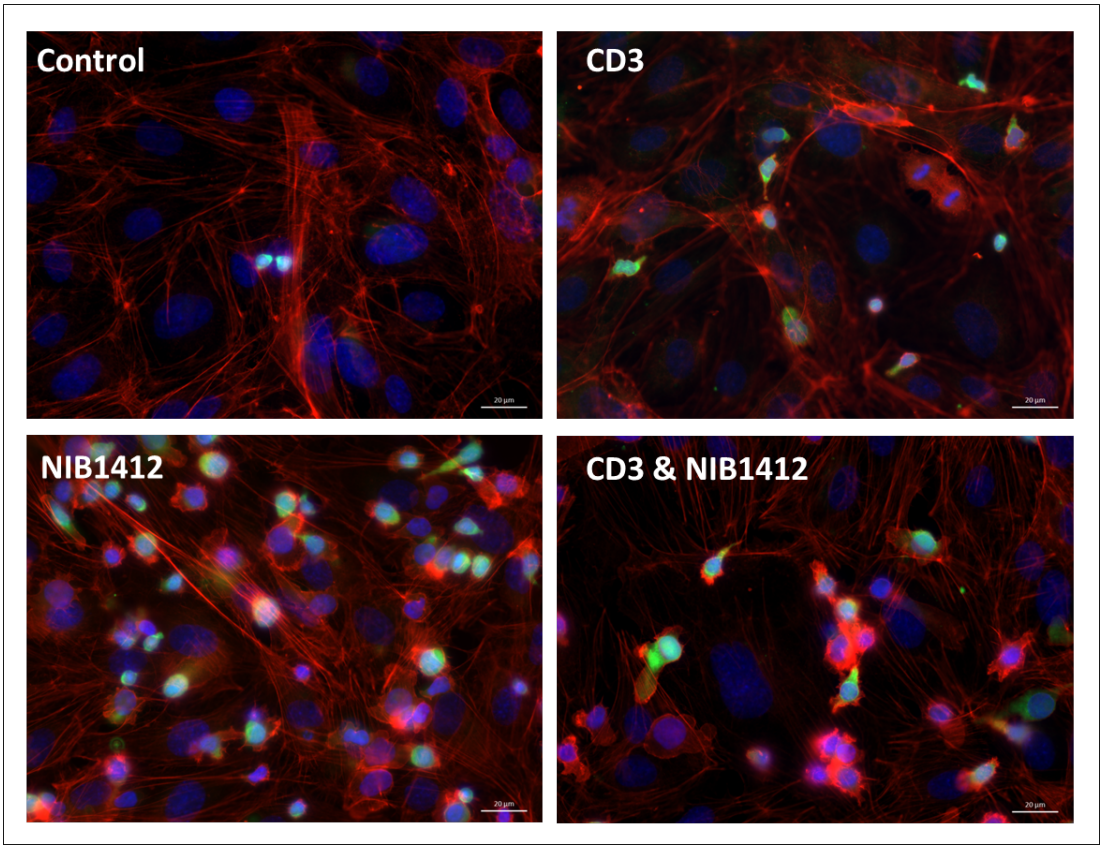

Figure 3.12: Enhanced adhesion of NIB1412-stimulated T_{EMS}

Immunofluorescent microscopy of HDMEC monolayer with adherent CMFDA-labelled T_{EMs} initially stimulated with the indicated antibodies and stained for F-actin and DNA using fluorescently labeled phalloidin (red) and DAPI (blue), respectively. (Scale bar = 20 microns). Phase optics was adjusted to emphasize adherent cells.

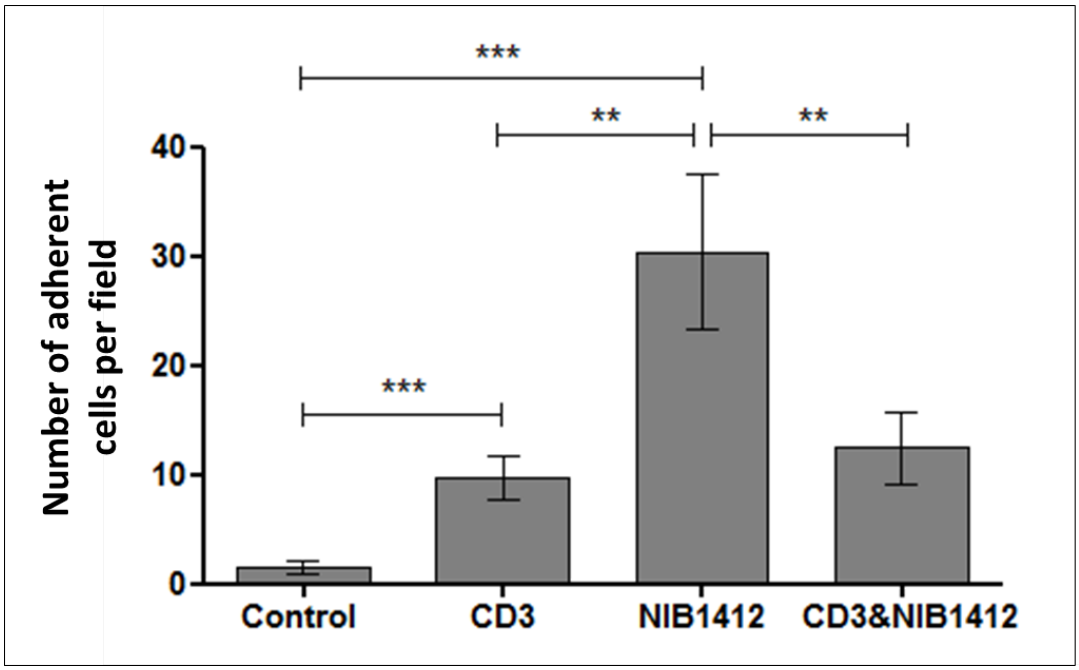

Figure 3.13: Enhanced adhesion of NIB1412-stimulated T_{EMS}

CMFDA-labelled T_{EMs} initially stimulated with the indicated antibodies were added to confluent HDMECs and incubated for 30 minutes. Cells were washed and the remaining adherent cells visualized under fluorescence microscopy. Vertical axis represents the number of adherent T_{EMs} per field (**p<0.01; ***p<0.001, unpaired t-test). Results from four independent donors are represented as means ± SD.

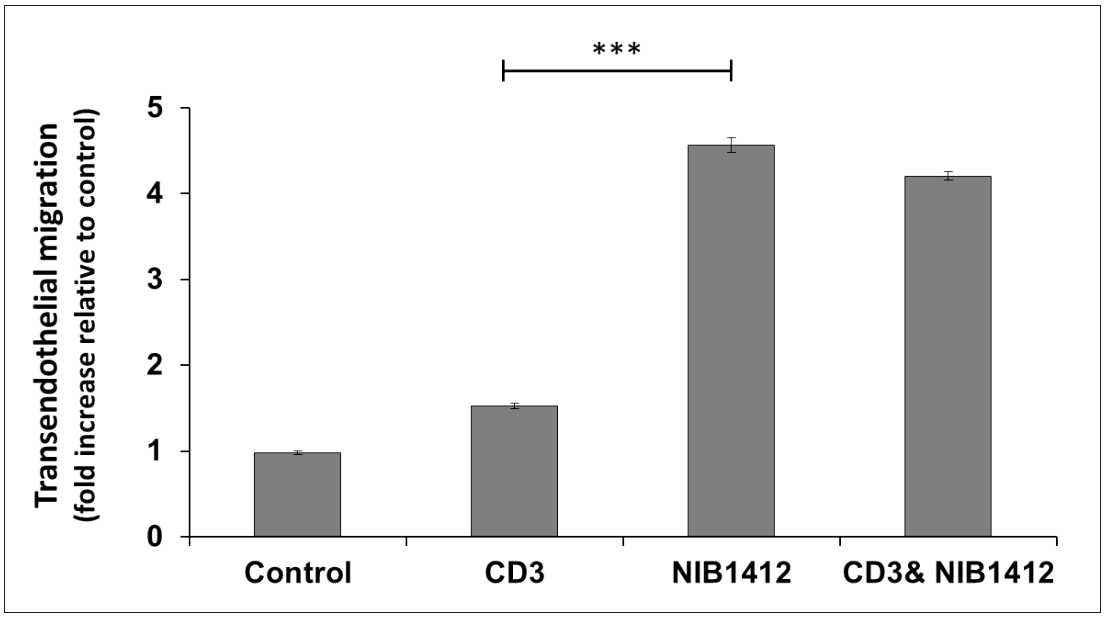

Figure 3.14: Enhanced transendothelial migration of NIB1412-stimulated T_{EMs}

Transmigration of stimulated $CD4^+$ T_{EMs} across HDMEC layer on transwell inserts. Transmigrated cells were quantified by fluorescence and the results are presented as the mean (± SD) number of transmigrated cells from 3 replicate wells per condition. Results are representative of three independent experiments (***p<0.001unpaired t-test).

3.3.6. Failure to upregulate cell surface PD-1 and CTLA-4 by CD28SA-activated $CD4^+$ effector memory T cells

Activation of T cells via the TCR/CD3 complex leads to upregulation of surface PD-1. Up to 18% of NIB1412-stimulated T_{EMs} expressed PD-1, which declined to ~ 3 to 6% from 48 hrs onwards (Figure 3.15).

Anti-CD3 stimulated T_{EMs} expressed high PD-1, which peaked around day 3 to about 60% and remained relatively constant up to 4 days post-activation. The proportion of PD-1^+ T_{EMs} on day 2 post-activation was up to 17-fold higher in the anti-CD3 mAb condition compared to the NIB1412 condition (Figure 3.15). From day 2 onwards, the proportion of anti-CD3-activated $CD4^+$ T_{EMs} expressing PD-1 was 11- to 12-fold higher compared to when they were stimulated with NIB1412. The combination of NIB1412 and anti-CD3 generally resulted in PD-1 expression intermediate to that of stimulation with either anti-CD3 or NIB1412 condition (Figure 3.15).

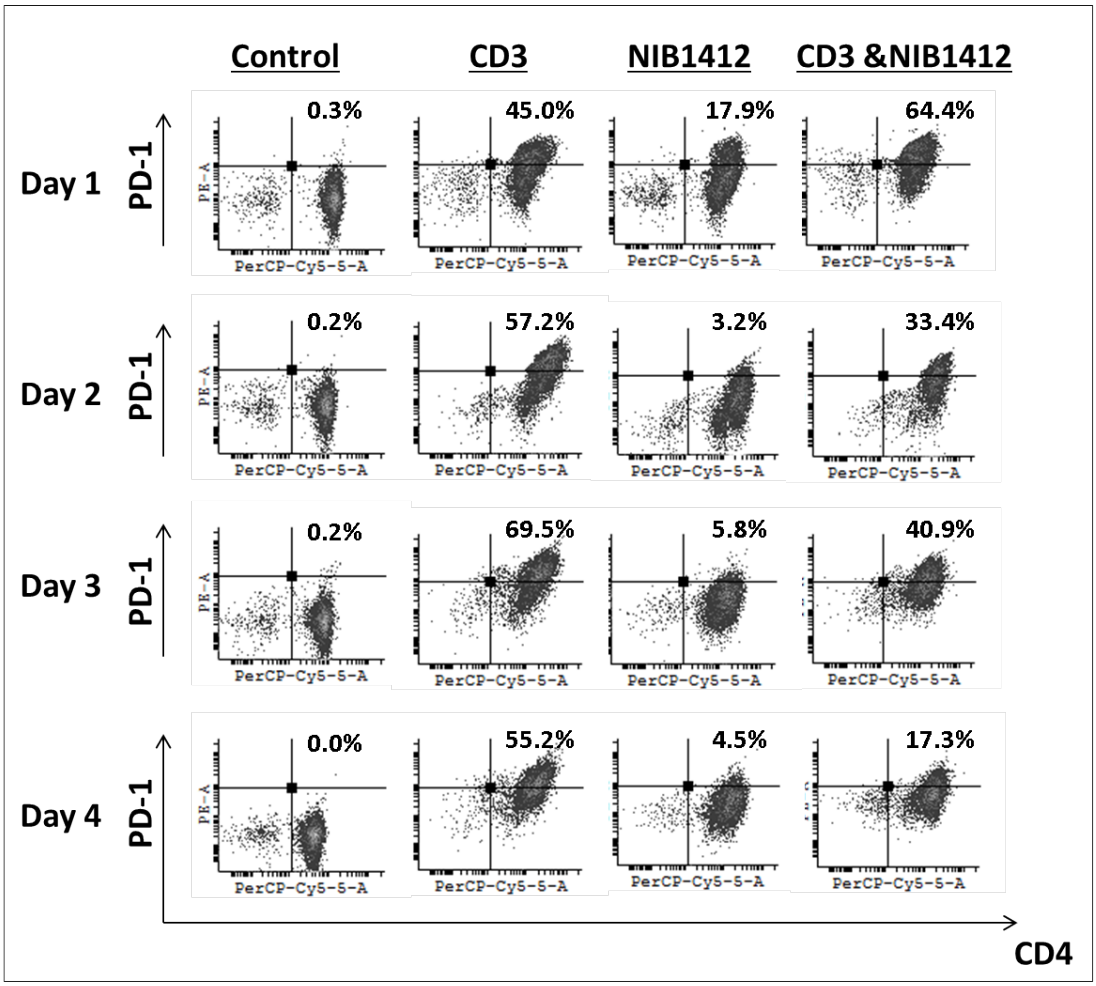

Figure 3.15: Failure of NIB1412-stimulated T_{EMS} to upregulate cell surface PD-1

Human $CD4^+$ T_{EM} were stimulated for 1 to 4 days with plate-bound anti-CD3 mAb (CD3, 5 µg/ml); NIB1412 (NIB1412, 10 µg/ml); anti-CD3 mAb and NIB1412 (CD3 & NIB1412); control category included cells without any treatment (Control). Cells were harvested at indicated time points and stained with fluorochrome-conjugated anti-CD4 and anti-PD-1 antibodies followed by flow cytometric analysis. Populations of $CD4^+PD\text{-}1^+$ cells are shown in the upper right quadrant as percentages of total T cells. Results are representative of four independent experiments.

Although surface staining of NIB1412-activated $CD4^+$ T cells showed a negligible surface PD-1 expression, intracellular staining of these cells revealed the presence of intracellular PD-1 (Figure 3.16).

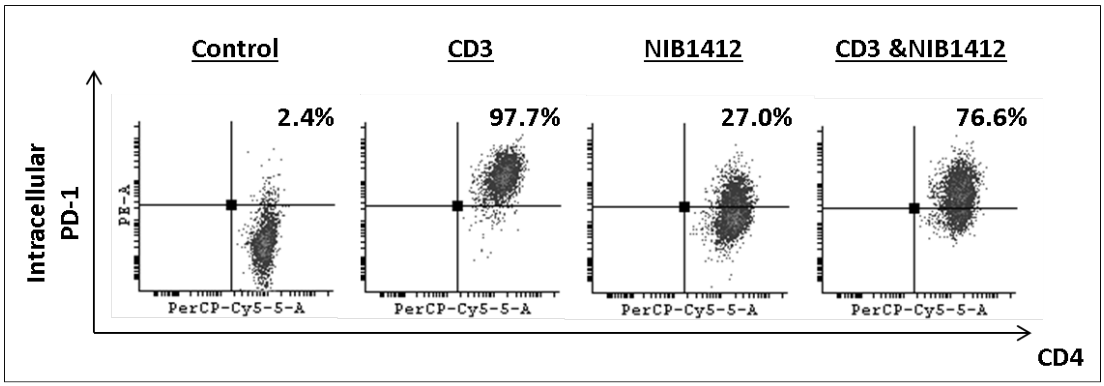

Figure 3.16: NIB1412-stimulated T_{EMS} express intracellular PD-1

Human $CD4^+$ T_{EM} were stimulated for 3 days with plate-bound anti-CD3 mAb (CD3, 5 µg/ml); NIB1412 (NIB1412, 10 µg/ml); anti-CD3 mAb and NIB1412 (CD3 & NIB1412); control category included cells without any treatment (Control). Cells were harvested and stained for intracellular PD-1 following fixation/permeabilization treatment. Population of $CD4^+$ $PD\text{-}1^+$ cells are shown in the upper right quadrant as percentages of total T cells. Results are representative of four independent experiments.

However, the PD-1 mRNA levels in NIB1412-activated $CD4^+$ T cells were significantly lower than anti-CD3 mAbs-activated cells (figure 3.17i). Moreover, CTLA-4 mRNA levels were also significantly lower in NIB1412-activated $CD4^+$ T cells than in anti-CD3 mAbs-activated cells (figure 3.17ii).

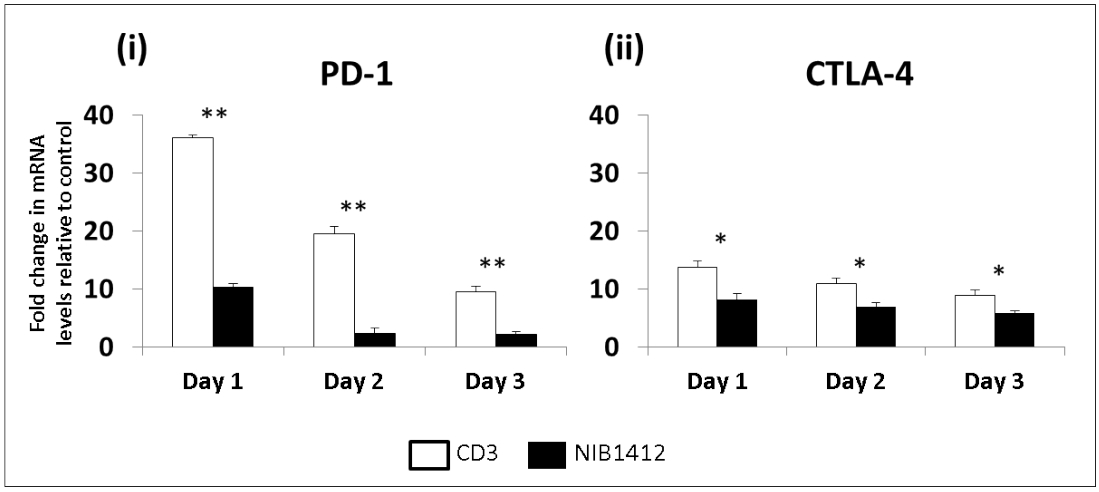

Figure 3.17: NIB1412-stimulated T_{EMS} have significantly lower PD-1 and CTLA-4 mRNA levels

Human $CD4^+$ T cells were stimulated with plate-bound anti-CD3 or NIB1412 for 1-3 Days. The mRNA levels of (i) PD-1 and (ii) CTLA-4 were determined by real-time RT-PCR. The mRNA levels were normalized to the loading control, GAPDH, and expressed as a fold increase of the PD-1 or CTLA-4 mRNA levels in unstimulated cells. Data represented as mean + S.D of triplicates. n=2 independent experiments. (*$P < 0.05$, **$P < 0.01$; t-test)

Our results show that NIB1412 stimulation of T_{EMs} results in a dysregulated phenotype in terms of minimal PD-1 and CTLA-4 expression, which prevents the input of normal negative regulatory signals to control T cell activation.

3.3.7. Absence of PD-1 mediated regulation of T cell function in CD28SA- stimulated T cells.

To determine whether the absence of PD-1 expression has a functional consequence on NIB1412-activated $CD4^+$ T cells, recombinant PD-L1 (rPD-L1) was used to engage the PD-1 expressed on activated T cells. The proportion of cells expressing IFNγ was decreased to half in $CD4^+$ T cells that were initially stimulated with anti-CD3 and then re-stimulated with anti-CD3+rPD-L1 (Figure 3.18). $CD4^+$ T cells that were initially stimulated with the CD3 and NIB1412 combination were unaffected in their IFNγ secretion upon re-stimulation with anti-CD3 and rPD-L1 (Figure 3.18). These results suggest that the presence of surface PD-1 enables a negative feedback response when bound to its ligand, which is absent in NIB1412-activated $CD4^+$ T cells and thus could lead to dysregulated functional outputs.

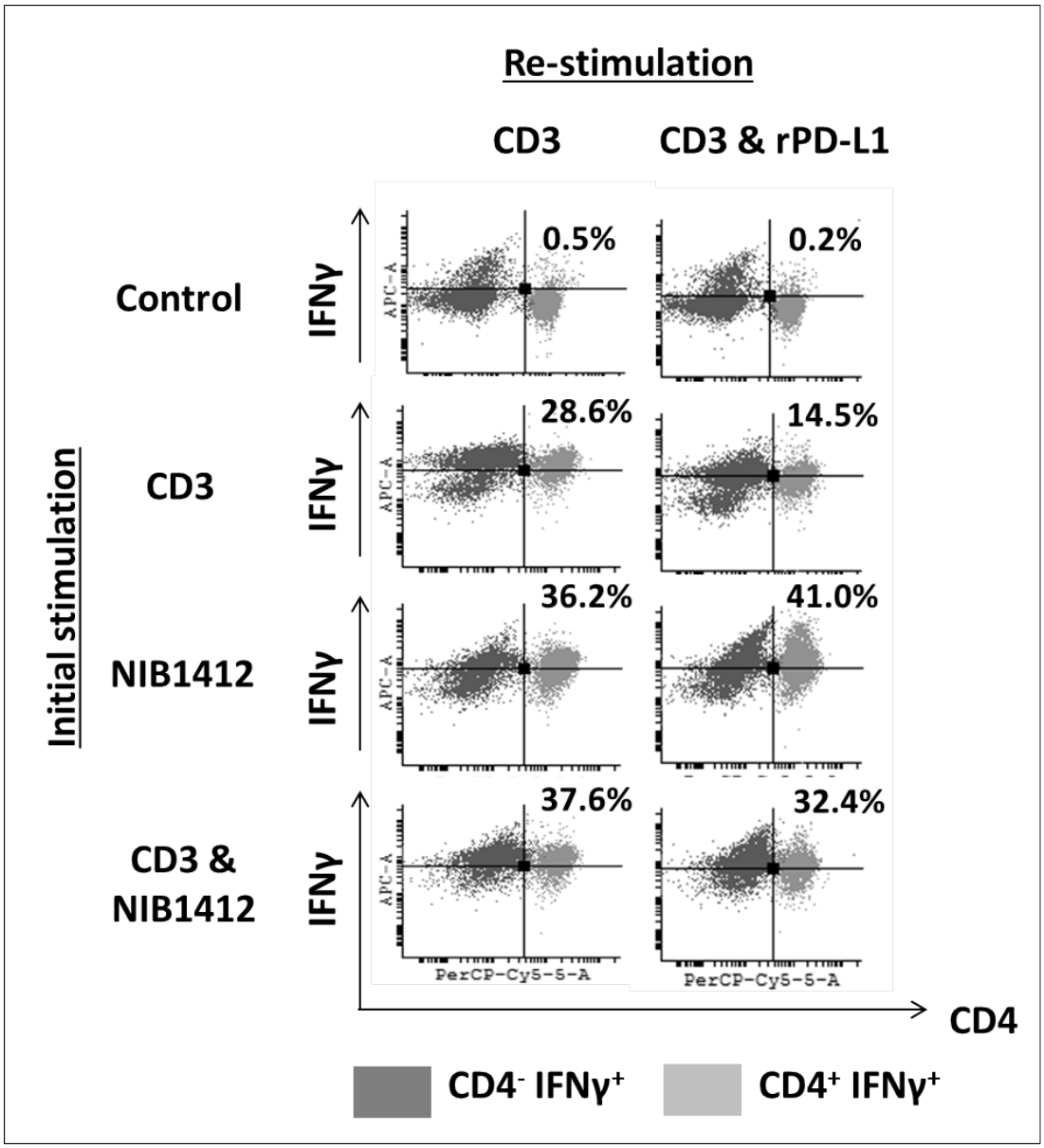

Figure 3.18: Absence of PD-1 mediated regulation in NIB1412- stimulated T cells

Human PBMCs were stimulated for 48h with plate-bound anti-CD3 mAb (CD3, 5 µg/ml); NIB1412 (NIB1412, 10 µg/ml); anti-CD3 mAb and NIB1412 (CD3 & NIB1412); control category included cells without any treatment (Control). Cells were then re-stimulated with anti-CD3 only (CD3, 1 µg/ml) or with anti-CD3 and 10 µg/ml of rPD-L1 (CD3 & rPD-L1). Cells were harvested and stained with fluorochrome-conjugated anti-CD4 antibody, fixed, permeabilized, stained with fluorochrome-conjugated anti-IFNγ antibody and analyzed by flow cytometry. The $CD4^+$ population is shown in light grey and the $CD4^-$ population in dark grey. The percentages of the $CD4^+$ $IFN\gamma^+$ cells are shown in the upper right quadrant. Results are representative of four independent experiments.

3.3.8. PD-1 engagement reduces phospho PTEN levels in T_{EMs} stimulated by anti-CD3 but not CD28SA

The engagement of CD28 on T cells leads to the activation of the phosphatidylinositol 3-kinase (PI3K)/ protein kinase B (Akt) pathway which is important for cell survival and growth [108]. Phosphatase and tensin homolog (PTEN), a lipid phosphatase, negatively regulates the PI3K/Akt pathway [109]. A recent study has shown that the engagement of the PD-1 pathway suppresses casein kinase 2 (CK2) and results in the inhibition of the stabilizing-phosphorylation of the Ser380-Thr382-Thr383 residue cluster of PTEN. This increases PTEN phosphatase activity which subsequently inhibits the phosphatidylinositol 3-kinase (PI3K)/Akt pathway (figure 1.7) [29].

Our results show that T_{EMs} stimulated with NIB1412 have significantly higher pPTEN levels compared to when stimulated with anti-CD3 mAb. T_{EMS} stimulated with anti-CD3 in the presence of rPD-L1 result in significantly diminished pPTEN compared to the anti-CD3 alone condition (Figure 3.19). The rPD-L1+NIB1412 condition showed similarly high pPTEN levels compared to the NIB1412 alone condition (Figure 3.19). Consistent with the previous result, CK2 expression was found to be significantly higher in T_{EMs} activated with NIB1412 than when stimulated with anti-CD3 mAb (Figure 3.20). The CK2 levels, although not significant, were reduced in T_{EM} stimulated with anti-CD3 in the presence of rPD-L1, but no reduction was observed in the rPD-L1+NIB1412 condition. These results point to the lack of engagement of the PD-1 mediated regulation of the PI3K-PTEN-CK2 signalling axis in CD28SA activated T cells.

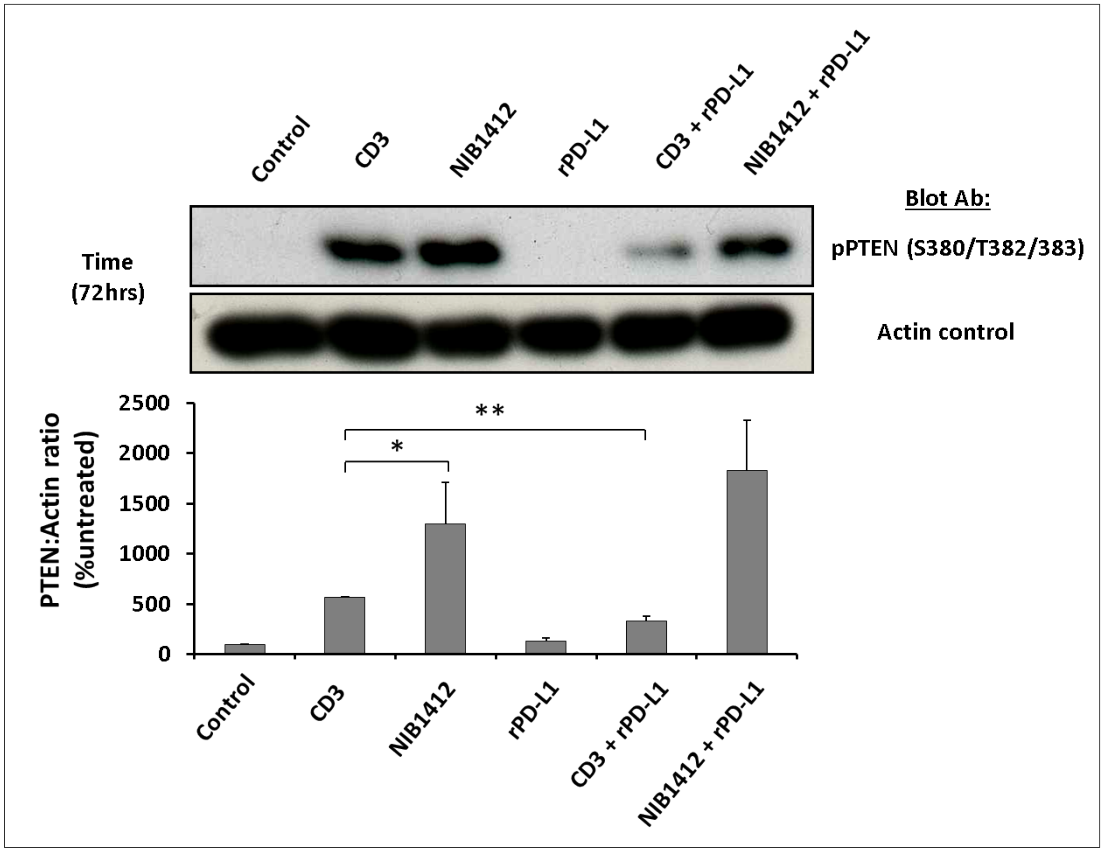

Figure 3.19: Effects of PD-1 engagement on phospho PTEN

Human $CD4^+$ T_{EMs} were stimulated with anti-CD3 mAb (CD3, 5 µg/ml); NIB1412 (NIB1412, 10 µg/ml); rPD-L1 (rPD-L1, 10µg/ml); with anti-CD3 mAb and rPD-L1 (CD3 + rPD-L1) or with NIB1412 and rPD-L1 (NIB1412 + rPD-L1). At the end of 72 hrs, the cells were lysed and extracted protein separated by SDS-PAGE. pPTEN – S380/T382/383 (47kDa) protein levels were assessed by immunoblotting and actin (45kDa) was used as loading control. Blot is representative of four independent experiments. pPTEN levels were quantified by densitometry, normalized to β-actin and expressed as a percentage of pPTEN levels in untreated cells. Data are represented as mean ± SEM of four independent experiments. Statistical analysis was performed using unpaired t-test (* $p<0.05$, ** $p<0.01$). Phospho PTEN – pPTEN

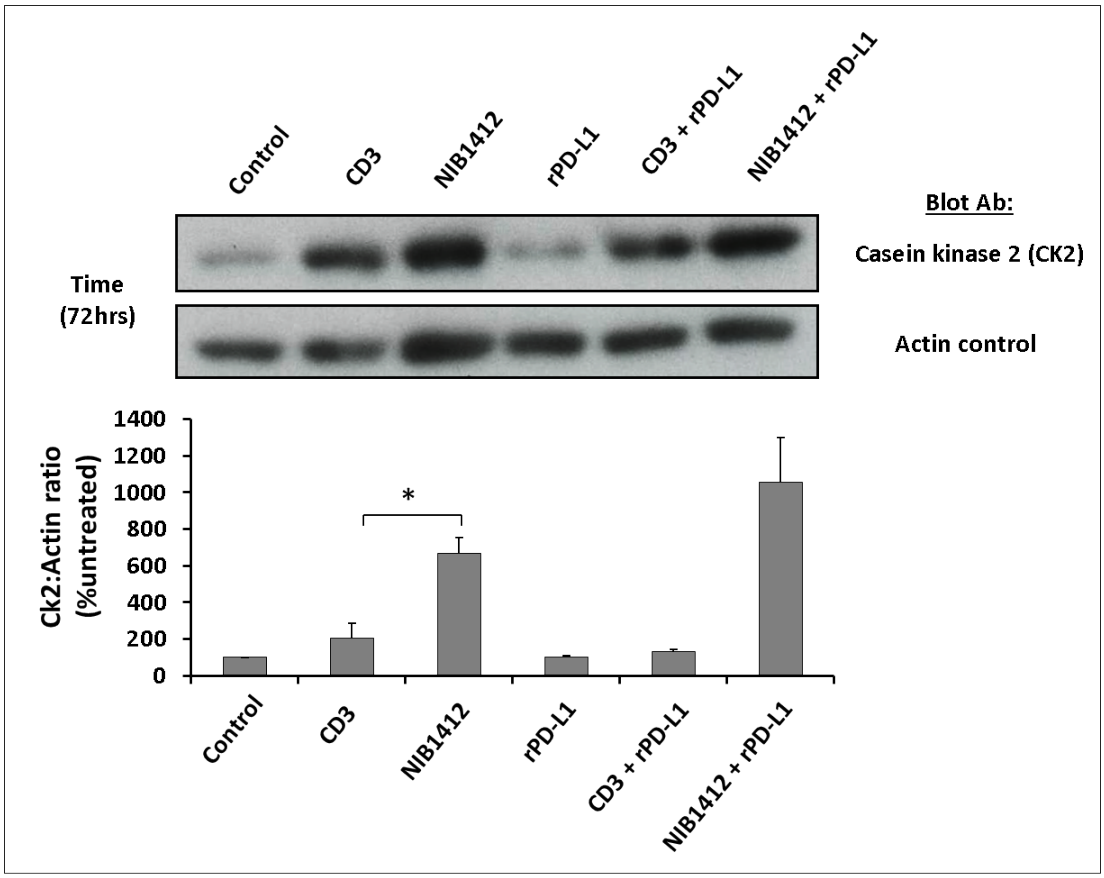

Figure 3.20: Effects of PD-1 engagement on CK2 levels

Human $CD4^+$ T_{EMs} were stimulated with anti-CD3 mAb (CD3, 5 µg/ml); NIB1412 (NIB1412, 10 µg/ml); rPD-L1 (rPD-L1, 10µg/ml); with anti-CD3 mAb and rPD-L1 (CD3 + rPD-L1) or with NIB1412 and rPD-L1 (NIB1412 + rPD-L1). At the end of 72 hrs, the cells were lysed and extracted protein separated by SDS-PAGE. CK2α (42kDa) protein levels were assessed by immunoblotting and actin (45kDa) was used as loading control. All blots are representative of four independent experiments. CK2 levels were quantified by densitometry, normalized to β-actin and expressed as a percentage CK2 levels in untreated cells. Data are represented as mean ± SEM of four independent experiments. Statistical analysis was performed using unpaired t-test (* $p<0.05$, ** $p<0.01$). Casein Kinase 2 – CK2

3.4. Discussion

TGN1412 is a CD28SA that caused an uncontrolled expansion of T cells with an accompanying cascade of proinflammatory cytokine release and infiltration of T cells into tissues, in all six healthy volunteers enrolled in a Phase I clinical study [92]-[97]. Despite initial recovery, their conditions deteriorated and this may be linked to a prolonged adverse response due to the dysregulation of the immune system by TGN1412.

We show that prolonged stimulatory signals, upregulation of the CCR5 receptor and the LFA-1 integrin on the cell surface, and lack of inhibitory receptors such as PD-1 in CD28SA-treated T cells are responsible for the hyperactive phenotype observed. We also showed the prolonged unrestricted proliferation in CD28SA-activated effector memory $CD4^+$ T cells. These results indicate the unrestricted expansion of a CD28SA-induced immune response, while the anti-CD3-induced immune response contracts post-activation. When T cells are activated with CD28SA and anti-CD3 in combination, the resulting phenotype expresses intermediate levels of PD-1, LFA-1 and CCR5, compared to when activated with either agonist on its own. This might suggest that anti-CD3 activation induces regulatory signals.

Enhanced and prolonged secretion of IL-2 and autocrine triggering of IL-2 receptors (IL-2Rs) could contribute to sustained proliferation of CD28SA-stimulated T cells. Data from our lab indicate that NIB1412-simulated T cell proliferation requires IL-2-IL-2R interaction (data from collaborator Stebbings et al.). Activation with anti-CD3 reduces levels of CD28 post-activation but these are reset and maintained at physiologically high levels from day 2. For CD28SA-activated T cells the CD28 receptor re-emerges within a short time frame following activation which makes it available for re-engagement by unbound CD28SA, leading to repeated upregulation and downregulation of the CD28 receptor and continuous induction of input signals. This may reflect the sustained signalling observed in previous studies [16]. Activation of T cells in combination with CD28SA and anti-CD3 shows a delay in CD28 receptor re-emergence until day 3, which reduces again at day 4. The presence of anti-CD3-mediated signals may influence CD28 receptor expression, and in turn reduce repeated stimulation by unbound CD28SA.

The contraction phase of T cell activation is mainly brought about through apoptosis induced via the Fas-FasL system, [110] and we have shown a diminished capacity of CD28SA stimulated T cells to upregulate Fas (CD95), which might explain the failure of these T cells to undergo normal contraction.

CD28SA-stimulated T cells also upregulate significant levels of HLA-DR and CD80, co-stimulatory molecules typically expressed by antigen presenting cells. Circulating T cells in HIV-1-infected individuals undergo a transition from a reactive to an antigen presenting phenotype by expressing both HLA-DR and CD80 molecules. The expression of these co-stimulatory receptors is thought to reflect the chronicity of the T cell activation [111]. Studies have shown that T cells acquire markers of antigen presentation from APCs [112]. Since we isolated the T_{EM} population from PBMCs prior to stimulation with NIB1412, it suggests that superagonist activation may lead to the endogenous upregulation of HLA-DR and CD80. This could enable T cell to T cell antigen presentation. In a heterogeneous mixture of cells CD28SA-activated T cells would be capable of activating a variety of T cells by acting as APCs. Furthermore, histological studies have revealed that CD80 expression can be detected on tissue-infiltrating T cells [113]. Taken together, the expression of LFA-1 and markers of antigen presentation suggests that CD28SA-activated T cells have a high tissue infiltration capability.

Effector memory cells respond to the inflammatory chemokines CCL3, CCL4 and CCL5, and upon re-stimulation up-regulate CCR5 and become tissue invasive [114]. TGN1412 can induce monocytes to secrete high levels of CCL5 within 2hrs of stimulation [115]. It is likely that CD28SA-induced upregulation of CCR5 was a contributing factor to the lymphocyte tissue invasion observed in the volunteers during the TGN1412 clinical trial. A prominent feature of the pathologic events in the trial patients was prolonged lymphocyte depletion from the circulation which was suggested to be related to unregulated T cell extravasation [92, 106]. LFA-1 is the predominant adhesion molecule on T cells [63] and plays an important role in extravasation of lymphocytes into inflamed tissue. Since NIB1412-stimulated T_{EMs} expressed high levels of LFA-1, it is possible that these cells might be more likely to undergo extravasation. We show enhanced adhesion and transendothelial

migration of NIB1412-stimulated T_{EMs} compared to anti-CD3-stimulated T_{EMS}. A variety of negative regulators are known to play roles in the resolution of T cell response with PD-1 being a key inhibitory receptor [11]. The PD-1 pathway has been shown to play crucial roles in the regulation of autoimmunity, transplantation immunity, infectious immunity, and tumour immunity [98]. The PD-1-PD-L1 interaction plays an important role during the contraction phase of the immune response [98]. PD-1 deficient experimental mouse models display a breakdown of tolerance and a higher susceptibility to proliferate with higher amounts of IFN-γ production [116], which leads to the development of spontaneous strain-dependent autoimmune diseases. The recognition that the PD-1 pathway provides strong negative signalling and is a dominant regulator of activated T cells has led to focus on development of therapeutic strategies aimed at manipulating this PD-1 [98]. Thus, PD-1 was chosen as a candidate receptor to see its potential lack of contribution in CD28SA-activated T cells. In our study, we show that CD28SA-activated T cells fail to upregulate PD-1 and the negative feedback conferred by the PD-1-PD-L1 interaction was found to be absent in these T cells. Further investigations are required in order to gain an understanding of the mechanisms that regulate PD-1 expression and function in this context.

Although, PD-1 was absent on the surface of CD28SA-activated $CD4^+$ T cells, it is present within the cytoplasm of these cells. PD-1 has been shown to be present in vesicles near the Golgi and in the trans-Golgi network [117]. Since PD-1 is known to be upregulated on the cell surface upon TCR triggering, it suggests that the fusion of PD-1-containing vesicles within the cytoplasm to the plasma membrane is dependent on signalling pathways that emanate from the TCR that are not engaged by CD28SA. The exact molecular signals that connect TCR to PD-1 upregulation require further definition.

We have shown that engagement of the PD-1 receptor by PD-L1 reduces PTEN phosphorylation in anti-CD3-stimulated T_{EMs} but not in CD28A-stimulated T_{EMs}. The presence of phosphorylated PTEN in CD28SA-stimulated T_{EMs} suggests that there is an absence of PTEN lipid phosphatase activity to inhibit the PI3K/AKT signaling axis, leaving the T cells in a hyper-proliferative state. Since the PI3K pathway regulates

diverse cellular activities such as growth, migration, survival, vesicular trafficking and glucose metabolism [118], it would be worth investigating key signalling proteins that branch from the PI3K nexus that may be dysregulated during CD28SA activation. The lack of a reliable biomarker predictive of uncontrolled T cell stimulation by TGN1412 was a key factor in the failure of preclinical safety testing of this immunostimulatory mAb. Detailed understanding of the target biology followed by identification and screening of target specific biomarkers for risk assessment is essential to improve the safety profile of biologics [87]. Our study demonstrates that CD28SA-stimulated T cells display a phenotype that is reflective of a predisposition to excessive activation and lack of regulation by PD-1 mediated inhibitory signals, which can potentially be used as biomarkers to predict the effects a T cell stimulatory biologic. However, the utility of testing for functionality of the PD-1 pathway as a biomarker of hazard needs further investigation and validation.

The metabolic program underlying the excessive activation of CD28SA-activated T cells is unknown. Since, both the activity and fate of T cells are directly linked to their metabolic profile; we decided to investigate the metabolic characteristics of CD28SA-stimulated T cells and compared them to T cells activated via the conventional CD3/TCR route. This is the subject of the next chapter of this thesis.

Chapter FOUR

CD28 superagonist activation of T cells induces a cancer cell-like metabolic program

4. CD28 superagonist activation of T cells induces a cancer cell-like metabolic program

4.1. Abstract

CD28 superagonist (CD28SA), a therapeutic immunomodulatory monoclonal antibody triggered rapid and exaggerated activation of $CD4^+$ effector memory T cells (T_{EM}) in humans with unwanted serious adverse effects. Distinct metabolic programs have been shown to determine the fate and responses of immune cells. Here, we show that human $CD4^+$ T_{EM} stimulated with CD28SA adopt a metabolic program similar to those of cancer cells with enhanced glucose utilization, lipid biosynthesis and proliferation in hypoxic conditions. Identification of metabolic profiles underlying hyperactive T cell activation provides a platform to test safety of immunostimulatory antibodies.

4.2. Introduction

CD28 Superagonists (CD28SAs) are monoclonal antibodies (mAbs) that crosslink CD28 co-stimulatory receptors resulting in potent T cell activation independent of concomitant T cell receptor (TCR) engagement [119]. The CD28SA, TGN1412, triggered an excessive and adverse cytokine release (cytokine storm) when administered to volunteers in a human Phase 1 clinical trial [92]. We and others have shown that CD28SA induces exaggerated activation, polyclonal expansion and migration of $CD4^+$ effector memory T cells (T_{EM}) [92, 120, 121]. The basis for this hyperactive dysregulated phenotype is the subject of much research and the lack of inhibitory inputs [121] has been suggested as one potential mechanism (see previous chapter). T cells need to undergo metabolic reprogramming in order to adapt to their changing metabolic needs as they progress from resting T cells to fully differentiated effectors and memory cells [69]. T cells use glucose as the primary nutrient source for energy generation and biomass production, although amino acids such as glutamine are also utilised [69]. Prior to activation, naive T cells have low metabolic requirements and rely on mitochondrial oxidative pathways for basal energy generation. Upon activation, T cells adopt a metabolic profile typified by aerobic glycolysis and basal oxidative phosphorylation (OXPHOS) [69].

Rapidly proliferating T cells require lipids to support membrane biogenesis and depending on the T cell subset, lipids may be acquired or synthesised (lipogenesis) [122]. T cells use distinct metabolic programs according to their differentiation state and immunological role. Studies have shown that $CD4^+$ T helper (Th) 1, Th2 and Th17 cells are highly glycolytic, while $CD4^+$ regulatory T cells have high lipid oxidation rates [123]. The metabolic phenotype of the TGN1412-target cell, $CD4^+$ T_{EM}, has not been studied. Importantly, the metabolic program that supports the dramatic hyperactivation and proliferation induced by CD28SA is currently unknown. We hypothesised that that superagonistic activation programs $CD4^+$ T_{EM} metabolism to favour enhanced glycolysis and lipogenesis. In order to establish whether CD28SA-stimulated T cells have a lipogenic phenotype, we defined the activity of key enzymes, ATP-citrate lyase (ACL) and acetyl-CoA carboxylase (ACC), involved in the net conversion of glucose to lipid.

4.3. Results

4.3.1. CD28SA-activated T cells display a hyperactive phenotype

We and others have previously shown that CD28SA-activation results in a hyperactive T cell phenotype [121, 124]. T cell activation triggers metabolic programs that promote biomass generation which is evident by an increase in cell size, termed blasting. We used a TGN1412-like CD28SA mAb, termed NIB1412 to stimulate $CD4^+$ T_{EM} and demonstrate that the percentage of blasting T cells in the CD28SA-stimulated condition is about 45% greater than in the CD3-activated condition (Figure 4.1).

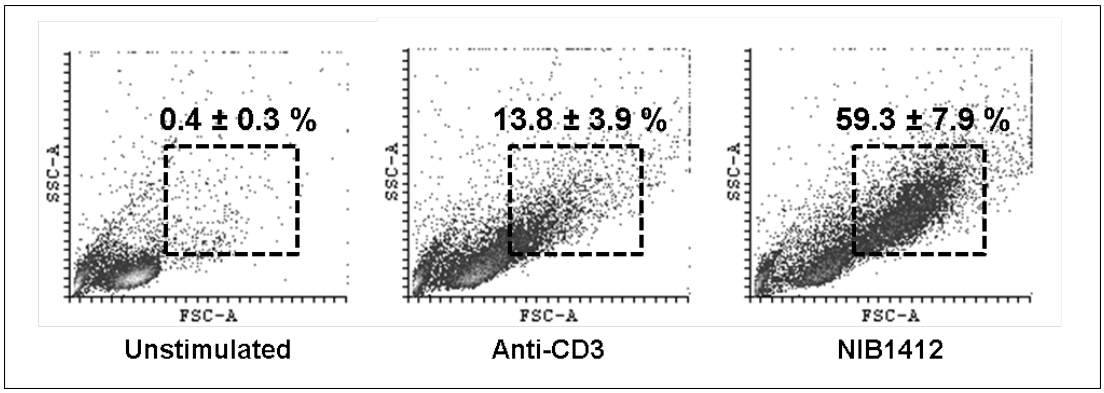

Figure 4.1: CD28SA activation results in greater blasting of $CD4^+$ T_{EM}

(a) Size (forward scatter [FSC]) and granularity (side scatter [SSC]) were quantified by flow cytometry. FSC and SSC were measured on purified human $CD4^+$ T_{EM} stimulated with anti-CD3 or CD28SA for 48 h. Percentages ± SD indicate T cell blasts. The data are representative of four independent experiments. NIB1412 – CD28SA.

4.3.2. CD28SA stimulation maximises OXPHOS potential

Activated immune cells prefer glycolysis over OXPHOS as it is around two orders of magnitude faster for biomass accumulation and proliferation [125]. Nevertheless, OXPHOS is necessary for cell-surface expression of the IL-2 receptor and thus vital for lymphocyte proliferation [126]. To assess the contribution of OXPHOS to meet the energy requirements during hyperactivation of $CD4^+$ T_{EM} upon CD28SA stimulation, we used extracellular flux analysis to measure oxygen consumption rates (OCR) and basal respiration, ATP production, maximal respiration and spare respiratory capacity (SRC) (see methods for details). CD28SA-stimulated T cells had higher basal respiration and ATP production when compared to CD3-activated $CD4^+$ T_{EM} (Figure 4.2 (a)). The high oxygen consumption and ATP production is indicative of enhanced rates of OXPHOS which occurs primarily in the mitochondria [127]. To determine whether CD28SA-stimulated T cells had more active mitochondrial mass, we stained $CD4^+$ T_{EM} with Mitotracker deep red and found that CD28SA-stimulation led to a higher quantity of actively respiring mitochondria than when activated with anti-CD3 mAbs (Figure 4.2 (b) and (c)). CD28SA-stimulated T cells also produced more mitochondrial reactive oxygen species (mitoROS) than CD3-activated $CD4^+$ T_{EM} (Figure 4.2 (d)) which is reflective of enhanced mitochondrial electron transport activity [128]. Collectively, these results indicate that CD28SA-activated cells

maximise their OXPHOS potential which is supported by their greater active mitochondrial mass.

To test whether, CD28SA-stimulated cells are reliant on OXPHOS for their hyperproliferation, we cultured activated $CD4^+$ T_{EM} under hypoxic or normoxic conditions. While, CD3-stimulated cells proliferated more in normoxic than in hypoxic condition (Figure 4.2 (e)), CD28SA-stimulated cells proliferated in both the conditions with higher rate of proliferation in hypoxic condition. This suggests that CD28SA activated T cells have a flexible metabolic program that reduces the reliance on OXPHOS for proliferation.

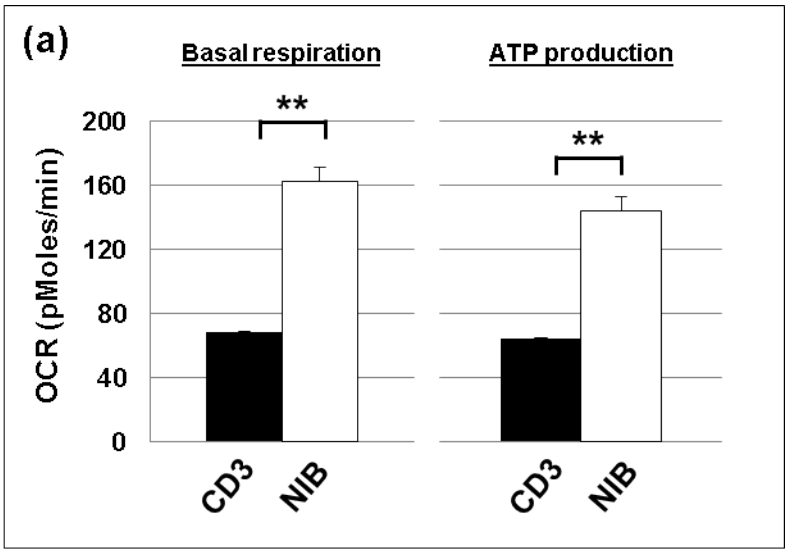
(a)
Basal respiration
ATP production
**
**
200
160
120
80
40
0
OCR (pMoles/min)
CD3
NIB
CD3
NIB

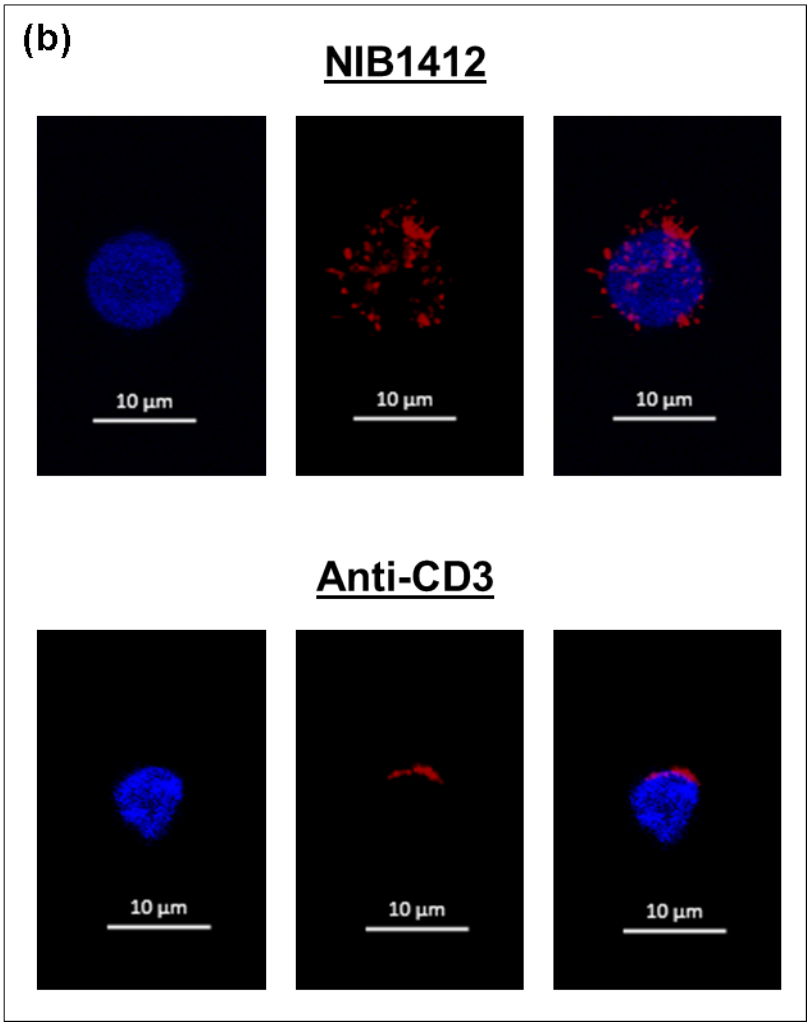
(b)
NIB1412
10 µm
10 µm
10 µm
Anti-CD3
10 µm
10 µm
10 µm

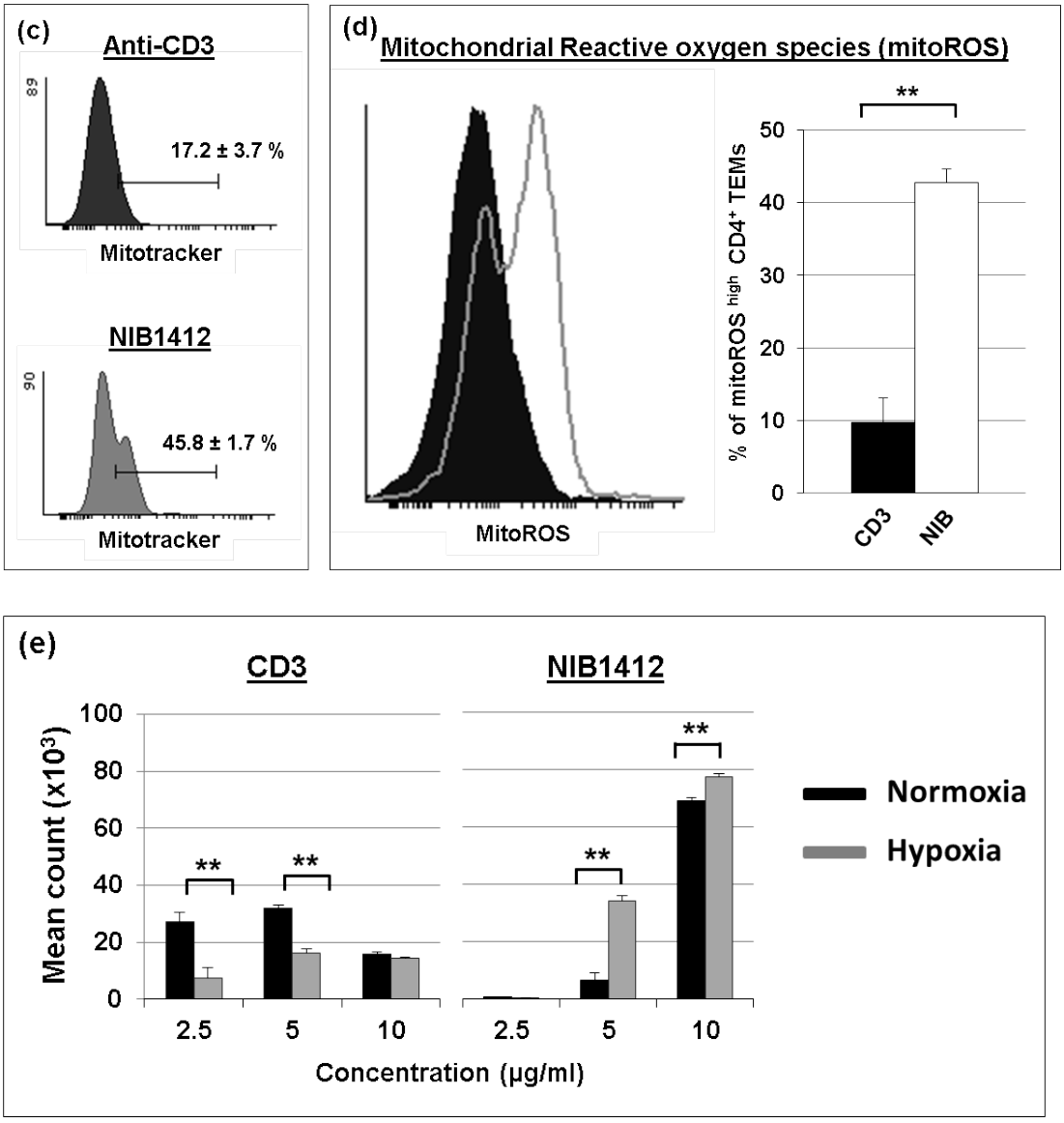

Figure 4.2: CD28SA stimulation maximizes OXPHOS potential

(a) Oxygen consumption rates (OCR; pMoles/min) of pre-activated human $CD4^+$ T_{EM}s were measured using the seahorse XF96 extracellular flux analyser in real time, under basal conditions and in response to sequential addition of Oligomycin (1 µM), 2,4-DNP (160 µM) and Antimycin A & Rotenone (1 µM). Mean OCR values representing basal respiration and ATP production are presented as bar charts. The bars represent the mean ± SD. The data are representative of three independent experiments, (*P < 0.05, **P < 0.01; unpaired, two-tailed Student's t-test).

(b) Immunofluorescent (IF) images of mitochondria. IF images show CD3- and CD28SA-stimulated human $CD4^+$ T_{EM} stained with Mitotracker (red) and Hoechst (blue); Far right quadrant represents merged image of the two stains; scale bars represent 10 µM.

(c) Mitochondria were stained with MitoTracker Deep Red or (d) MitoSOX™ Red Mitochondrial Superoxide Indicator, and the staining intensities were quantified by flow cytometry. Data represent the mean percent of cells ± SD (n=3) staining positive for mitochondria, or mitochondrial ROS (mitoROS), with the mean percent of mitoROS presented in a bar graph. The bars represent the mean ± SD (n=3). ** denotes P-value < 0.01 as calculated by an unpaired, two-tailed Student's t-test

(e) Human $CD4^+$ T_{EM} were stimulated with the indicated concentrations of plate-bound antibodies and incubated in normoxic (20% O_2) or hypoxic (5% O_2) conditions. Proliferation was measured three days post-activation by 3H-labeled thymidine incorporation. The vertical axis represents mean cpm ± SD from triplicate wells. The data are representative of three independent experiments, (*P< 0.05, **P< 0.01; unpaired two-tailed t-test). NIB1412 – CD28SA.

4.3.3. CD28SA stimulation maximises glucose utilization

We next measured extracellular acidification rates (ECAR), a marker of glycolysis, and found that CD28SA-stimulated $CD4^+$ T_{EM} displayed significantly higher glycolysis and lacked glycolytic reserve compared to CD3-stimulated cells (Figure 4.3 (a)). This result indicates that CD28SA-activated cells adopt a metabolic program that maximises basal glycolytic rate. We tested whether the high glycolytic rate was associated with altered glycolytic machinery in $CD4^+$ T_{EM}. The enzyme GAPDH is critical component of the glycolytic pathway that generates pyruvate from glucose (figure 1.8). Studies have shown that GAPDH shuttles between nuclear and cytoplasmic compartments, with cytoplasmic GAPDH being active in glycolysis [129] while nuclear GAPDH is thought to be involved in the initiation of apoptotic cascades [130] and promoting gene transcription [131]. We examined the cellular distribution of GAPDH by immunofluorescence and observed that the distribution of GAPDH staining was coincident with the nuclear contours in CD3-stimulated $CD4^+$ T_{EM}. In contrast, CD28SA-stimulated $CD4^+$ T_{EM} had more dispersed cytosolic distribution of GAPDH (Figure 4.3 (b)). Increased glycolytic rates need to be fuelled by a commensurate increase in the uptake of glucose which is predominantly mediated by the glucose transporter, GLUT1 in T cells [132]. In addition to TCR activation, CD28 costimulation acting through the PI3K/Akt pathway is an important component in increasing glycolytic flux essential for cell proliferation [73]. The

uptake of the fluorescent glucose analog 2-NBDG (Fig 4.3 (c) (i)) and cell surface expression of GLUT1 (Figure 4.3 (c) (ii)) were both higher in CD28SA-stimulated $CD4^+$ T_{EM} than in CD3-stimulated cells.

The ratio of the basal ECAR to OCR indicates the cellular preference for glycolysis versus OXPHOS [133]. Figure 4.3 (d) (i) shows the ECAR/OCR ratio of CD28SA- and CD3-stimulated T cells cultured (in base media with glutamine only) in the absence of glucose (-Glu) or in the presence of glucose (+Glu). In the -Glu condition the ECAR/OCR ratio was significantly lower in CD28SA-stimulated cells than CD3-stimulated cells. In the +Glu condition CD28SA-stimulated cells had a significantly higher ECAR/OCR ratio than CD3-stimulated cells. These plots demonstrate that in the presence of glucose CD28SA-stimulated cells preferentially drive glycolysis, while CD3-stimulated cells also drive OXPHOS. Collectively these results show that CD28SA stimulation drives an adaptable metabolic program that maximises glucose utilisation to drive both OXPHOS and glycolysis depending on glucose availability. This was demonstrated by the cell viability in glucose deficient conditions. The viability of CD28SA-stimulated cells was unaffected after 24hrs while more than 50% of the CD3-stimulated cells died (Figure 4.3 (d) (ii)).

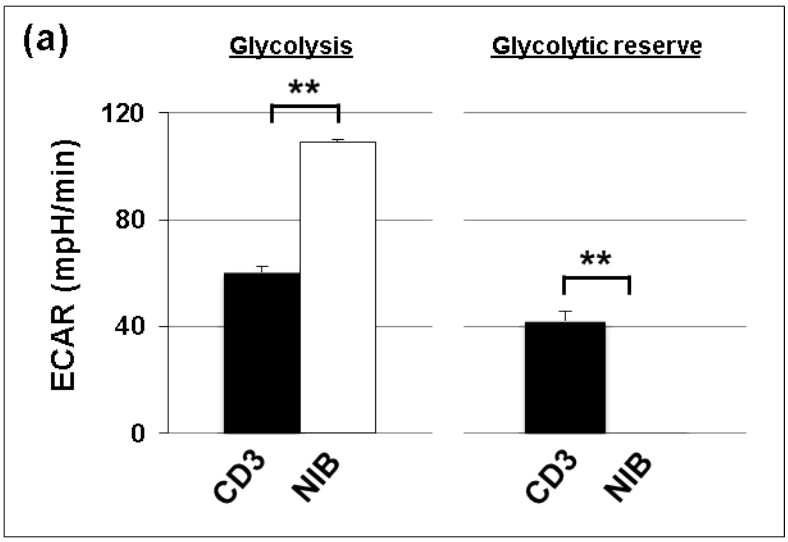
(a)
Glycolysis
Glycolytic reserve
**
**
120
80
40
0
ECAR (mpH/min)
CD3
NIB
CD3
NIB

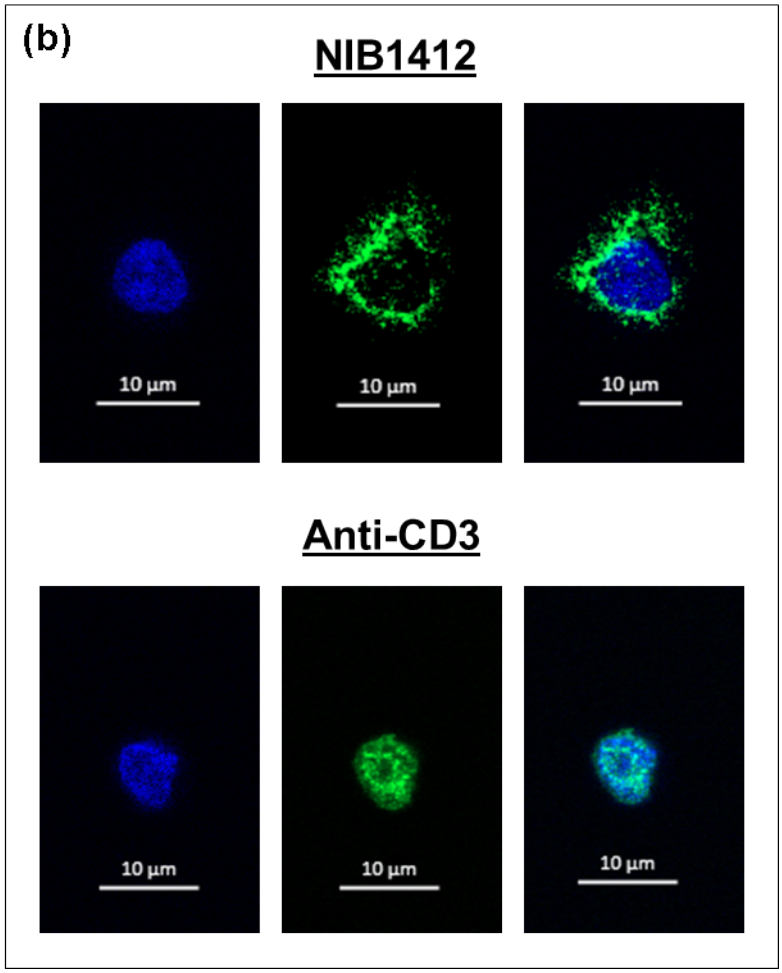
(b)
NIB1412
10 µm
10 µm
10 µm
Anti-CD3
10 µm
10 µm
10 µm

(c)

Fluorescent glucose analog (2NBDG) uptake

(i)

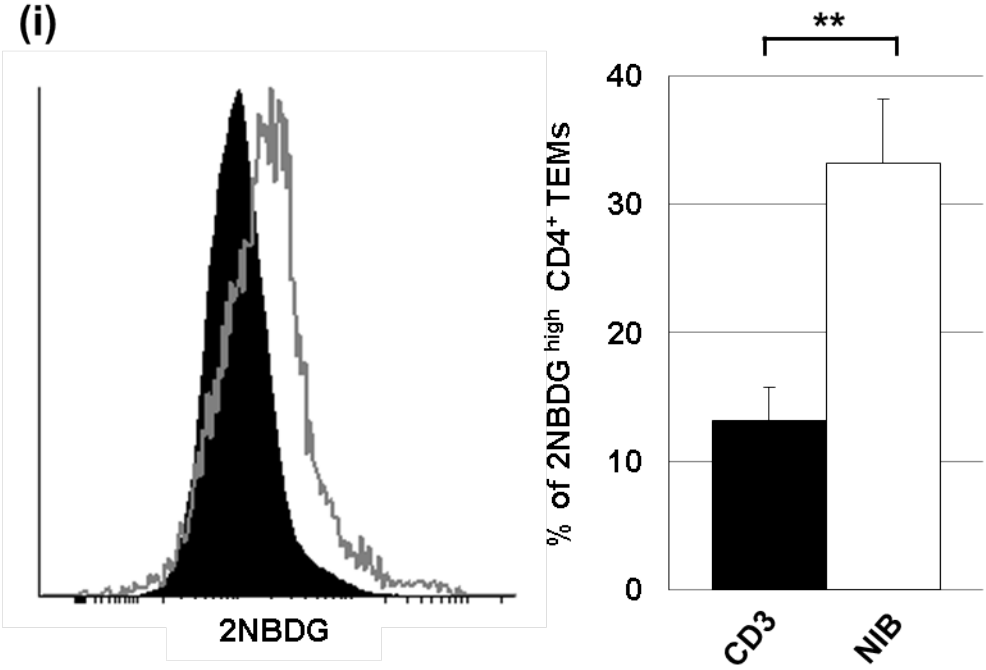

(ii) Cell surface expression of Glut1

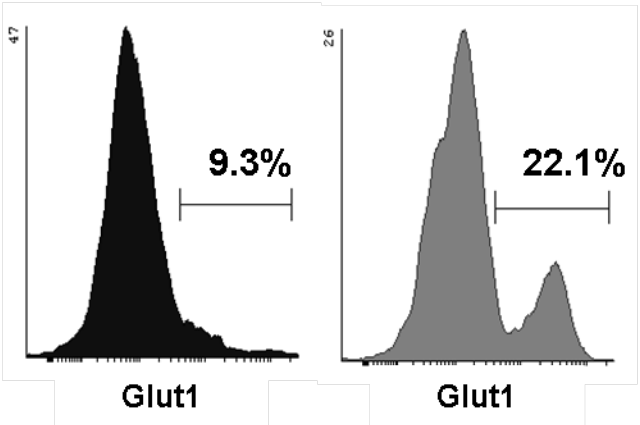

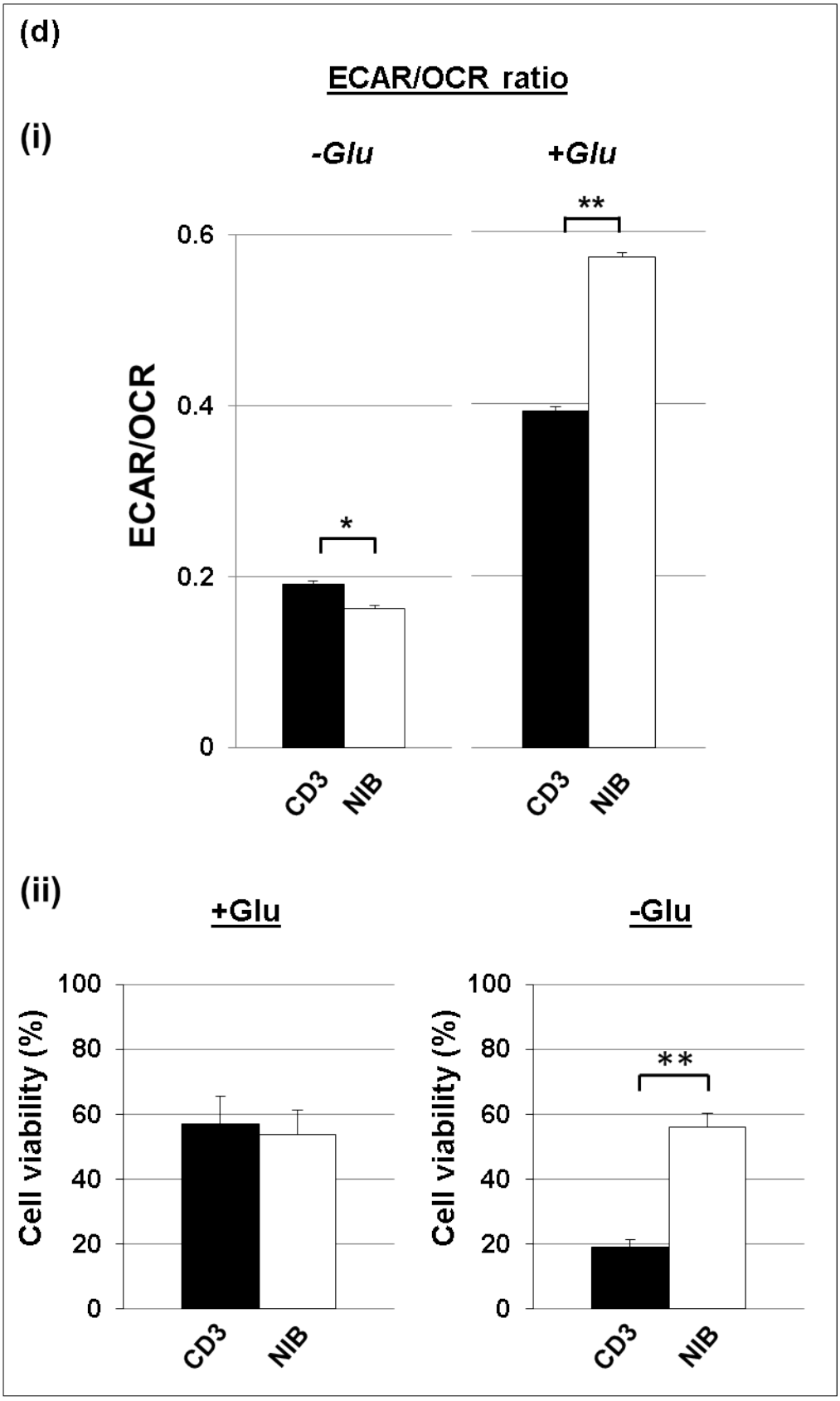

Figure 4.3: CD28SA stimulation maximises glucose utilization

(a) Extracellular acidification rates (ECAR; mpH/min) of pre-activated human $CD4^+$ T_{EMs} were measured using the seahorse XF96 extracellular flux analyzer in real time, under basal conditions

and in response to sequential addition of glucose (10 mM), Oligomycin (1 µM) and 2-deoxy-D-glucose (2-DG) (100 mM). Mean ECAR values representing glycolysis and glycolytic reserve are presented as bar charts. The bars represent the mean ± SD. The data are representative of three independent experiments, (*P < 0.05, **P < 0.01; unpaired two-tailed t-test).

(b) Immunofluorescence images show CD3-and CD28SA-stimulated human $CD4^+$ T_{EM} at 48 h post-activation stained with anti-GAPDH (green) and DAPI (blue); scale bars represent 10 µm. Far right quadrant represents merged image of the two stains.

(c) Human $CD4^+$ T_{EM} were stimulated with anti-CD3 or CD28SA for 48 h. Cells were then incubated with 2-NBDG for 30mins and the amount of (i) 2NBDG uptake was measured by flow cytometry, with the mean percent of 2-NBDG positive $CD4^+$ T_{EM} presented in a bar graph. The bars represent the mean ± SD (n=3). ** denotes P-value < 0.01 as calculated by an unpaired, two-tailed Student's t-test. Cells were also stained for (ii) Glut1 expression.

(d) Basal ECAR and OCR of pre-activated human $CD4^+$ T_{EMs} were measured using the seahorse XF96 extracellular flux analyzer in real time, with the (i) ECAR/OCR ratio presented as bar charts. The bars represent the mean ± SD. The data are representative of three independent experiments, (*P< 0.05, **P< 0.01; two-tailed unpaired t-test). (ii) Cell viability of CD3- and CD28SA-stimulated human $CD4^+$ T_{EM} cultured for 24 h in the presence or absence of glucose. Percentage of viable cells was determined by using trypan blue. The data are representative of three independent experiments. ** denotes P-value < 0.01 as calculated by an unpaired, two-tailed Student's t-test.

NIB1412 – CD28SA.

4.3.4. CD28SA-activated T cells are metabolically programmed to favour lipogenesis

Mitochondrial fatty acid oxidation (FAO; β-oxidation) is a source of acetyl CoA that is used in the TCA cycle for energy generation through OXPHOS [134]. Carnitine palmitoyl transferase (CPT1a) is a metabolic enzyme that controls the rate-limiting step in mitochondrial FAO [135]. To determine whether mitochondrial FAO contributes to OXPHOS, we measured changes in SRC in the presence of the CPT1a inhibitor, etomoxir. In both +Glu and -Glu conditions, around 80% of FAO contributed to the SRC of CD3-stimulated $CD4^+$ T_{EM}. In contrast, only about 30% of FAO contributed to the SRC of CD28SA-stimulated cells in -Glu while there was no contribution of FAO to the SRC in the +Glu conditions (Figure 4.4 (a)).

IL-2-secreting $CD8^+$ effector memory T cells store exogenous long-chain fatty acids in lipid droplets which are then mobilized for mitochondrial FAO [122]. In contrast,

$CD8^+$ memory T cells were shown to use extracellular glucose to synthesise fatty acids for neutral lipid stores [122], which then undergo lipolysis to supply fatty acids for FAO as well as for incorporation into cellular membrane structures. The lipid reserve of T cells is determined by the balance between lipogenesis and rate of FAO [122]. The low rate of FAO in CD28SA-activated $CD4^+$ T_{EM} suggested the possibility that these cells are potentially increasing their lipid reserve. LipidTox staining revealed that CD28SA stimulation (Figure 4.4 (b) (i)) induces a significantly greater accumulation of neutral lipids in $CD4^+$ T_{EM} than when activated with anti-CD3 mAbs (Figure 4.4 (b) (ii)). This was confirmed and quantified by flow cytometry (Figure 4.4 (b) (iii)).

Lipogenesis requires the availability of acetyl-CoA which is an essential substrate for the endogenous biosynthesis of fatty acids. Increased glycolysis can shunt glucose-derived pyruvate into the mitochondria to be decarboxylated to acetyl-CoA, and then condensed with oxaloacetate to form citrate [136]. Citrate is then exported from the mitochondria via the malate-citrate shuttle system and used as a substrate for ATP-citrate lyase (ACL) [137]. We measured the acetyl-CoA content and demonstrate that total acetyl-CoA levels were significantly higher in CD28SA-stimulated $CD4^+$ T_{EM} than in CD3-stimulated cells (Figure 4.4 (c) (i)). ACL is a key cytosolic enzyme that catalyses the generation of acetyl-coenzyme A (CoA) from mitochondria-derived citrate. Acetyl-CoA is then carboxylated to malonyl-CoA by acetyl-CoA carboxylase (ACC) which subsequently results in fatty acid synthesis. The activity of ACL and ACC are increased by serine phosphorylation [138, 139].

The increased lipogenesis in CD28SA-stimulated cells is reflected by the hyperactivity of the lipogenic enzymes, ACL and ACC as determined by their phosphorylation status (Figure 4.4 (c) (ii)). CD28SA stimulation of T cells is known to induce high IL-2 secretion [104]. To rule out the influence of the CD28SA-secreted IL-2 on the *de novo* lipogenesis, we also activated $CD4^+$ T_{EM} with anti-CD3 in combination with IL-2 (aCD3+IL-2), and with anti-CD3 in combination with conventional anti-CD28 (aCD3+aCD28). Since ACC is the rate-limiting enzyme in regulating fatty acid synthesis [140], we measured its activity in these conditions. As can be seen in the results, CD28SA-stimulated cells had significantly greater ACC

phosphorylation than any of the other conditions (Figure 4.4 (c) (iii)). This indicates that the enhanced lipogenic program in CD28SA-activated $CD4^+$ T_{EM} is not secondary to IL-2 effects.

ACL and ACC represent committed steps in channelling glucose-derived metabolites towards a lipid biosynthetic fate which is regulated by PI3K/Akt signalling [141]. This is consistent with the activation of the PI3K pathway by engagement of CD28 by the superagonistic mAb [16]. The Acetyl CoA that feeds lipogenesis is primarily derived from citrate [142]. The citrate can be produced from glucose-derived pyruvate that enters the TCA cycle. A recent study has shown that in cancer cells, glutamine can enter the TCA cycle and also become a source of citrate for *de novo* lipogenesis through reductive carboxylation of glutamine-derived α-ketoglutarate (α-KG) [143] (Figure 1.8). An elevated αKG/citrate ratio was shown to be the principal driving force for reductive glutamine metabolism [143]. We observed that CD3-stimulated $CD4^+$ T_{EM} possessed a high relative αKG/citrate ratio of 2.2± 0.3, suggesting ongoing reductive glutamine metabolism (Figure 4.4 (d)). In contrast, CD28SA-stimulated cells had a low relative α-KG/citrate ratio of 0.6± 0.1 indicative of an absence of reductive carboxylation (Figure 4.4 (d)). Collectively, these results show that CD28SA-stimulated cells have a dominant program of endogenous biosynthesis of fatty acids, which is not accompanied by preferential reductive glutamine metabolism. Cancer cells display increased glycolytic flux where intermediate metabolites are channelled towards acetyl-CoA generation for use in *de novo* fatty acid biosynthesis [144]. We used a variety of different immortal cell lines to assess the activity of ACL and ACC, markers of *de novo* lipogenesis. Figure 4.5 shows ACL and ACC expression in liver hepatocellular cells (HepG2), HeLa cells, ovarian tumour cell line A2780 and the malignant melanoma cell line A375. Increased de novo lipogenesis is a hallmark of cancer cells, and a high glucose-to-lipid flux is correlated with increased proliferative capacity. Our results show that CD28SA stimulation induces a similar metabolic phenotype, where increased glycolytic flux correlates with elevated *de novo* lipogenesis and reduced fatty acid oxidation.

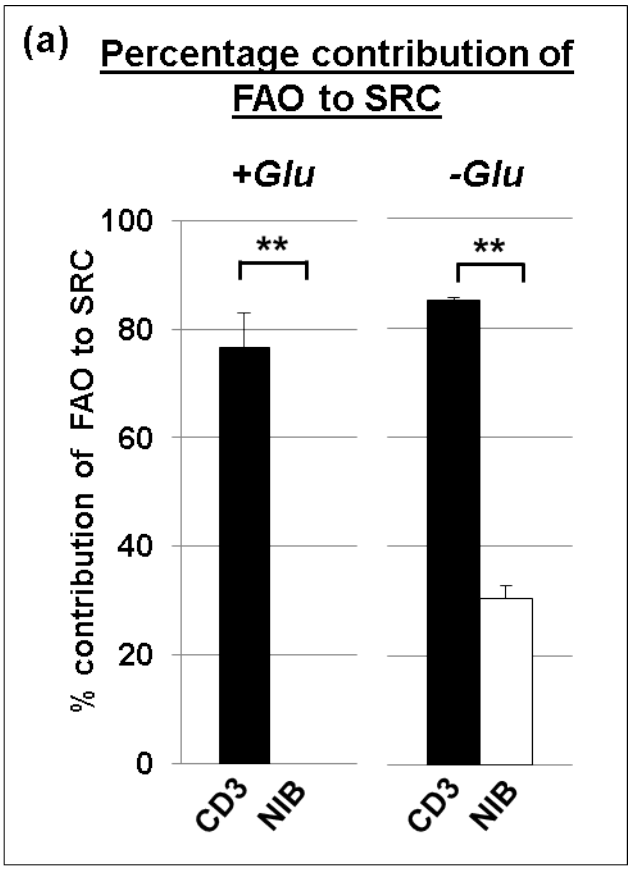
(a)
Percentage contribution of FAO to SRC
+Glu
-Glu
% contribution of FAO to SRC
100
80
60
40
20
0
**
**
CD3
NIB
CD3
NIB

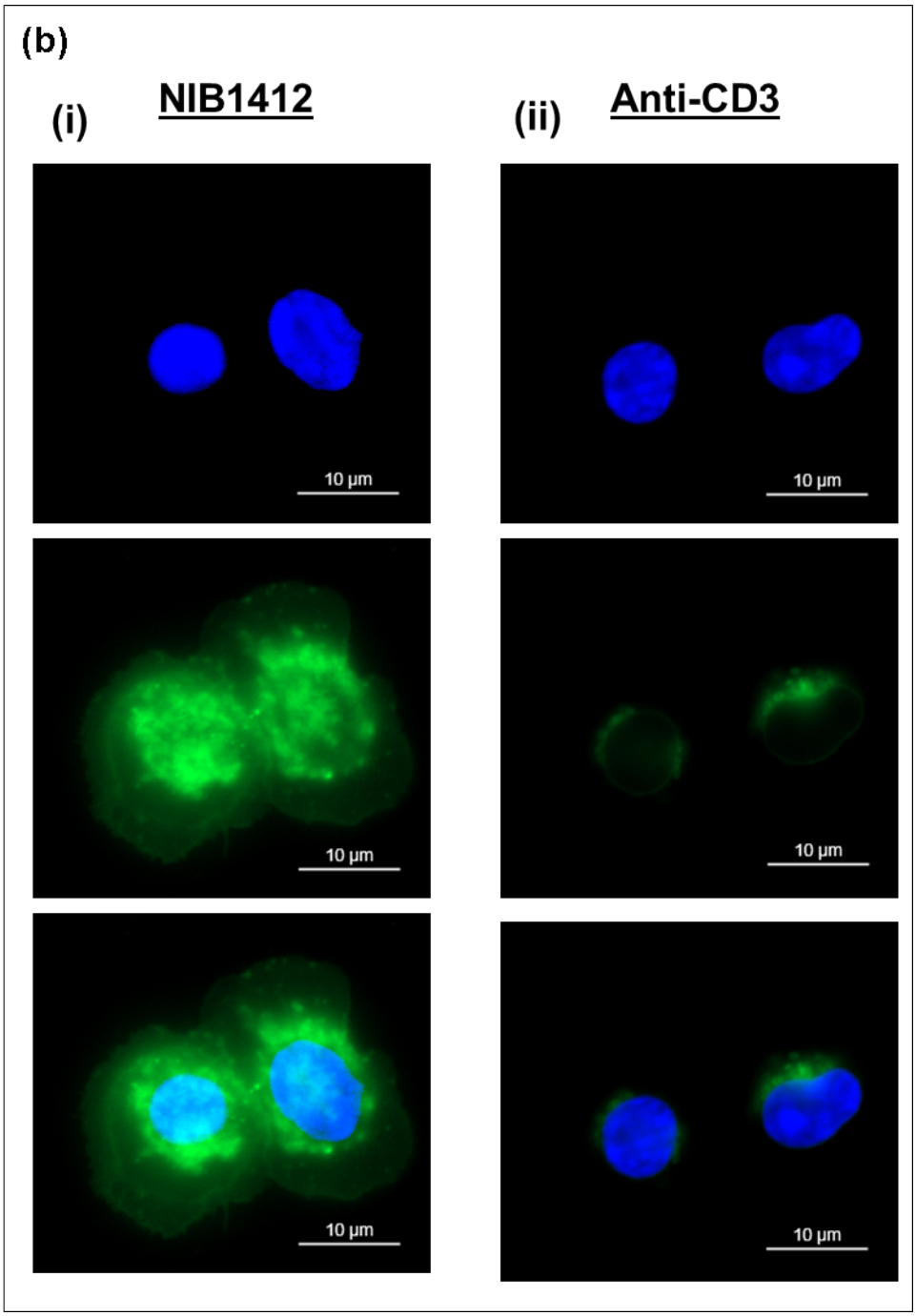
(b)
(i)
NIB1412
(ii)
Anti-CD3
10 µm
10 µm
10 µm
10 µm
10 µm
10 µm

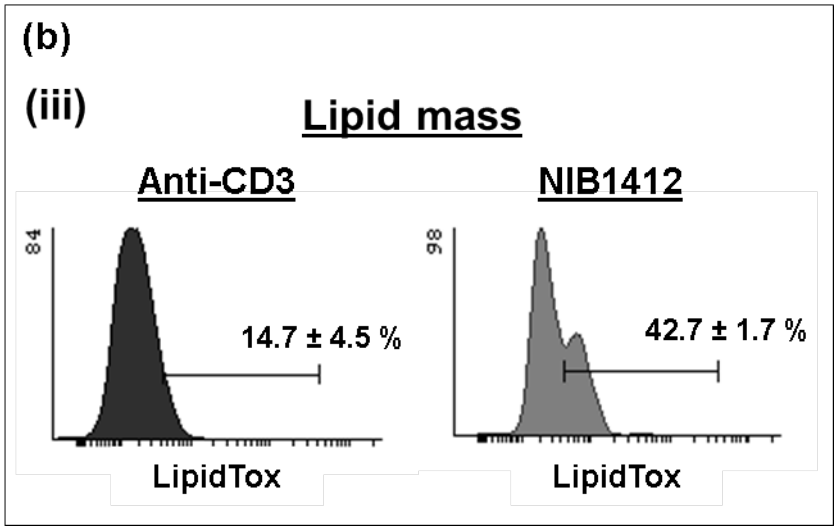
(b)
(iii)
Lipid mass
Anti-CD3
NIB1412
84
98
14.7 ± 4.5 %
42.7 ± 1.7 %
LipidTox
LipidTox

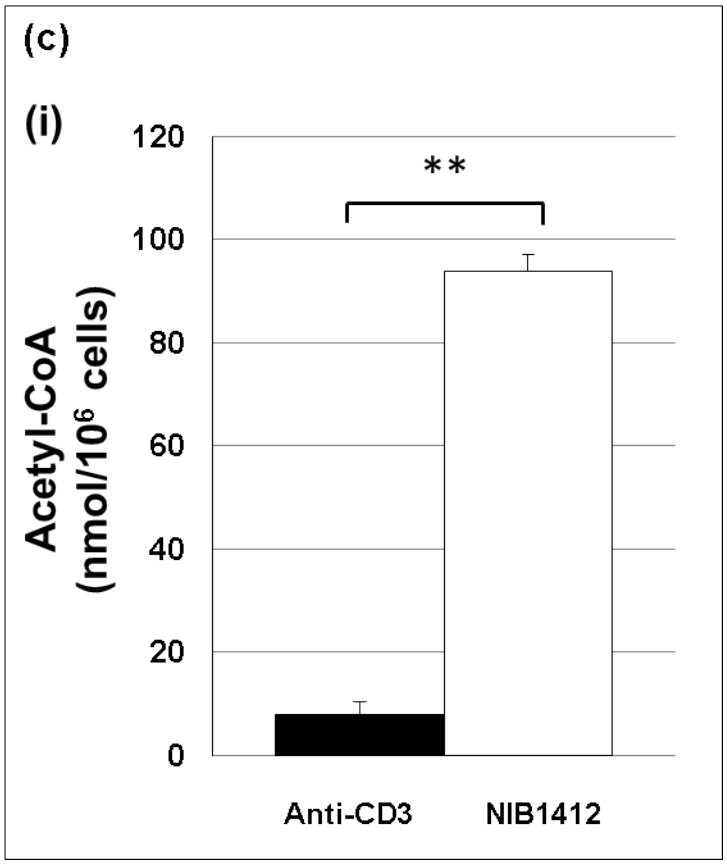
(c)
(i)
120
100
80
60
40
20
0
**
Acetyl-CoA
(nmol/10^6 cells)
Anti-CD3
NIB1412

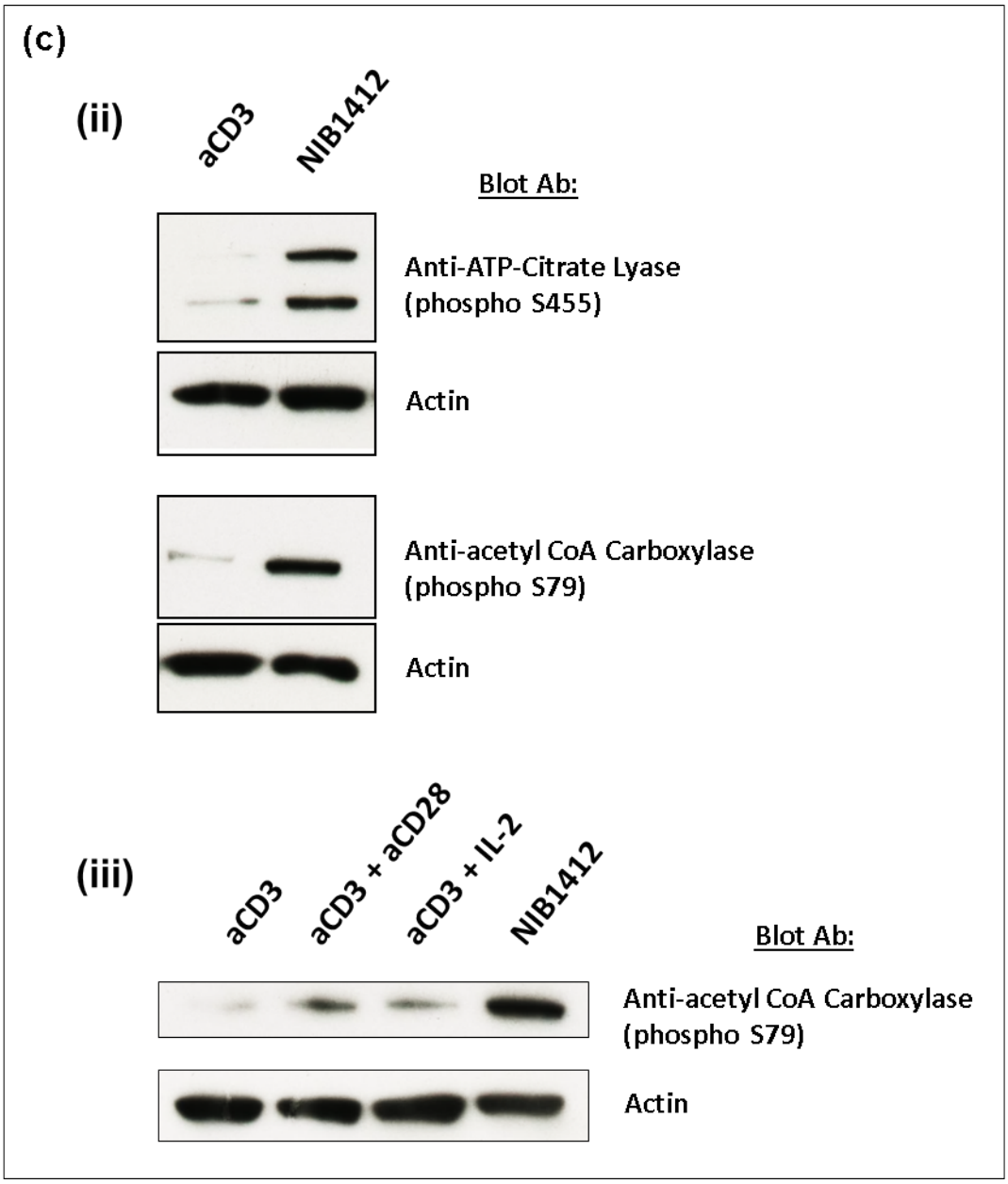
(c)
(ii)
aCD3
NIB1412
Blot Ab:
Anti-ATP-Citrate Lyase
(phospho S455)
Actin
Anti-acetyl CoA Carboxylase
(phospho S79)
Actin
(iii)
aCD3
aCD3 + aCD28
aCD3 + IL-2
NIB1412
Blot Ab:
Anti-acetyl CoA Carboxylase
(phospho S79)
Actin

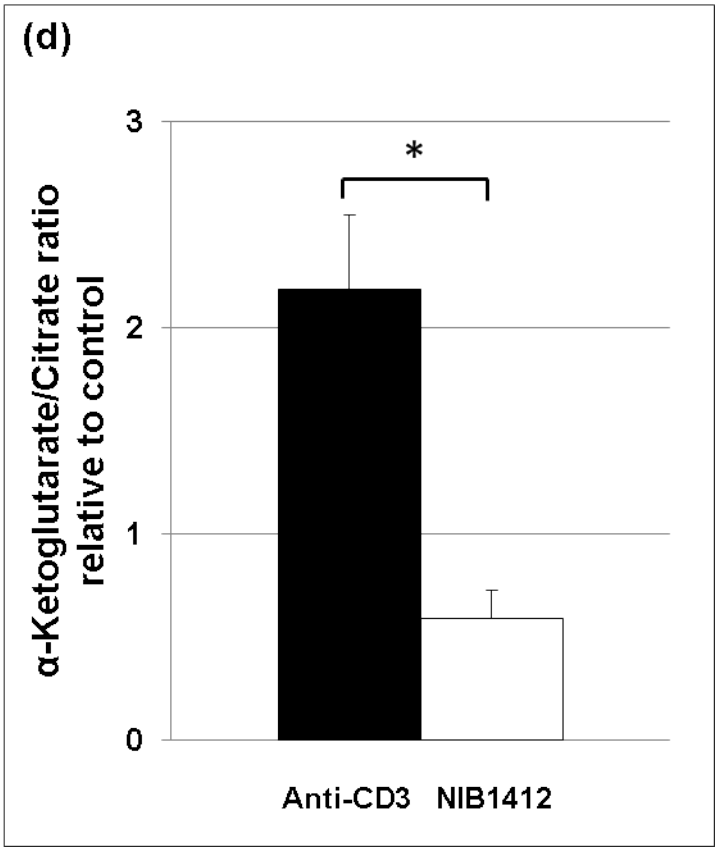

Figure 4.4: CD28SA activation induces *de novo* lipogenesis

(a) Oxygen consumption rates (OCR; pMoles/min) of pre-activated human $CD4^+$ T_{EMs} were measured using the seahorse XF96 extracellular flux analyser in real time, under basal conditions and in response to sequential addition of Oligomycin (1 µM), 2,4-DNP (160 µM) and Antimycin A & Rotenone (1 µM). Etomoxir (200 µM) or media was injected after 2,4-DNP injection. The SRC (quantitative difference between maximal uncontrolled OCR [± etomoxir treatment] and initial basal OCR) was calculated and presented as the percentage contribution of FAO to SRC in bar charts. The bars represent the mean ± SD. The data are representative of three independent experiments, (** denotes P-value < 0.01 as calculated by an unpaired, two-tailed Student's t-test).

(b) Immunofluorescence images show (i) CD28SA- and (ii) CD3-stimulated $CD4^+$ T_{EM} at 48 h post-activation stained with LipidTOX (green) and DAPI (blue); scale bars represent 10 µm. Far bottom quadrant represents merged image of the two stains. (iii) LipidTOX staining was quantified by flow cytometry. Data represent the mean percent of cells ± SD (n=3) staining positive for neutral lipids.

(c) (i) Relative levels of acetyl-CoA in anti-CD3- and NIB1412-stimulated human $CD4^+$ T_{EMs} at 48 h post-activation; mean ± SD of triplicates (**P < 0.01; unpaired two-tailed Student's t-test). (ii) Western blot analysis of p-ACL (125kDa) and p-ACC (250kDa), and (iii) p-ACC with IL-2 condition, in anti-CD3- and CD28SA-stimulated $CD4^+$ T_{EM} at 48 h post-activation. Actin (45kDa) was used as a loading control.

(d) Alpha-ketoglutarate-to-citrate ratio in CD3- and CD28SA-stimulated human $CD4^+$ T_{EM} at 48 h post-activation, presented as bar charts. The bars represent the mean ± SD of triplicates (*P < 0.05; unpaired two-tailed Student's t-test).

NIB1412 – CD28SA.

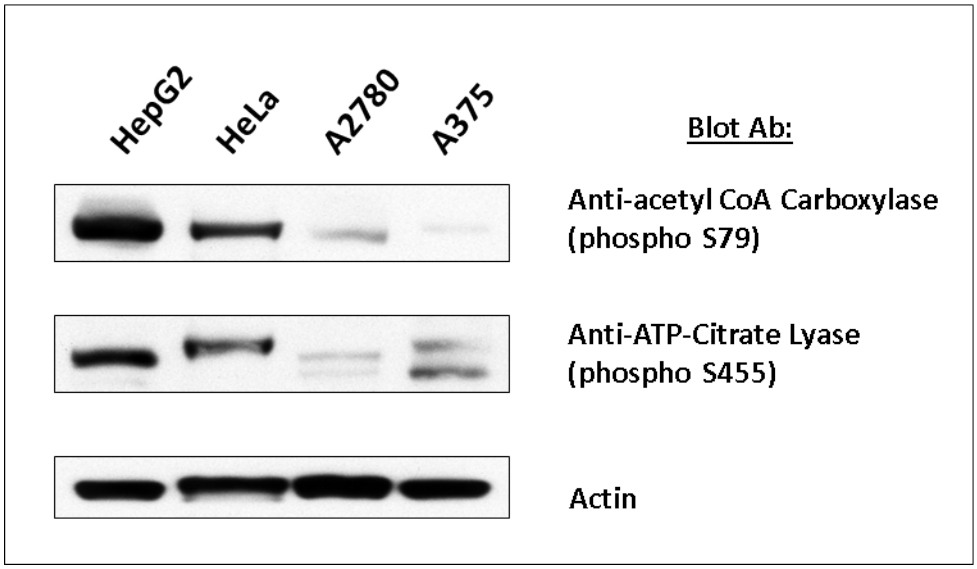

Figure 4.5: Immortalized cell lines display markers for *de novo* lipogenesis

Western blot analysis of p-ACC (250kDa) and p-ACL (125kDa) in liver hepatocellular cells (HepG2), human cervical cancer cells (HeLa), human ovarian tumour cell line (A2780) and human malignant melanoma cell line (A375). Actin (45kDa) was used as a loading control.

We also analysed the autophagy protein LC3 to reveal the autophagic activity in CD28SA-stimulated cells. As shown in figure 4.6, NIB1412-stimulated T_{EMS} had significantly higher levels of LC3 II than anti-CD3-stimulated cells.

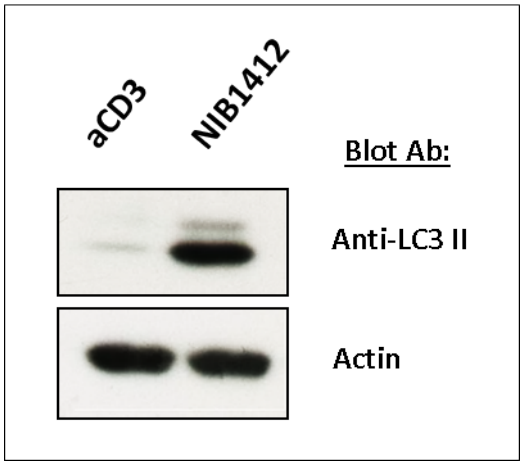

Figure 4.6: CD28SA activation induces autophagy

Western blot analysis of endogenous LC3 expression from human $CD4^+$ T_{EMS} activated with anti-CD3 mAbs or NIB1412. The modification of LC3-I (18kDa) to LC3-II (16kDa) indicates autophagic activity. Actin (45kDa) was used as a loading control.

4.4. Discussion

Immunostimulatory mAbs are common in clinical trials as a strategy to increase immune responses. The dramatic immunostimulatory activity comes with side effects such as the induction of pro-inflammatory mediators and organ-specific autoimmunity. Recognising metabolic patterns in immune cells treated with therapeutic mAbs could serve as novel biomarkers of hazard. For example, aberrant nutrient uptake and utilization, together with increased *de novo* lipid biosynthesis could lead to dysregulated immune cell number and function.

Hyperactive cells such as cancer cells are known to undergo a metabolic shift towards glycolysis and pronounced increase in *de novo* lipid biosynthesis, to promote rapid cell proliferation and migration. Accumulated neutral lipid stores are then mobilized to provide free fatty acids to promote production of signalling lipids, for incorporation into cellular membranes or for the production of ATP via β-oxidation [145]. Prior to activation, idle T cells have low metabolic requirements and rely on mitochondrial oxidative pathways for basal energy generation. Upon activation T cells adopt a metabolic profile typified by aerobic glycolysis and basal OXPHOS. T cells use distinct metabolic programs according to their differentiation state and immunological role. Studies have shown that $CD4^+$ T helper (Th) 1, Th2 and Th17 cells are highly glycolytic, while $CD4^+$ regulatory T cells have high lipid oxidation rates [123]. The metabolic program of $CD4^+$ effector memory T cells is unknown. Here we show the bioenergetic profile adopted by T_{EM}s that have been activated via the conventional TCR/CD3 pathway and through maximal CD28 stimulation using a CD28SA.

Previous studies have shown that IL-2 secreting $CD8^+$ T_{EM}s store exogenously derived fatty acids, while $CD8^+$ memory T cells use extracellular glucose for the endogenous biosynthesis of fatty acids to support mitochondrial FAO [122]. Although the dynamics of fatty acid utilization for FAO hasn't been shown in $CD4^+$ T cells, in this report we propose that CD28SA stimulation enables $CD4^+$ T_{EM}s to maximize glucose utilization and promote endogenous biosynthesis of fatty acids. The increased lipogenesis in CD28SA-stimulated cells is reflected by the hyperactivity of the lipogenic enzymes, ATP citrate lyase and acetyl-CoA carboxylase

(figure 4.4 (c)). In contrast to anti-CD3-stimulated cells, CD28SA-stimulated cells had accumulated intracellular levels of neutral lipids (figure 4.4 (b) iii) which further support the CD28SA-induced exacerbated endogenous biosynthesis of fatty acids. *De novo* fatty acid biosynthesis is not only required to synthesize new membranes for cell proliferation but also to facilitate the formation of lipid rafts for increased signalling of cell surface receptors associated with pro-stimulation [144]. This is in agreement with our previous report [121] where we showed an upregulation of pro-stimulatory receptors on CD28SA-stimulated cells.

The irreversible injury of respiration in normal cells gives rise to the malignant transformation towards a cancer phenotype. Cancer cells display an altered metabolism characterised by increased rates of intracellular glucose import, higher rate of glycolysis associated with reduced pyruvate oxidation and increased lactic acid production. A key distinguishing feature of cancer cell metabolism is reduced fatty acid oxidation and increased *de novo* fatty acid synthesis [146], to promote rapid cell proliferation and migration [147]. Although the dynamics of fatty acid utilization for FAO hasn't been shown in $CD4^+$ T_{EM}, in this report we propose that CD28SA stimulation enables $CD4^+$ T_{EM} to maximize glucose utilization and promote endogenous biosynthesis of fatty acids.

A common component of the cancer phenotype is adaptation to hypoxia, which requires increased glycolysis. Furthermore, poor prognosis, increased tumour aggressiveness and invasiveness are correlated with increased glucose uptake [148]. ACL and ACC expression in liver hepatocellular cells (HepG2), HeLa cells, ovarian tumour cell line A2780 and the malignant melanoma cell line A375 were also determined. Increased de novo lipogenesis is a hallmark of cancer cells, and a high glucose-to-lipid flux is correlated with increased tumour aggressiveness. ACL is the regulator of the key step that converts high glycolytic flux into increased lipid synthesis, required for membrane production during cell proliferation [149]. The glycolytic phenotype together with upregulated ACL activity thus confers a significant proliferative advantage to cancer cells. The elevated expression of ACL and ACC in CD28SA-activated T cells corresponds with their elevated proliferative

capacity and increased migration/tissue invasion; characteristics shared by cancer cells.

Autophagy is a cellular degradation pathway for the clearance of damaged or redundant proteins and organelles. The degradation products of the recycled intracellular constituents can be funnelled into biosynthetic pathways or used as an alternative energy source to maintain cell viability. Rapidly proliferating cancer cells have high metabolic demands and heavily rely on autophagy to supply biosynthetic metabolites [150]. Here, we show that CD28SA-activated T cells display high expression of the autophagy marker LC3-II. Thus, autophagy significantly contributes to the high metabolic demands of CD28SA-activated T cells.

A significantly higher mitochondrial mass and mitoROS was observed in CD28SA-stimulated cells compared to anti-CD3 stimulated cells. MitoROS production is regulated by mitochondrial membrane potential ($\Delta\psi m$), metabolic state of mitochondria and O_2 concentration[151]. The mitochondrial mass itself is not positively correlated with mitoROS as mitochondrial biogenesis also increases the expression of several antioxidant enzymes [152]. Mitochondrial mass and $\Delta\psi m$ are known to be significantly increased in cells during cell cycle, particularly when they are at the S phase [153] and we have shown in a previous study [121] that a high proportion of CD28SA-stimulated cells are in S-phase at 48hrs post-activation and onwards. Thus, the elevated mitochondrial mass and mitoROS might be due to the rapid cell proliferation induced by CD28SA activation. Studies have shown that an increase in mitochondrial mass results in an increase in overall mitochondrial function, with a boost in residual OXPHOS capacity and an increase in overall ATP generating capacity [154, 155]. This concurs with the results shown in figure 4.2 (a); elevated mitochondrial mass coincides with high basal respiration and high ATP production in CD28SA-stimulated T cells.

In summary, we have shown that CD28SA activation induces a T cell metabolic program that is geared towards maximal glucose utilization, endogenous lipid synthesis and less dependency on OXPHOS. We have also defined ACL and ACC as the molecular components that enable this metabolic program to operate. Our

study provides insights into the remarkable capacity of T cells to adopt a variety of distinct metabolic programming depending on the pathways that are engaged. Our results may also have implications and utility in drug development as dysregulated metabolic patterns in immune cells treated with therapeutic mAbs could serve as novel biomarkers of hazard or risk identification. For example, aberrant nutrient uptake and utilization, together with increased *de novo* lipid biosynthesis could be indicative of excessive immunostimulatory potential of the therapeutic mAb. Metabolic studies that compare a number of immunostimulatory therapeutic mAbs are required to examine this further.

Overall, metabolic patterns are important in determining the functional potential of effector T cells. Here we have looked at a potent immune stimulant and the resulting metabolic program adopted by effector memory $CD4^+$ T cells. The next chapter looks at functional output and metabolic profiles of TCR-activated cytotoxic $CD8^+$ T cells that have suffered inhibition by a potent immune suppressant; TGF-β. We also examine whether a mitochondria localised antioxidant can rescue the TGF-β-imposed T cell suppression.

Chapter FIVE

Defining the role of oxidative stress in TGF-β-associated functional and metabolic alterations in T cells

5. Defining the role of oxidative stress in TGF-β-associated functional and metabolic alterations in T cells

5.1. Abstract

TGF-β has profound inhibitory effects on the immune system by directly inhibiting T cell proliferation and activation. Here we investigate the effects of the mitochondrial ROS scavenger Tiron in mouse transgenic F5-TCR $CD8^+$ T cells activated in the presence of TGF-β. T cells stimulated with NP68 in the presence of Tiron had significantly greater mitochondrial respiration and glycolysis. Upon TCR re-stimulation, T cells activated with NP68 in the presence of Tiron had significantly higher IFN-γ and IL-2 production. We demonstrate that Tiron neutralizes the TGF-β-mediated suppressive effects and restores $CD8^+$ effector functions. We propose that immunotherapies targeted to counteract the immunosuppressive effects of tumor-derived TGF-β could be supplemented with antioxidants to help restore $CD8^+$ T cell-mediated tumor eradication.

5.2. Introduction

The majority of immunomodulatory mAbs are aimed at enhancing the anti-tumour effects of T cells but fail in light of tumour-derived TGF-β, an immunosuppressive cytokine that effectively inhibits the generation of a cytotoxic T cell response. Interfering with TGF-β-induced immune suppressive mechanisms could maximise the therapeutic effectiveness of immunomodulatory mAbs in eliciting anti-tumour activity. Tumour cells utilize a number of immune evasion strategies that take advantage of the LAG-3, TGF-β, and cell-intrinsic PD-1 inhibitory pathway of T cells. Tumour cells express the ligands to the inhibitory receptors expressed on T cells and evade elimination by the immune system. Tumour cells secrete TGF-β to enhance metastagenicity while inhibiting cytotoxic T cell-mediated immune responses [7]. TGF-β has profound inhibitory effects on the immune system by directly inhibiting T cell proliferation and activation. The significance of TGF-β is reflected in TGF- β null mice which present lymphocyte-mediated multifocal inflammation [156]. TGF-β exerts its functional effects by inducing prolonged generation of reactive oxygen

species (ROS) and persistent disruption of mitochondrial membrane potential [157]. In addition, TGF-β suppresses the transcriptional activity of the genes related to mitochondrial biogenesis and function [158].

The redox status of a cell can regulate various responses ranging from proliferation and activation, to cell death. Although there are multiple sources of reactive oxygen species (ROS) in the cell, mitochondrial metabolism represents the major source of ROS production and it has been recently shown that mitochondrial ROS (mitoROS) directly stimulate the production of proinflammatory cytokines via distinct molecular pathways [159]. ROS are thought to modulate T cell reactivity by enhancing and prolonging the antigen specific proliferative response in T cells. Optimal ROS levels are required for proper T cell activation and are important in determining T cell fate [160]. Low ROS levels leads to improper TCR stimulation with low activation and proliferation, whereas high ROS levels can lead to increased apoptosis due DNA damage and activation of p53 induced-genes. Depending on the redox state, ROS production can switch T cells towards a more hyporesponsive or proliferative phenotype. Persistent and prolonged ROS production can lead to oxidative stress and is thought to play an important role in the hyporesponsiveness of T cells in various inflammatory conditions [161]. In contrast, ROS production shortly after TCR engagement in resting T cells can act as an amplifier of Ca^{2+}-dependent steps in T cell activation and is essential for activation-induced IL-2 secretion [162]. Mammalian cells have a number of antioxidant enzymes to scavenge mitoROS. The SOD family of antioxidant enzymes catalyse the dismutation of $O_2^{\cdot-}$ to H_2O_2, which is then quickly reduced to water by two other enzymes, catalase and glutathione peroxidase (GPx) [151].

Since TGF-β deregulates cellular redox state and appears to inhibit mitochondrial respiration and ATP synthesis, we focused our attention on the mitochondria-localized synthetic ROS scavenger Tiron (Sodium 4,5-dihydroxybenzene-1,3-disulfonate), to determine whether this antioxidant can rescue the suppressive effects of TGF-β on TCR-activated T cells. The present study evaluates the effect of Tiron on T cell metabolism, LAG-3 and IL-2R (CD25) receptor expression and its effects on TCR re-stimulation-induced T cell proliferation and, IL-2 and IFNγ

production. To induce antigen-specific T cell activation we utilized a TCR transgenic mouse model wherein the TCR (F5-TCR) of the $CD8^+$ T cells can specifically be activated by an antigenic peptide, NP68.

5.3. Results

5.3.1. TGF-β reduces TCR-induced LAG-3 and CD25 expression and inhibits T cell proliferation

To assess the effect of TGF-β on the proliferative ability of mouse F5 lymphocytes, we stimulated T cells with various concentrations of NP68 in the presence or absence of TGF-β. TGF-β significantly ($p<0.01$) reduced TCR-induced proliferation at all concentrations of NP68 (figure 5.1).

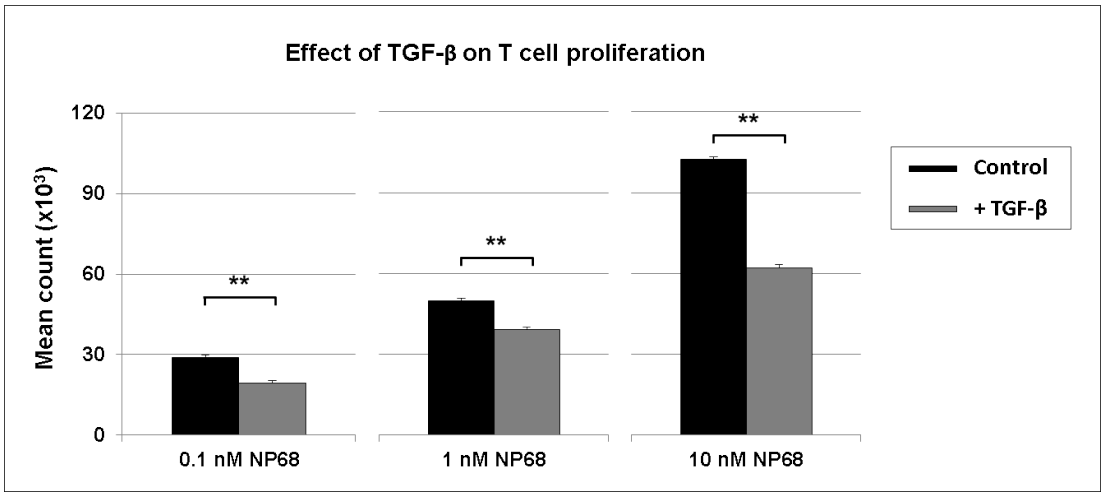

Figure 5.1: TGF-β suppresses TCR-stimulated T cell proliferation

Mouse F5 CD8 T cells were stimulated with the indicated concentrations of antigenic peptide NP68 and proliferation was measured three days post-activation by ^{3}H-labeled thymidine incorporation. The vertical axis represents mean cpm ± SD from triplicate wells. The data are representative of four independent experiments, (**$p < 0.01$; unpaired t-test).

Upon T cell stimulation, expression of cell surface receptors indicates differentiation of the naive $CD8^+$ T cell population into activated CTLs. Cytokines play a vital role in maintaining the homeostasis of $CD8^+$ T cells. In order to assess whether TGF-β influences the expression of surface receptors, we assessed the expression of a range of stimulatory (CD25, CD137 and CD69) and inhibitory (LAG-3, PD-1, BTLA, TIM-3 and TIGIT) receptors on $CD8^+$ T cells activated with a range of NP68

concentrations (0 to 1µM) in the presence or absence of TGF-β by flow cytometry. TGF-β was found to only influence the expression of CD25 and LAG-3 receptors on T cells activated with 1nM NP68 (figure 5.2). NP68 at 1nM was shown to be the optimal working concentration and was predominantly used for the rest of this study.

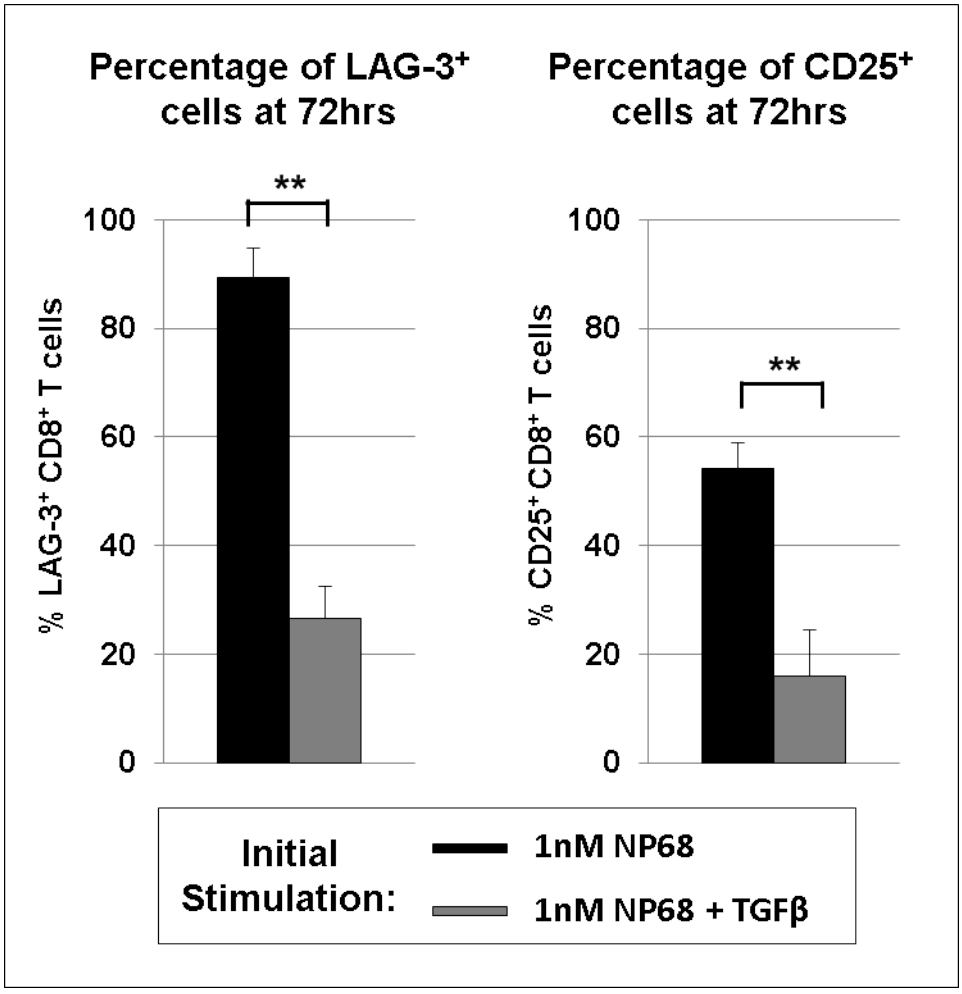

Figure 5.2: TGF-β significantly reduces LAG-3 and CD25 expression on TCR-stimulated T cells

Mouse F5 CD8 T cells were stimulated with 1nM of antigenic peptide NP68. Cells were harvested at 72hours post-activation and stained with fluorochrome-conjugated anti-CD8 and anti-LAG-3 or anti-CD25 antibodies followed by flow cytometric analysis. The mean percent of $CD8^+$ cells staining positive for LAG-3 or CD25 are presented in a bar graph. The bars represent the mean± SD (n=3). (**p< 0.01; unpaired ttest)

In addition to TGF-β, the influence of IL-6 and IL-23, cytokines that promote tumor growth, and the influence of IL-2, a cytokine that mediates tumor regression, on CD25 and LAG-3 receptor expression was also examined (figure 5.3). IL-6 has both

pro-inflammatory and anti-inflammatory properties while IL-23 is thought to be involved in the negative regulation of CD8 T cell functions [163].

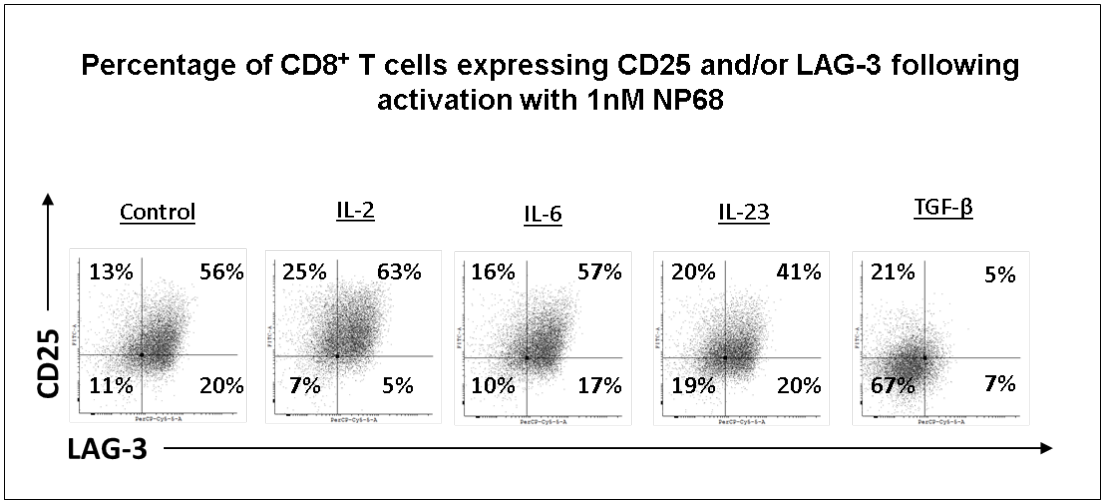

Figure 5.3: Influence of other cytokines on LAG-3 and CD25 expression

Mouse F5 CD8 T cells were stimulated with 1nM of antigenic peptide NP68 in the presence of IL-2, IL-6, IL-23 or TGF-β. Cells were harvested at 72hours post-activation and stained with fluorochrome-conjugated anti-CD8 and anti-LAG-3 or anti-CD25 antibodies followed by flow cytometric analysis. Populations of cells are shown in each quadrant as percentages of total T cells staining positive or negative for the respective markers. Results are representative of four independent experiments.

Since TGF-β reduces LAG-3 receptor expression on activated $CD8^+$ T cell, we assessed whether the functional output was also affected. Our results show that IFN-γ secretion of T cells that were stimulated with NP68 in the presence of TGF-β was reduced when re-stimulated at 72hours with NP68-pulsed dendritic cells (DCs) in the presence of LAG-3 blockade (figure 5.4). We used matured DC for re-stimulation since they express the LAG-3 ligand MHC class II.

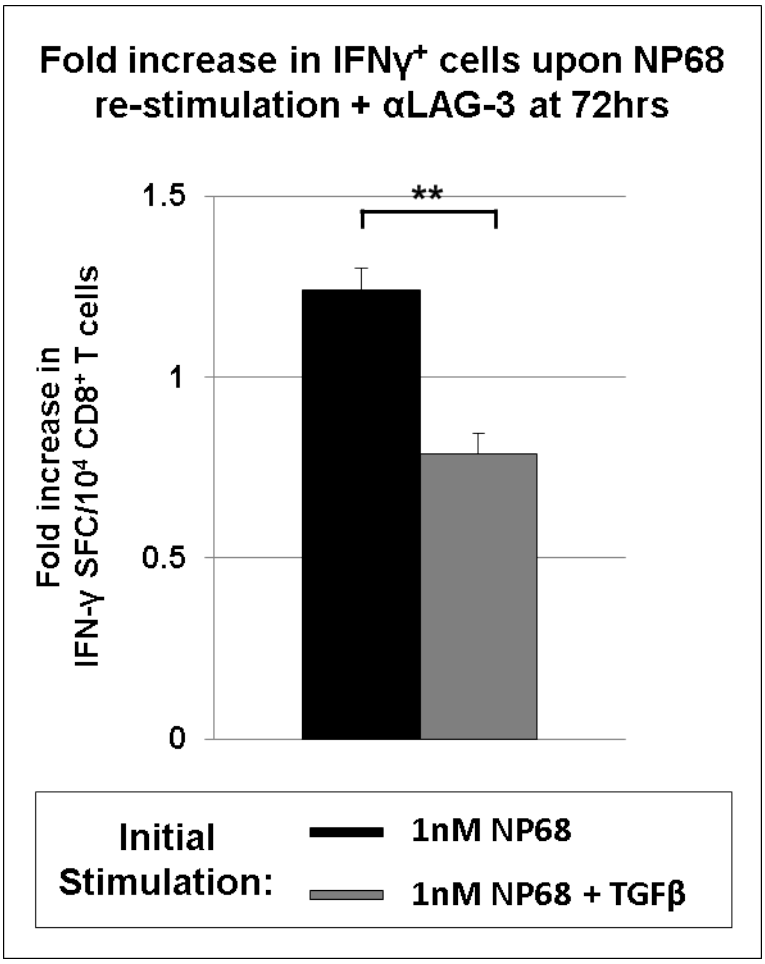

Figure 5.4: TGF-β experienced T cells are less responsive to LAG-3 blocking

Matured mouse dendritic cells were pulsed with 1nM of antigenic peptide NP68 and incubated with F5 CD8 T cells in a DC: T cell ratio of 1:20 for 12hours. The figure shows the results of the IFN-γ specific ELISpot assays (triplicate means± SD; **p< 0.01; unpaired ttest)

To test whether CD25 and LAG-3 are functionally important, a T cell proliferation assay with IL-2 supplementation or LAG-3 blockade was done (figure 5.5). The binding of IL-2 to CD25 enhances proliferation while addition of LAG-3 blocking antibody also increases proliferation. This shows that CD25 expression is important for IL-2-mediated survival while LAG-3 expression inhibits proliferation under physiological conditions.

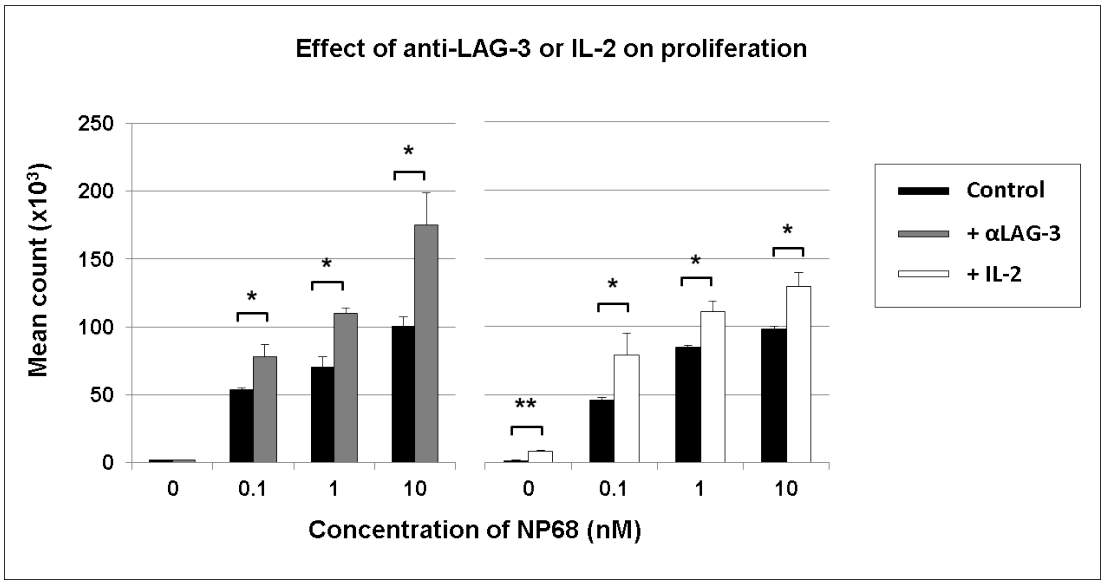

Figure 5.5: IL-2 supplementation or LAG-3 blockade increases T cell proliferation

Mature DCs were pulsed with increasing concentrations of NP68 antigenic peptide and then co-cultured with F5 CD8 T cells for 72 h. ^{3}H-labeled thymidine (^{3}H-Thy) was added for the last 16 h. Proliferation of T cells was determined by scintillation counting of incorporated ^{3}H-Thy. Data are presented as mean ^{3}H-Thy scintillation counts ± S.D. (*p< 0.05; **p< 0.01; unpaired ttest)

5.3.2. MitoROS scavenger increases TGF-β-induced reduction in LAG-3 and CD25 expression

We next investigated whether we could rescue the reduction in LAG-3 and CD25 expression on NP68-activated T cells that suffered inhibition by TGF-β with the mitochondrial ROS scavenger Tiron (added 24hrs after T cell activation as mitoROS produced upon TCR stimulation is essential for T cell expansion [164]). The population of T cells stimulated with 1nM NP68 in the presence of Tiron had significantly ($p<0.01$) higher LAG-3 and CD25 expression than T cells stimulated with NP68 only at 72 hours (figure 5.6). Furthermore, Tiron countered the TGF-β-induced reduction in LAG-3 and CD25 expression (figure 5.6).

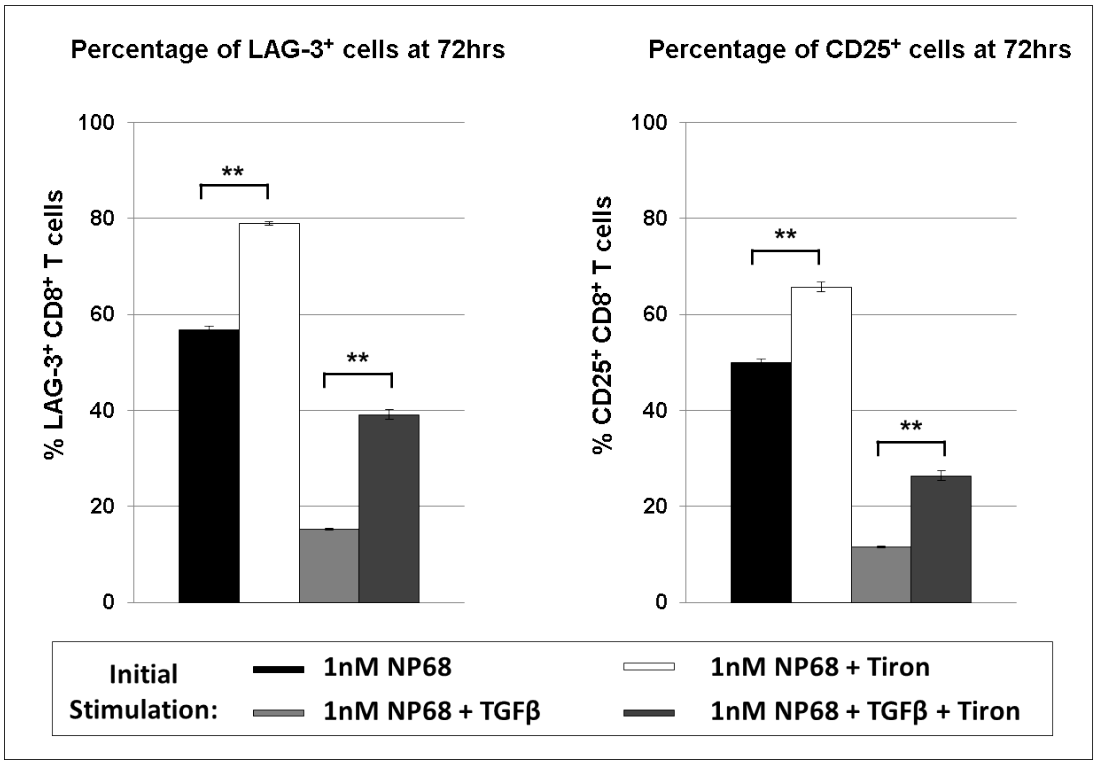

Figure 5.6: Tiron supplementation increases LAG-3 and CD25 expression on TCR-stimulated T cells

Mouse F5 CD8 T cells were stimulated with 1nM NP68 ± TGFβ (5ng/ml) ± Tiron (250µM). Cells were harvested at 72hours post-activation and stained with fluorochrome-conjugated anti-CD8 and anti-LAG-3 or anti-CD25 antibodies followed by flow cytometric analysis. The mean percent of $CD8^+$ cells staining positive for LAG-3 or CD25 are presented in a bar graph. The bars represent the mean± SD (n=3). (**p< 0.01; unpaired ttest)

5.3.3. MitoROS scavenger increases T cell proliferation of TGF-β-experienced T cells upon TCR re-stimulation

We investigated whether we could rescue the reduction in proliferation of NP68-activated T cells that suffered inhibition by TGF-β with the mitochondrial ROS scavenger Tiron. Since TGF-β reduces the surface expression of CD25 and LAG-3 on T cells, we also examined whether the Tiron-induced rescue of CD25 and LAG-3 expression has an influence on T cell proliferation when re-stimulated in the presence of IL-2 or LAG-3 blocking antibodies. T cells were initially stimulated with 1nM NP68 ± TGFβ (5ng/ml) ± Tiron (250µM) for 72hours. At the end of the time point cells were re-stimulated with 1nM NP68 with either IL-2 (250 units/ml) or LAG-3 blocking antibody (5µg/ml). T cells stimulated with NP68 in the presence of Tiron had significantly greater ($p<0.01$) proliferation at re-stimulation than T cells

stimulated with NP68 only. Furthermore, Tiron countered the TGF-β-induced reduction in T cell proliferation. The presence of IL-2 at re-stimulation had a significant ($p<0.01$) impact on T cell proliferation in all conditions (figure 5.7). T cells that were initially stimulated with NP68 ± TGF-β were unaffected by LAG-3 blocking antibodies. The presence of Tiron at initial stimulation lead to higher T cell proliferation upon re-stimulation in the presence of LAG-3 blockade (figure 5.7).

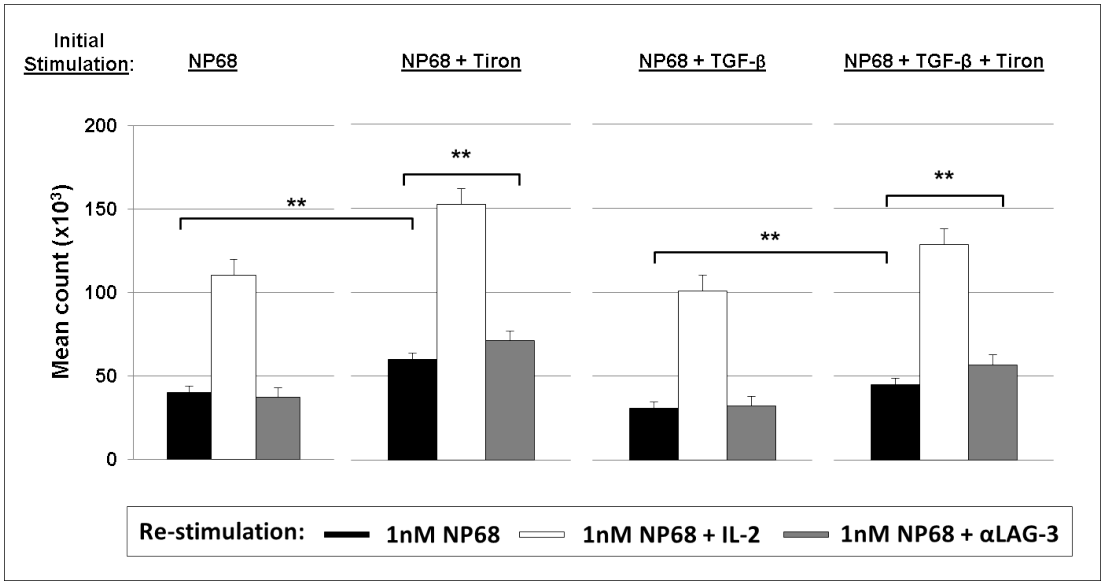

Figure 5.7: Tiron supplementation increases T cell proliferation on TCR re-stimulation

Mouse F5 CD8 T cells were stimulated with 1nM NP68 ± TGFβ (5ng/ml) ± Tiron (250μM) for 72hours and then re-stimulated with 1nM NP68 in the presence of IL-2 or anti-LAG-3 for 72hours. ^{3}H-labeled thymidine (^{3}H-Thy) was added for the last 16 h. Proliferation of T cells was determined by scintillation counting of incorporated ^{3}H-Thy. Data are presented as mean ^{3}H-Thy scintillation counts ± S.D. (*p< 0.05; **p< 0.01; unpaired ttest)

The difference in LAG-3 blockade seen in the presence of Tiron may be due to an upregulation of the LAG-3 ligand MHC II among the splenocyte population. We have shown by flow cytometry that T cells activated with NP68 ± TGF-β express negligible amounts of MHC II but in the presence of Tiron express significantly higher, detectable levels of MHC II (figure 5.8).

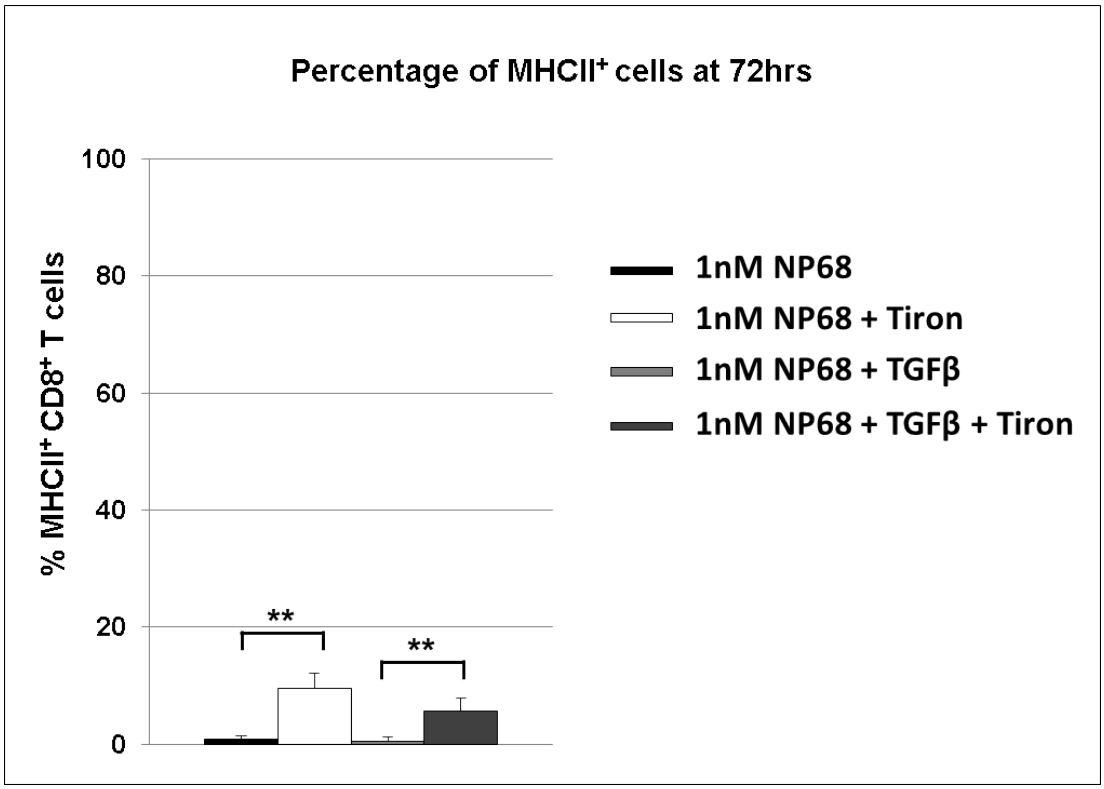

Figure 5.8: Tiron induces MHC II expression on CD8$^+$ T cells

Mouse F5 CD8 T cells were stimulated with 1nM NP68 ± TGFβ (5ng/ml) ± Tiron (250µM). Cells were harvested at 72hours post-activation and stained with fluorochrome-conjugated anti-CD8 and anti-MHC II antibodies followed by flow cytometric analysis. The mean percent of CD8$^+$ cells staining positive for MHC II are presented in a bar graph. The bars represent the mean± SD (n=3). (**p< 0.01; unpaired ttest)

5.3.4. MitoROS scavenger increases CD8+ IFN-γ and IL-2 production of TGF-β-experienced T cells upon TCR re-stimulation

IFN-γ and IL-2 production are hallmarks of activated T cells, and the T cell derived IL-2 in turn stimulates other T cells to produce IFN-γ [165]. Since TGF-β is known to inhibit IL-2 and IFN-γ cytokine production in CD8$^+$ T cells, we examined whether Tiron supplementation to NP68-activated T cells that suffered inhibition by TGF-β can rescue the observed reduction in IFN-γ and IL-2 production. As shown in figure 5.9, IFN-γ and IL-2 production are significantly increased ($p<0.01$) upon NP68 re-stimulation in T cells that were initially activated with Tiron supplementation. In contrast, T cells that were initially activated with NP68 and TGF-β had lower ($p<0.05$) IFN-γ production compared to T cells initially stimulated with only NP68.

Tiron supplementation after initial TCR stimulation was able to counter the reduction in IFN-γ production caused by TGF-β.

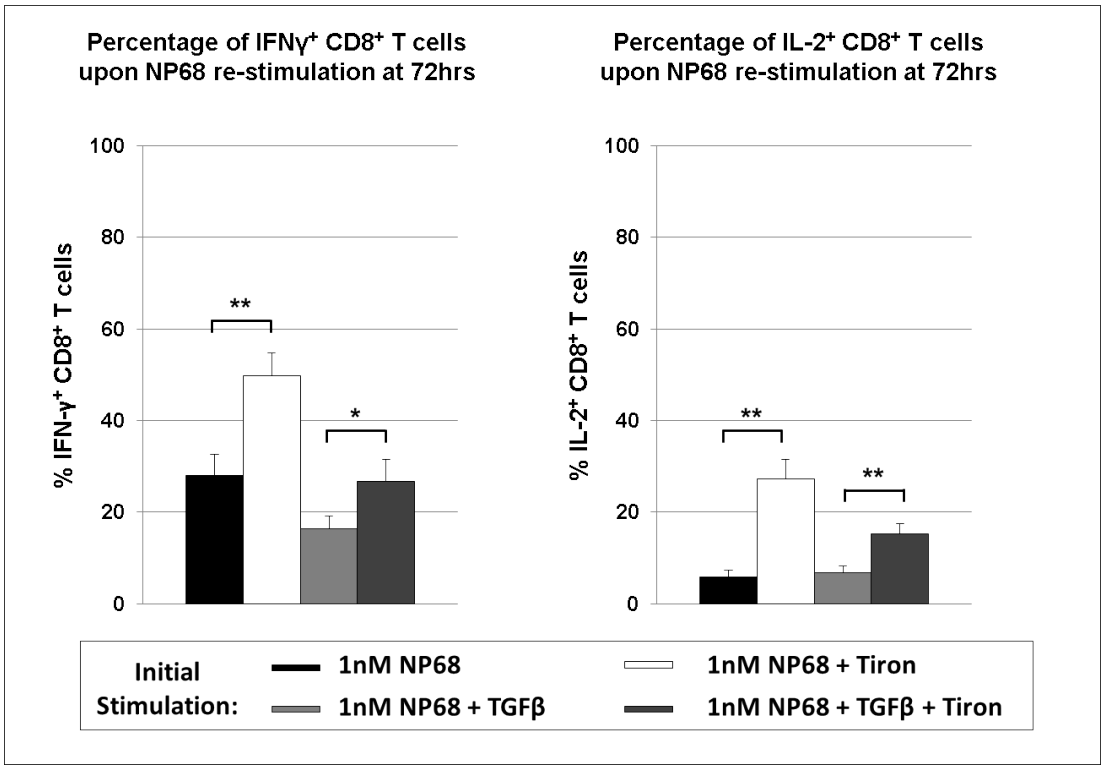

Figure 5.9: Tiron increases CD8$^+$ IFN-γ and IL-2 production upon TCR re-stimulation

Mouse F5 CD8 T cells were stimulated with 1nM NP68 ± TGFβ (5ng/ml) ± Tiron (250µM) for 72hours, washed and then re-stimulated with 1nM NP68 for 6hours with GolgiStop added after 1hour. Cells were harvested and stained with fluorochrome-conjugated anti-CD8, and then fixed and stained for intracellular cytokine production with fluorochrome-conjugated anti-IL-2 and anti-IFN-γ followed by flow cytometric analysis. The mean percent of CD8$^+$ cells staining positive for IL-2 or IFN-γ are presented in a bar graph. The bars represent the mean± SD (n=3). (**p< 0.01; unpaired ttest)

5.3.5. MitoROS scavenger suppresses TGF-β-induced CREB activation

In TCR-activated $CD8^+$ T cells TGF-β represses the cytotoxic *IFN-γ* gene via activation of the cAMP responsive element binding protein (CREB) [7]. CREB is activated by a number of growth factors, hormones and stress signals that trigger its phosphorylation. In macrophages, the TGF-β-ROS-CREB signaling axis is known to trigger apoptosis as well as oxidative stress and DNA damage. The DNA damage mediated survival signaling then further elevates CREB activation [60]. Here we show that NP68 activated T cells display CREB activation, which is increased further in the presence of TGF-β. The addition of Tiron decreases CREB activation in NP68-activated T cells. Interestingly, the addition of Tiron to T cells activated with NP68 in the presence of TGF-β display further reduction in CREB phosphorylation (figure 5.10).

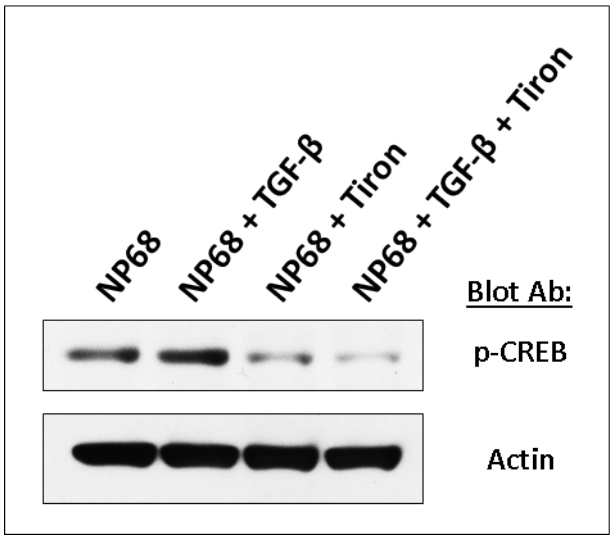

Figure 5.10: TGF-β-induced CREB is repressed by Tiron supplementation

Western blot analysis of phospho-CREB (43kDa) in Mouse F5 $CD8^+$ T cells stimulated with 1nM NP68 ± TGFβ (5ng/ml) ± Tiron (250μM) for 72hours. Actin (45kDa) was used as a loading control.

5.3.6. MitoROS scavenger increases glycolysis and decreases mitochondrial respiration of TGF-β-experienced T cells following primary stimulation

To uncover the relative contribution of OXPHOS and glycolysis to the energy demands of T cells activated with NP68 in the presence of Tiron, we measured O_2 consumption rates (OCR) and extracellular acidification rates (ECAR), respectively. The OCR values are shown as bar charts in figure 5.11 (a).

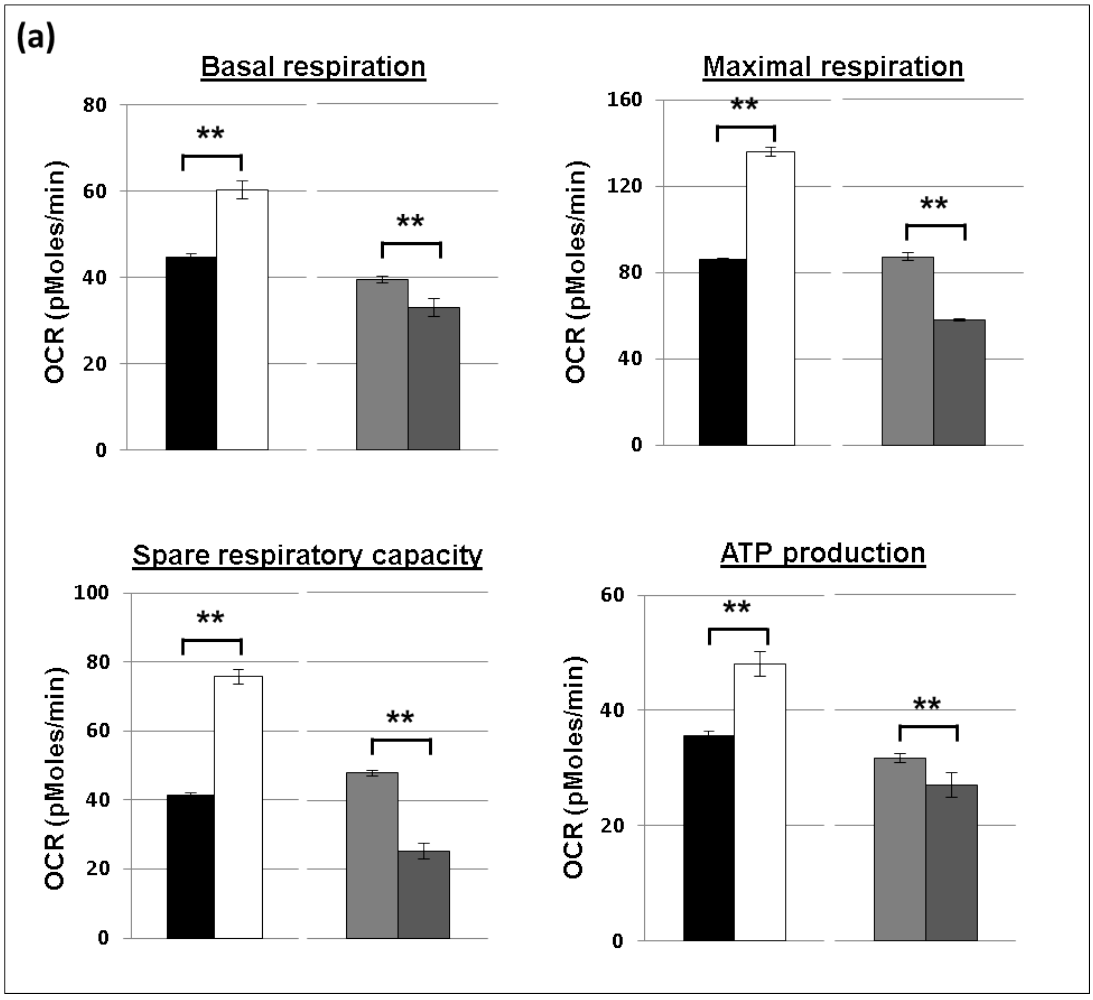

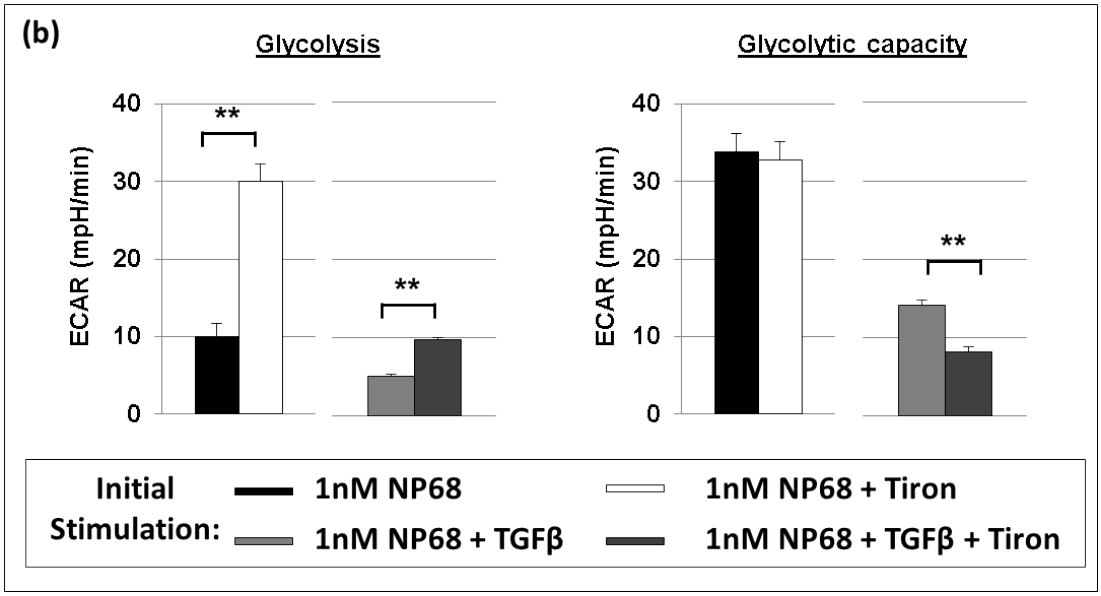

Figure 5.11: Tiron supplementation promotes T cell metabolism

(a) O_2 consumption rates (OCR; pMoles/min) were measured using the seahorse XF96 extracellular flux analyzer in real time, under basal conditions and in response to sequential addition of Oligomycin (1µM), 2,4-DNP (160µM) and Antimycin A & Rotenone (1 µM). Mean OCR values representing basal respiration, maximal respiration, spare respiratory capacity (SRC) and ATP production are presented as bar charts. The bars represent the mean± SD. The data are representative of three independent experiments, (**P< 0.01; unpaired ttest).

(b) Extracellular acidification rate (ECAR; mpH/min) was measured using the seahorse XF96 extracellular flux analyzer in real time, under basal conditions and in response to sequential addition of glucose (10mM), Oligomycin (1 µM) and 2-deoxy-D-glucose (2-DG) (100mM). Mean ECAR values representing glycolysis and glycolytic capacity are presented as bar charts. The bars represent the mean± SD. The data are representative of three independent experiments, (**P< 0.01; unpaired ttest).

We observed a significant ($p<0.01$) increase in basal respiration, maximal respiration, spare respiratory capacity (SRC) and ATP production in T cells activated with NP68 in the presence of Tiron. In contrast, for T cells that were activated with NP68 and TGF-β, Tiron significantly ($p<0.01$) reduced all of the above mentioned metabolic parameters. T cells activated with NP68 in the presence of Tiron displayed significantly ($p<0.01$) higher glycolysis than T cells activated with NP68 ± TGF-β (figure 5.11 (b)). Although there was no difference in glycolytic capacity between NP68-stimulated and NP68 + Tiron-stimulated T cells, Tiron decreased the glycolytic capacity of T cells activated with NP68 in the presence of TGF-β. These

results indicate that T cells activated in the presence of Tiron adopt a metabolic program that maximizes basal glycolytic rate.

5.3.7. MitoROS scavenger increases glycolysis and decreases mitochondrial respiration of TGF-β-experienced T cells following secondary stimulation

Since elevated proliferation, IL-2 and IFN-γ production were observed following secondary stimulation, we investigated the relative contribution of OXPHOS and glycolysis to the energy demands of TCR-re-stimulated T cells that experienced a primary stimulation of NP68 ± TGFβ ± Tiron. T cells were activated with 1nM NP68 ± TGFβ (5ng/ml) ± Tiron (250µM) for 72hours and then re-stimulated with 1nM NP68 for 48hours (figure 2.1). The OCR values of the T cell at the end of this time point are shown as bar charts in figure 5.12 (a).

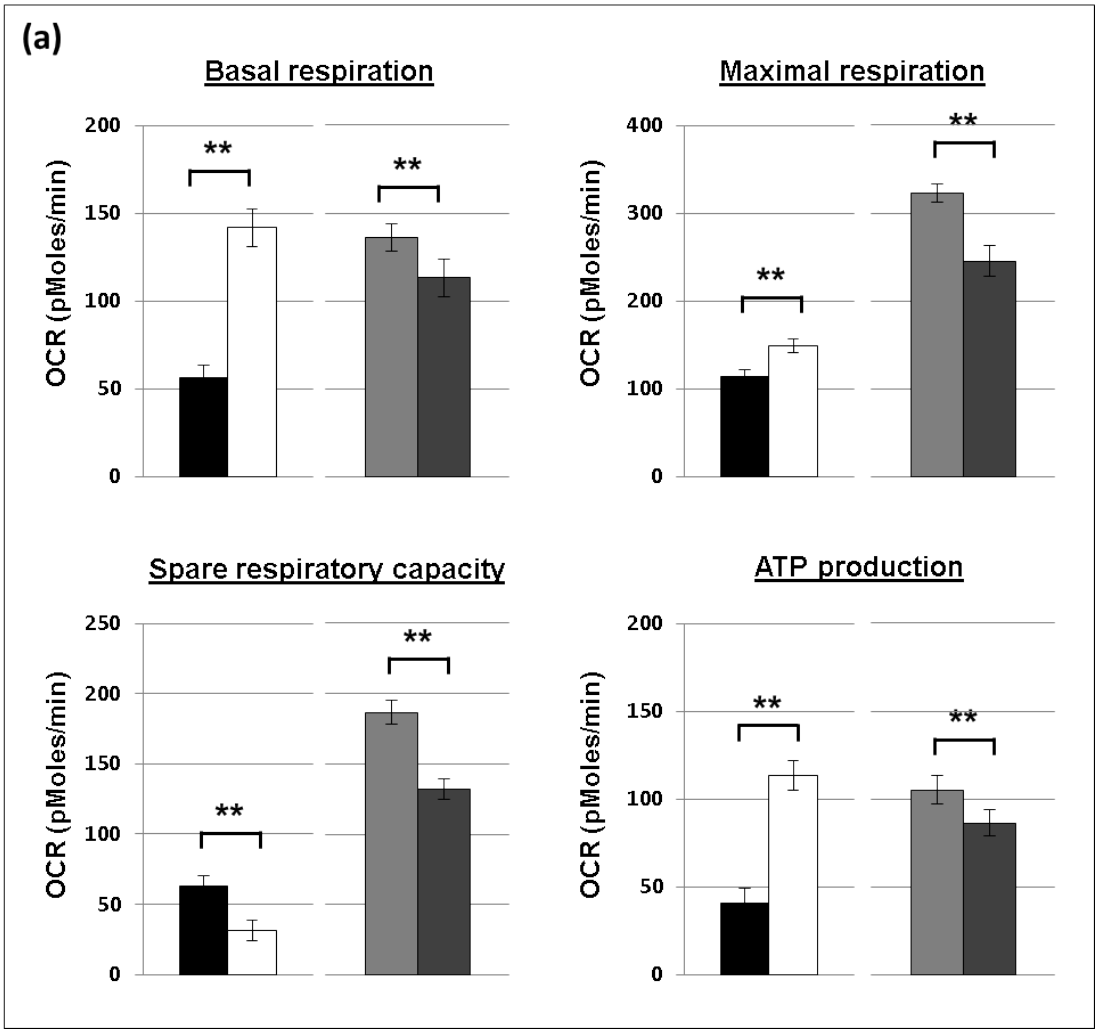

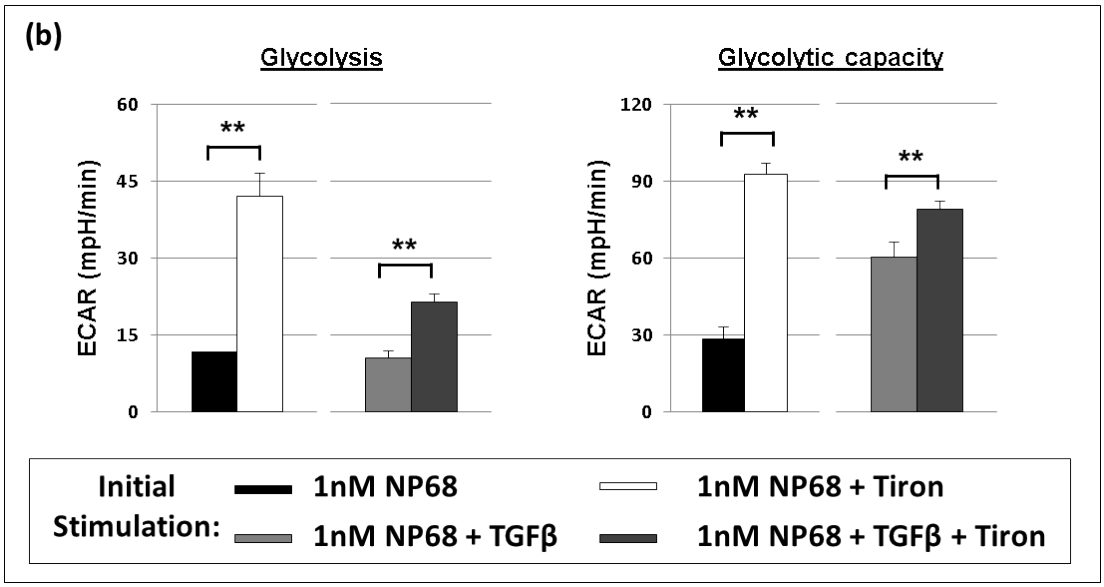

Figure 5.12: T cells activated in the presence of Tiron display higher glycolysis at re-stimulation

(a) O_2 consumption rates (OCR; pMoles/min) were measured using the seahorse XF96 extracellular flux analyzer in real time, under basal conditions and in response to sequential addition of Oligomycin (1µM), 2,4-DNP (160µM) and Antimycin A & Rotenone (1 µM). Mean OCR values representing basal respiration, maximal respiration, spare respiratory capacity (SRC) and ATP production are presented as bar charts. The bars represent the mean± SD. The data are representative of three independent experiments, (**P< 0.01; unpaired ttest).

(b) Extracellular acidification rate (ECAR; mpH/min) was measured using the seahorse XF96 extracellular flux analyzer in real time, under basal conditions and in response to sequential addition of glucose (10mM), Oligomycin (1 µM) and 2-deoxy-D-glucose (2-DG) (100mM). Mean ECAR values representing glycolysis and glycolytic capacity are presented as bar charts. The bars represent the mean± SD. The data are representative of three independent experiments, (**P< 0.01; unpaired ttest).

We observed a significant ($p<0.01$) increase in basal respiration, maximal respiration, spare and ATP production in T cells initially activated with NP68 in the presence of Tiron. Interestingly, the SRC at re-stimulation was significantly lower for T cells initially activated with NP68 + Tiron than cells activated with NP68 only. All other metabolic parameters followed a similar pattern to that shown in figure 5.11 (a), but at higher OCR values. T cells with a primary stimulation of NP68 ± TGF-β + Tiron displayed significantly ($p<0.01$) higher glycolysis after secondary stimulation than T cells that received a primary stimulus of NP68 ± TGF-β (figure 5.12 (b)). Compared to the metabolic profile after primary stimulation, re-stimulation made a profound difference to the glycolytic capacity. T cells with a primary stimulation of

NP68 ± TGF-β + Tiron displayed significantly ($p<0.01$) higher glycolytic capacity following secondary stimulation than T cells that received a primary stimulus of NP68 ± TGF-β (figure 5.12 (b)). These results indicate that TCR-activated T cells in the presence of Tiron adopt a metabolic program that maximizes glycolysis when re-stimulated.

5.3.8. Paradoxical increase of mitoROS in TGF-β-experienced activated T cells treated with mitoROS scavenger

Mitochondria are the main cellular source of energy and ROS in response to metabolic demands and/or cellular stress. Although very high levels of mitoROS can directly damage cellular components, mitoROS functions as a signaling molecule to adapt to stress and is required for normal cell homeostasis. In addition, mitoROS can constitutively promote cell proliferation [166]. Since we found that Tiron supplementation promoted T cell proliferation and cytokine production upon TCR-re-stimulation, we determined mitoROS levels at 48hours following Tiron supplementation (figure 2.1). The mitoROS levels of NP68 ± TGF-β-stimulated T cells significantly increased with Tiron supplementation (figure 5.13 (a)). Cell viability was similar for NP68 ± Tiron, but the presence of Tiron in NP68 + TGFβ-activated T cells significantly decreased cell viability (figure 5.13 (b)).

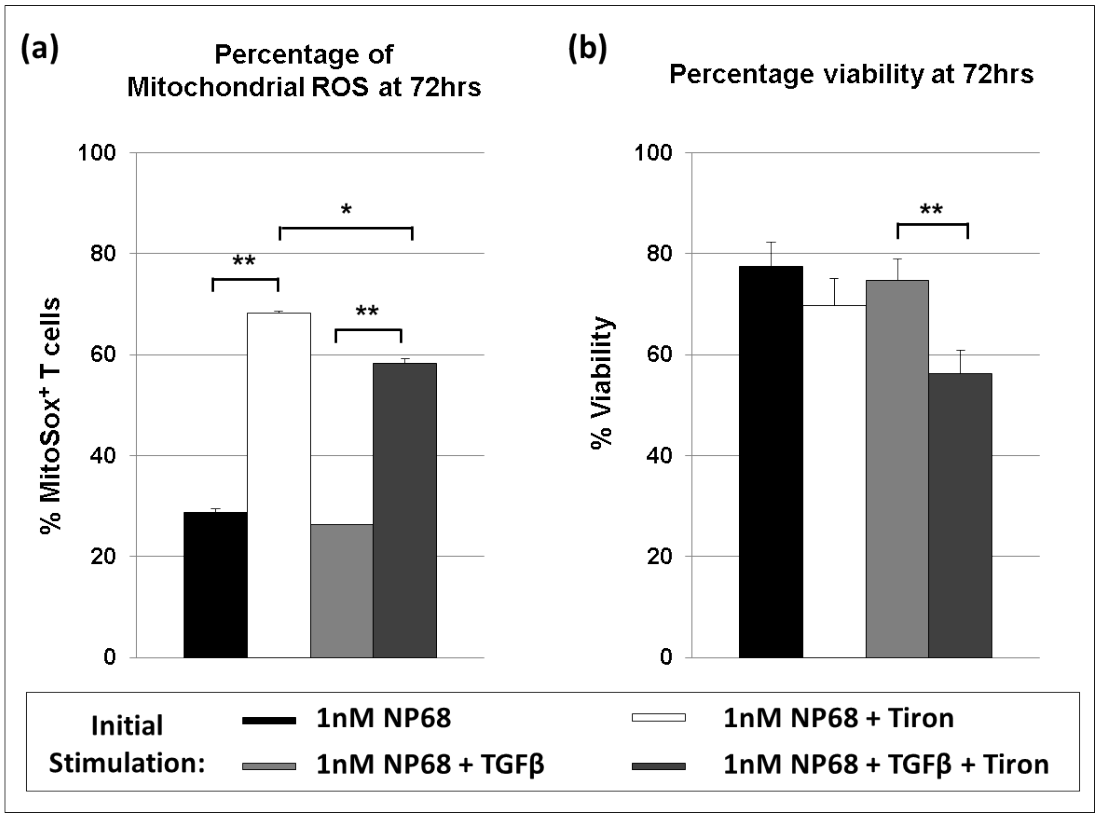

Figure 5.13: Tiron supplementation increases mitoROS

(a) Mouse F5 CD8 T cells were stimulated with 1nM NP68 ± TGFβ (5ng/ml) ± Tiron (250µM). Cells were harvested at 72hours post-activation and stained with MitoSOX™ Red Mitochondrial Superoxide Indicator and the staining intensities were quantified by flow cytometry. The mean percent of $CD8^+$ cells staining positive for mitoROS are presented in a bar graph. The bars represent the mean± SD (n=3). (*p<0.05; **p< 0.01; unpaired ttest)

(b) Cell viability of F5 CD8 T cells stimulated with NP68 ± TGFβ ± Tiron cultured for 72hrs. Percentage of viable cells determined using a trypan blue assay. The data are representative of three independent experiments, (**P< 0.01; unpaired ttest).

5.4. Discussion

The immunosuppressive effect imposed by TGF-β on T cells is a determinant factor for viral persistence and tumorigenesis. TGF-β plays an active role in suppressing anti-viral T cell responses and inhibiting T cell-mediated tumour clearance. Antigen-specific $CD8^+$ effector T cells that had undergone recent TCR stimulation are known to have increased mitochondrial potential (ΔΨm) and high levels of ROS. During the contraction phase the ΔΨm decreases but the superoxide levels remain the same. The reduced ΔΨm leads to membrane permeability and subsequent caspase activation [167]. Mitochondrial ROS generation is required for the TGF-β-mediated expression of genes [168].

A previous study investigated the effects of a metalloporphyrin-mimetic compound with superoxide dismutase activity on lymphocytic choriomeningitis virus (LCMV)-specific $CD8^+$ T cells. Treatment with this antioxidant reduced the expansion and contraction of antigen-specific $CD8^+$ T cells during primary activation and had no effect on secondary activation [169]. This study highlighted the importance of ROS during T cell expansion and contraction following primary stimulation. The purpose of the experiments presented here was to determine the effect of a mitochondria-localized antioxidant, Tiron, on the functional outcomes of TCR-activated $CD8^+$ T cells that have suffered inhibition by TGF-β.

Our data shows that Tiron supplementation to antigen-specific $CD8^+$ T cells that have suffered inhibition by TGF-β, display increased the proliferative capacity and effector functions at secondary stimulation. Data from the present study demonstrate that TCR-stimulated T cells with Tiron supplementation have a distinct functional response upon re-stimulation. Tiron permeates lipid membranes freely and preferentially localizes to the mitochondria where it can modulate intracellular electron transfer reactions as an antioxidant by scavenging free radicals [170]. Tiron promoted increased activation parameters of TCR re-stimulated T cells. We showed that TGF-β reduces the expression levels of LAG-3 and CD25 receptors, and also suppressed T cell proliferation. We demonstrated that Tiron was able to increase the TGF-β-induced reduction of LAG-3 and CD25 receptor expression levels. Interestingly, the surface marker expression of CD25 and LAG-3 increased in Tiron-

treated NP68-stimulated T cells compared to the non-treatment NP68 only condition. The changes in expression of surface receptors might prime the Tiron-experienced cells for a greater response upon re-stimulation. Our data show that Tiron also elevated activation parameters of re-stimulated T cells that were initially activated in the presence of TGF-β. Furthermore, we showed that TGF-β-induced CREB following primary stimulation is repressed by Tiron supplementation.

The mitochondrial respiratory chain is the major source of ROS. Excessive mitoROS levels can induce cell death while non-toxic levels serve as important signalling molecules to regulate cell growth, survival and proliferation [171]. It is thought that MitoROS could possibly modulate redox regulated processes such as the activation of growth-related genes (c-fos and c-jun), the alterations of protein kinases activity (tyrosine kinases, JNK, p38 and ERK), oxidative inactivation of protein phosphatases (PTEN and PP2A) and activation of transcription factors (AP-1 and NF-kB) [171, 172]. Any deregulation in mitoROS production could affect enzymes susceptible to redox regulation and trigger unfavourable cellular outcomes including unwanted or aberrant cell growth and/or proliferation. Several studies have also implicated mitoROS in lymphocyte apoptosis. The involvement of mitoROS and CREB during TCR/CD28 activation of cytotoxic $CD8^+$ T cells, together with downstream signalling events of LAG-3, TGF-β and IL-2 receptors are shown in the schematic below (figure 5.14).

Surprisingly, in contrast to T cells that were activated with NP68 ± TGF-β, T cells activated with NP68± TGF-β with Tiron supplementation had an elevated level of mitoROS at 72hrs. It is important to note that increased mitoROS is not always equivalent to oxidative stress that results in cellular damage. Elevated ROS may result in the specific redox-dependent cell signalling below the required threshold to induce oxidative damage leading to cell death. Re-stimulation at this time point enabled the Tiron-experienced T cells to secrete more IL-2 cytokine and proliferate at greater rates. Importantly, TCR-activated $CD8^+$ T cells that have suffered inhibition by TGF-β displayed reduced proliferation and cytokine secretion at re-stimulation, which was overcome when Tiron was supplemented following the primary TCR stimulation. This may be due to an upregulated antioxidant capacity

that enables adaptation to higher intrinsic oxidative stress caused by the higher mitochondrial activity to fuel the observed elevated functional outputs. T cells activated with NP68 in the presence of Tiron have an increased basal respiration and higher rates of glycolysis at 72hours. These cells attained an increased immune cell response upon re-stimulation as reflected by their elevated levels of pro-inflammatory cytokine secretion and proliferation.

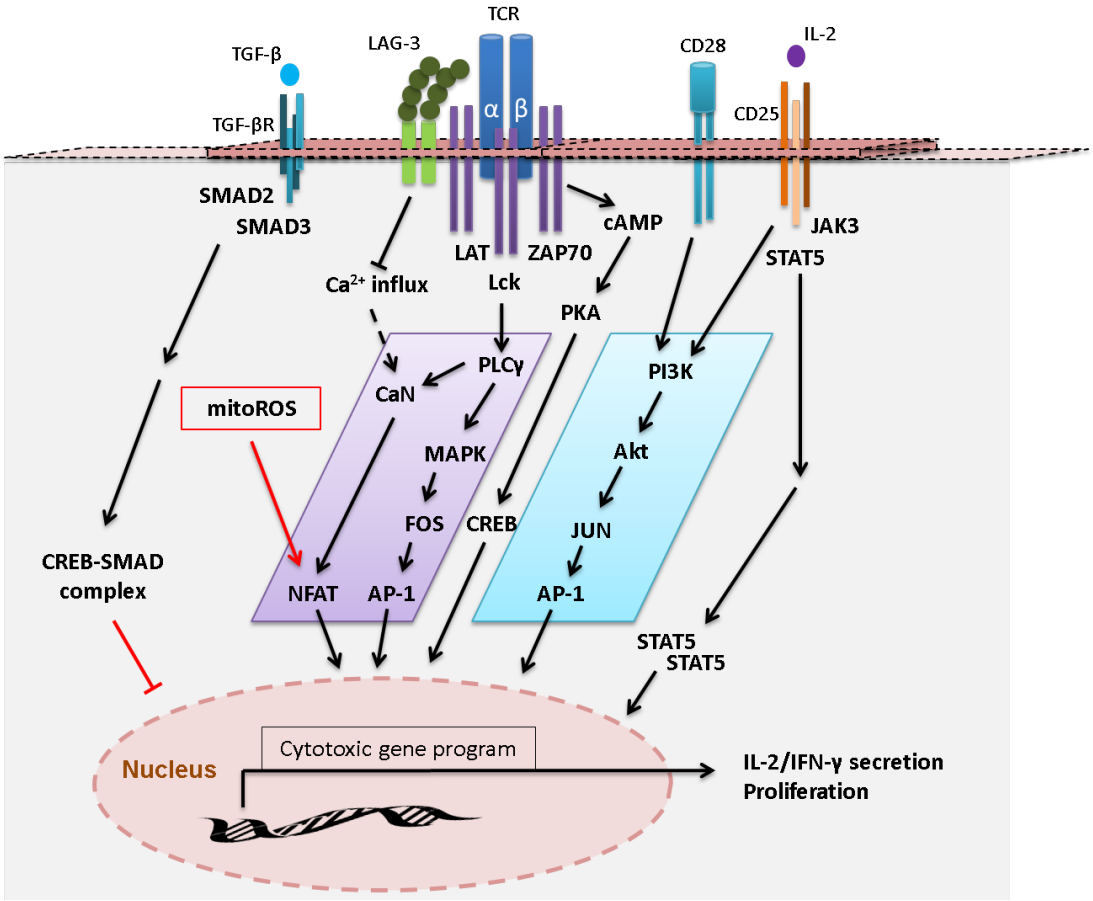

Figure 5.14: Involvement of mitoROS and CREB during T cell activation

TCR triggering of $CD8^+$ T cells activates a number of signalling pathways that ultimately results in the expression of cytotoxic gene products such as IFN-γ, which are responsible for CTL-mediated anti-tumour cytotoxicity. Downstream signalling from LAG-3, TGF-β and IL-2 receptors influence the gene response program. TGF-β-induced CREB may cooperate with SMADs to repress IFN-γ gene expression in T cells. MitoROS may contribute to enhanced nuclear localization of the transcription factor NFAT in order to increase IL-2 gene expression.

In addition, we also found that Tiron-treated NP68-stimulated T cells express detectable, albeit low levels of MHC class II molecules. Since mouse T cells lack the

capability to synthesise MHC class II molecules [173], it is likely that the observed expression was a result of MHC class II transfer from antigen presenting cells to T cells [174]. T cells that acquire MHC class II: peptide complexes are thought to act as APCs and induce proliferation and IL-2 secretion by resting T cells [174]. Thus, the supplementation of Tiron may influence global effector functions by enabling T cells to interact with additional T cell.

Collectively, these observations suggest that mitochondria-localized antioxidants may alter the sensitivity of T cells that have suffered inhibition by TGF-β to TCR-induced secondary stimulation. Further studies are required to see whether supplementation of a mitochondrial ROS scavenger following primary stimulation of T cells, upregulates the cellular antioxidant capacity that would enable adaptation to higher intrinsic oxidative stress caused by higher mitochondrial activity to meet the energy demands of elevated functional outputs at secondary stimulation.

Chapter SIX

Final Discussion

6. Final Discussion

Recent advances in immune mediated therapy have signalled a new era in the treatment of cancer (as well as other indications such as autoimmune disease and infectious disease), with opportunities for curative responses. These therapies are largely based on T cell Immunomodulatory monoclonal antibodies (mAbs) that are either direct agonists or relieve T cell inhibitory signals [86]. At the same time, however, these mAbs can be associated with a risk of serious adverse effects, which include systemic induction of proinflammatory cytokines (cytokine release syndrome) and organ-specific autoimmunity, which arise from dysregulated activation of the T cells [96]. In the recent past, one such serious adverse event was witnessed during a Phase I trial with TGN1412, a humanized CD28-specific superagonistic mAb (CD28SA) originally intended for the treatment of B cell chronic lymphocytic leukaemia and rheumatoid arthritis, which caused severe immune-mediated toxicity (cytokine release syndrome) in healthy volunteers [92]. The underlying mechanism involved substantial proliferation and extravasation of effector memory T cells (T_{EM}s), and life-threatening cytokine storm with highly elevated levels of a number of pro-inflammatory cytokines [97]. Detailed understanding of the target biology and identification of target specific biomarkers/functional parameters for risk assessment would be highly beneficial and aid our understanding of the safety profile of T cell modulatory mAbs in general [87]. While significant focus in recent times has been on assessing the potential of immunomodulatory mAbs to induce enhanced cytokine release, much less attention has been paid to other aspects of T cell biology including non-physiological activation phenotype/functions, migration characteristics and metabolism.

Here, a humanized superagonistic anti-CD28 antibody (NIB1412) and conventional anti-CD3 mAbs were used to demonstrate unlike conventional TCR/CD3 activation triggered by CD28SA. Activation by CD28SA lead to elevated proliferation with a higher percentage of T_{EM} (the main responding population to CD28SA activation) remaining in S-phase, reduced apoptosis, high secretion of IL-2, high expression of

TCR with fluctuating expression levels of CD28, elevated expression of stimulatory markers GITR and CD137, high level expression of markers of antigen presentation; HLA-DR and CD80, elevated expression levels of LFA-1, CCR5 and CXCR4, enhanced adhesion and migratory capacity, low level expression of co-inhibitory receptors; CTLA-4 and PD-1, and finally in the presence of recombinant PD-L1, CD28SA-activated T_{EM}s display an absence of PD-1-mediated regulation together with elevated expression of phospho-PTEN and CK2.

Distinct metabolic profiles have been reported for various T cell subtypes and upon activation with different agonists. These metabolic profiles are directly linked to T cell effector functions and contribute to pathology such as cancer and autoimmunity, by influencing key cellular events. Thus it was deemed important to elucidate the metabolic profile of CD28SA-activated cells to understand their energy needs and how it may affect effector functions. The metabolic profile of CD28SA-activated T cells was found to include maximal OXPHOS potential and glucose utilization, together with *de novo* lipogenesis as demonstrated by high activity of ACL and ACC. CD28SA stimulation was also found to induce autophagy. A high glycolytic flux into increased lipid synthesis, increased cell migration and autophagy are characteristics observed in aggressive and invasive tumours.

The PD-1 co-inhibitory receptor has been shown to be a powerful negative regulator of activated T cells. In the absence of PD-1-mediated signals, there is an increased propensity for T cells to expand with stronger accompanying inflammatory cascades. Regulation of T cell activation by PD-1 therefore represents a key characteristic of physiological behaviour and has the potential to report on the nature of T cell activation induced by a T cell mAb. Given the absence of PD-1-mediated regulation together with the distinct metabolic phenotype observed for CD28SA activation, a framework for biomarker design to predict adverse immune-mediated effects that arise as a consequence of immunostimulatory mAbs-induced excessive T cell activation can be developed. In addition, a detailed understanding of activation parameters, degree of regulation, migration capacity and metabolic programs adopted by the target cell upon mAb action may inform the drug developer in his choice of target and lead candidates.

The cytokine milieu in the microenvironment of affected tissues also influences the functional outcome of immunomodulatory mAbs. The immunosuppressive cytokine TGF-β attenuates the cytotoxic T cell-mediated anti-tumour immune responses and may also reduce the effectiveness of immunotherapy. Agents that block TGF-β and its signalling pathway are under development at both the pre-clinical and clinical stages. In the present study, the activation parameters and the metabolic program adopted by T cells that have suffered inhibition by TGF-β was investigated. It was demonstrated that TGF-β suppresses TCR-stimulated T cell proliferation and significantly reduces LAG-3 and CD25 expression on TCR-stimulated T cells. TGF-β experienced T cells were also found to be less responsive to LAG-3 blocking. The relief of TGF-β-induced oxidative stress by supplementation of a mitochondrial ROS scavenger was found to increase LAG-3 and CD25 expression, proliferative capacity, effector cytokine (IL-2 and IFN-γ) production and glycolysis in TCR-stimulated T cells. Instead of targeting TGF-β during immunomodulatory mAb-based cancer therapy, the supplementation of a mitochondrial ROS scavenger could negate the effects of TGF-β-induced suppression.

The CD28SA is thought to induce maximal activation of the CD28 receptor and thus all observed parameters that were shown to be elevated compared to physiological CD3/TCR activation, may be directly linked to the signalling components of the CD28 signalling pathway. Several outstanding questions remain regarding CD28SA activation and how it by-passes inhibitory receptor expression, and whether the lack of inhibitory inputs is the cause behind the altered metabolic program. Since an upregulation of pro-stimulatory receptors (e.g. CD137, GITR, HLA-DR and CD80) was observed, each one of these receptors may also feed into signalling events that influence the metabolic profile. Future investigations should be directed towards addressing these key questions.

References

1. Charles A Janeway, J., Paul Travers, Mark Walport, and Mark J Shlomchik., *Immunobiology*, in *The Immune System in Health and Disease*2001, Garland Science: New York.

2. Russell, J.H. and T.J. Ley, *Lymphocyte-mediated cytotoxicity.* Annu Rev Immunol, 2002. **20**: p. 323-70.
3. Sun, B. and Y. Zhang, *Overview of Orchestration of CD4+ T Cell Subsets in Immune Responses.* Adv Exp Med Biol, 2014. **841**: p. 1-13.
4. Sallusto, F., J. Geginat, and A. Lanzavecchia, *Central memory and effector memory T cell subsets: function, generation, and maintenance.* Annu Rev Immunol, 2004. **22**: p. 745-63.
5. Broere, F., et al., *Principles of Immunopharmacology*. 3rd ed. T cell subsets and T cell-mediated immunity, ed. M.J.P. F.P. Nijkamp. 2011, Birkhäuser Basel: Birkhäuser Basel.
6. Blohm, U., et al., *Solid tumors "melt" from the inside after successful CD8 T cell attack.* Eur J Immunol, 2006. **36**(2): p. 468-77.
7. Thomas, D.A. and J. Massague, *TGF-beta directly targets cytotoxic T cell functions during tumor evasion of immune surveillance.* Cancer Cell, 2005. **8**(5): p. 369-80.
8. Sykulev, Y., *T cell receptor signaling kinetics takes the stage.* Sci Signal, 2010. **3**(153): p. pe50.
9. Acuto, O., V. Di Bartolo, and F. Michel, *Tailoring T-cell receptor signals by proximal negative feedback mechanisms.* Nat Rev Immunol, 2008. **8**(9): p. 699-712.
10. Wange, R.L., *LAT, the linker for activation of T cells: a bridge between T cell-specific and general signaling pathways.* Sci STKE, 2000. **2000**(63): p. re1.
11. Thaventhiran., T., et al., *T Cell Co-inhibitory Receptors: Functions and Signalling Mechanisms.* Journal of Clinical and Cellular Immunology, 2012. **S12-004**.
12. Acuto, O. and F. Michel, *CD28-mediated co-stimulation: a quantitative support for TCR signalling.* Nat Rev Immunol, 2003. **3**(12): p. 939-51.
13. Boomer, J.S. and J.M. Green, *An enigmatic tail of CD28 signaling.* Cold Spring Harb Perspect Biol, 2010. **2**(8): p. a002436.
14. Schraven, B. and U. Kalinke, *CD28 superagonists: what makes the difference in humans?* Immunity, 2008. **28**(5): p. 591-5.
15. Hunig, T. and K. Dennehy, *CD28 superagonists: mode of action and therapeutic potential.* Immunol Lett, 2005. **100**(1): p. 21-8.
16. Waibler, Z., et al., *Signaling signatures and functional properties of anti-human CD28 superagonistic antibodies.* PLoS One, 2008. **3**(3): p. e1708.
17. Xu, C., et al., *Regulation of T cell receptor activation by dynamic membrane binding of the CD3epsilon cytoplasmic tyrosine-based motif.* Cell, 2008. **135**(4): p. 702-13.
18. Liu, J.O., *The yins of T cell activation.* Sci STKE, 2005. **2005**(265): p. re1.
19. Zhu, Y., S. Yao, and L. Chen, *Cell surface signaling molecules in the control of immune responses: a tide model.* Immunity, 2011. **34**(4): p. 466-78.
20. Sinclair, N.R., *Why so many coinhibitory receptors?* Scand J Immunol, 1999. **50**(1): p. 10-3.
21. Odorizzi, P.M. and E.J. Wherry, *Inhibitory receptors on lymphocytes: insights from infections.* J Immunol, 2012. **188**(7): p. 2957-65.
22. Daeron, M., et al., *Immunoreceptor tyrosine-based inhibition motifs: a quest in the past and future.* Immunol Rev, 2008. **224**: p. 11-43.
23. Vivier, E. and M. Daeron, *Immunoreceptor tyrosine-based inhibition motifs.* Immunol Today, 1997. **18**(6): p. 286-91.
24. Lorenz, U., *SHP-1 and SHP-2 in T cells: two phosphatases functioning at many levels.* Immunol Rev, 2009. **228**(1): p. 342-59.

25. Chemnitz, J.M., et al., *SHP-1 and SHP-2 associate with immunoreceptor tyrosine-based switch motif of programmed death 1 upon primary human T cell stimulation, but only receptor ligation prevents T cell activation.* J Immunol, 2004. **173**(2): p. 945-54.
26. Keir, M.E., et al., *PD-1 and its ligands in tolerance and immunity.* Annu Rev Immunol, 2008. **26**: p. 677-704.
27. Bennett, F., et al., *Program death-1 engagement upon TCR activation has distinct effects on costimulation and cytokine-driven proliferation: attenuation of ICOS, IL-4, and IL-21, but not CD28, IL-7, and IL-15 responses.* J Immunol, 2003. **170**(2): p. 711-8.
28. Sheppard, K.A., et al., *PD-1 inhibits T-cell receptor induced phosphorylation of the ZAP70/CD3zeta signalosome and downstream signaling to PKCtheta.* FEBS Lett, 2004. **574**(1-3): p. 37-41.
29. Patsoukis, N., et al., *PD-1 increases PTEN phosphatase activity while decreasing PTEN protein stability by inhibiting casein kinase 2.* Mol Cell Biol, 2013. **33**(16): p. 3091-8.
30. Yokosuka, T., et al., *Programmed cell death 1 forms negative costimulatory microclusters that directly inhibit T cell receptor signaling by recruiting phosphatase SHP2.* J Exp Med, 2012. **209**(6): p. 1201-17.
31. Vermeulen, K., D.R. Van Bockstaele, and Z.N. Berneman, *The cell cycle: a review of regulation, deregulation and therapeutic targets in cancer.* Cell Prolif, 2003. **36**(3): p. 131-49.
32. Patsoukis, N., et al., *Selective Effects of PD-1 on Akt and Ras Pathways Regulate Molecular Components of the Cell Cycle and Inhibit T Cell Proliferation.* Sci Signal, 2012. **5**(230): p. ra46.
33. Quigley, M., et al., *Transcriptional analysis of HIV-specific CD8+ T cells shows that PD-1 inhibits T cell function by upregulating BATF.* Nat Med, 2010. **16**(10): p. 1147-51.
34. Fife, B.T., et al., *Interactions between PD-1 and PD-L1 promote tolerance by blocking the TCR-induced stop signal.* Nat Immunol, 2009. **10**(11): p. 1185-92.
35. Keir, M.E., G.J. Freeman, and A.H. Sharpe, *PD-1 regulates self-reactive CD8+ T cell responses to antigen in lymph nodes and tissues.* J Immunol, 2007. **179**(8): p. 5064-70.
36. Schlierf, B., et al., *Rab11b is essential for recycling of transferrin to the plasma membrane.* Exp Cell Res, 2000. **259**(1): p. 257-65.
37. Goldberg, M.V. and C.G. Drake, *LAG-3 in Cancer Immunotherapy.* Curr Top Microbiol Immunol, 2011. **344**: p. 269-78.
38. Li, N., et al., *Metalloproteases regulate T-cell proliferation and effector function via LAG-3.* EMBO J, 2007. **26**(2): p. 494-504.
39. Li, N., et al., *Biochemical analysis of the regulatory T cell protein lymphocyte activation gene-3 (LAG-3; CD223).* J Immunol, 2004. **173**(11): p. 6806-12.
40. Workman, C.J., K.J. Dugger, and D.A. Vignali, *Cutting edge: molecular analysis of the negative regulatory function of lymphocyte activation gene-3.* J Immunol, 2002. **169**(10): p. 5392-5.
41. Triebel, F., *LAG-3: a regulator of T-cell and DC responses and its use in therapeutic vaccination.* Trends Immunol, 2003. **24**(12): p. 619-22.
42. Workman, C.J., et al., *Lymphocyte activation gene-3 (CD223) regulates the size of the expanding T cell population following antigen activation in vivo.* J Immunol, 2004. **172**(9): p. 5450-5.
43. Gajewski, T.F., et al., *Absence of CTLA-4 lowers the activation threshold of primed CD8+ TCR-transgenic T cells: lack of correlation with Src homology domain 2-containing protein tyrosine phosphatase.* J Immunol, 2001. **166**(6): p. 3900-7.

44. Valk, E., et al., *T cell receptor-interacting molecule acts as a chaperone to modulate surface expression of the CTLA-4 coreceptor.* Immunity, 2006. **25**(5): p. 807-21.
45. Baroja, M.L., et al., *Inhibition of CTLA-4 function by the regulatory subunit of serine/threonine phosphatase 2A.* J Immunol, 2002. **168**(10): p. 5070-8.
46. Hurchla, M.A., et al., *B and T lymphocyte attenuator exhibits structural and expression polymorphisms and is highly Induced in anergic CD4+ T cells.* J Immunol, 2005. **174**(6): p. 3377-85.
47. Steinberg, M.W., T.C. Cheung, and C.F. Ware, *The signaling networks of the herpesvirus entry mediator (TNFRSF14) in immune regulation.* Immunol Rev, 2011. **244**(1): p. 169-87.
48. Zhu, C., A.C. Anderson, and V.K. Kuchroo, *TIM-3 and its regulatory role in immune responses.* Curr Top Microbiol Immunol, 2011. **350**: p. 1-15.
49. Meyaard, L., *The inhibitory collagen receptor LAIR-1 (CD305).* J Leukoc Biol, 2008. **83**(4): p. 799-803.
50. Jansen, C.A., et al., *Regulated expression of the inhibitory receptor LAIR-1 on human peripheral T cells during T cell activation and differentiation.* Eur J Immunol, 2007. **37**(4): p. 914-24.
51. Sathish, J.G., et al., *Constitutive association of SHP-1 with leukocyte-associated Ig-like receptor-1 in human T cells.* J Immunol, 2001. **166**(3): p. 1763-70.
52. Stengel, K.F., et al., *Structure of TIGIT immunoreceptor bound to poliovirus receptor reveals a cell-cell adhesion and signaling mechanism that requires cis-trans receptor clustering.* Proc Natl Acad Sci U S A, 2012. **109**(14): p. 5399-404.
53. Yu, X., et al., *The surface protein TIGIT suppresses T cell activation by promoting the generation of mature immunoregulatory dendritic cells.* Nat Immunol, 2009. **10**(1): p. 48-57.
54. Cao, H. and P.R. Crocker, *Evolution of CD33-related siglecs: regulating host immune functions and escaping pathogen exploitation?* Immunology, 2011. **132**(1): p. 18-26.
55. Crocker, P.R. and P. Redelinghuys, *Siglecs as positive and negative regulators of the immune system.* Biochem Soc Trans, 2008. **36**(Pt 6): p. 1467-71.
56. Malek, T.R. and A.L. Bayer, *Tolerance, not immunity, crucially depends on IL-2.* Nat Rev Immunol, 2004. **4**(9): p. 665-74.
57. Malek, T.R. and I. Castro, *Interleukin-2 receptor signaling: at the interface between tolerance and immunity.* Immunity, 2010. **33**(2): p. 153-65.
58. Schroder, K., et al., *Interferon-gamma: an overview of signals, mechanisms and functions.* J Leukoc Biol, 2004. **75**(2): p. 163-89.
59. Li, M.O., et al., *Transforming growth factor-beta regulation of immune responses.* Annu Rev Immunol, 2006. **24**: p. 99-146.
60. Singh, R., B.S. Shankar, and K.B. Sainis, *TGF-beta1-ROS-ATM-CREB signaling axis in macrophage mediated migration of human breast cancer MCF7 cells.* Cell Signal, 2014. **26**(7): p. 1604-15.
61. Dykstra, M., et al., *Location is everything: lipid rafts and immune cell signaling.* Annu Rev Immunol, 2003. **21**: p. 457-81.
62. Marelli-Berg, F.M., et al., *The highway code of T cell trafficking.* J Pathol, 2008. **214**(2): p. 179-89.
63. Hogg, N., I. Patzak, and F. Willenbrock, *The insider's guide to leukocyte integrin signalling and function.* Nat Rev Immunol, 2011. **11**(6): p. 416-26.
64. Smith, A., et al., *The role of the integrin LFA-1 in T-lymphocyte migration.* Immunol Rev, 2007. **218**: p. 135-46.
65. Perez, O.D., et al., *Leukocyte functional antigen 1 lowers T cell activation thresholds and signaling through cytohesin-1 and Jun-activating binding protein 1.* Nat Immunol, 2003. **4**(11): p. 1083-92.

66. Alkhatib, G., *The biology of CCR5 and CXCR4.* Curr Opin HIV AIDS, 2009. **4**(2): p. 96-103.
67. Yamane, H. and W.E. Paul, *Memory CD4+ T cells: fate determination, positive feedback and plasticity.* Cell Mol Life Sci, 2012. **69**(10): p. 1577-83.
68. Pearce, E.L., et al., *Fueling immunity: insights into metabolism and lymphocyte function.* Science, 2013. **342**(6155): p. 1242454.
69. Pearce, E.L. and E.J. Pearce, *Metabolic pathways in immune cell activation and quiescence.* Immunity, 2013. **38**(4): p. 633-43.
70. Mihaylova, M.M. and R.J. Shaw, *The AMPK signalling pathway coordinates cell growth, autophagy and metabolism.* Nat Cell Biol, 2011. **13**(9): p. 1016-23.
71. Nagy, E. and W.F. Rigby, *Glyceraldehyde-3-phosphate dehydrogenase selectively binds AU-rich RNA in the NAD(+)-binding region (Rossmann fold).* J Biol Chem, 1995. **270**(6): p. 2755-63.
72. Jacobs, S.R., et al., *Glucose uptake is limiting in T cell activation and requires CD28-mediated Akt-dependent and independent pathways.* J Immunol, 2008. **180**(7): p. 4476-86.
73. Frauwirth, K.A., et al., *The CD28 signaling pathway regulates glucose metabolism.* Immunity, 2002. **16**(6): p. 769-77.
74. Murphy, M.P. and R.M. Siegel, *Mitochondrial ROS fire up T cell activation.* Immunity, 2013. **38**(2): p. 201-2.
75. Baenke, F., et al., *Hooked on fat: the role of lipid synthesis in cancer metabolism and tumour development.* Dis Model Mech, 2013. **6**(6): p. 1353-63.
76. Csibi, A., et al., *The mTORC1 pathway stimulates glutamine metabolism and cell proliferation by repressing SIRT4.* Cell, 2013. **153**(4): p. 840-54.
77. Weinberg, S.E. and N.S. Chandel, *Futility sustains memory T cells.* Immunity, 2014. **41**(1): p. 1-3.
78. Maryanovich, M. and A. Gross, *A ROS rheostat for cell fate regulation.* Trends Cell Biol, 2013. **23**(3): p. 129-34.
79. Yang, Z. and D.J. Klionsky, *Eaten alive: a history of macroautophagy.* Nat Cell Biol, 2010. **12**(9): p. 814-22.
80. Russell, R.C., et al., *ULK1 induces autophagy by phosphorylating Beclin-1 and activating VPS34 lipid kinase.* Nat Cell Biol, 2013. **15**(7): p. 741-50.
81. Nazarko, V.Y. and Q. Zhong, *ULK1 targets Beclin-1 in autophagy.* Nat Cell Biol, 2013. **15**(7): p. 727-8.
82. Boya, P., F. Reggiori, and P. Codogno, *Emerging regulation and functions of autophagy.* Nat Cell Biol, 2013. **15**(7): p. 713-20.
83. Wang, R.C., et al., *Akt-mediated regulation of autophagy and tumorigenesis through Beclin 1 phosphorylation.* Science, 2012. **338**(6109): p. 956-9.
84. Tanida, I., T. Ueno, and E. Kominami, *LC3 and Autophagy.* Methods Mol Biol, 2008. **445**: p. 77-88.
85. Kabeya, Y., et al., *LC3, a mammalian homologue of yeast Apg8p, is localized in autophagosome membranes after processing.* EMBO J, 2000. **19**(21): p. 5720-8.
86. Pardoll, D.M., *The blockade of immune checkpoints in cancer immunotherapy.* Nat Rev Cancer, 2012. **12**(4): p. 252-64.
87. Sathish, J.G., et al., *Challenges and approaches for the development of safer immunomodulatory biologics.* Nat Rev Drug Discov, 2013. **12**(4): p. 306-24.
88. Chames, P., et al., *Therapeutic antibodies: successes, limitations and hopes for the future.* Br J Pharmacol, 2009. **157**(2): p. 220-33.
89. Scott, A.M., J.D. Wolchok, and L.J. Old, *Antibody therapy of cancer.* Nat Rev Cancer, 2012. **12**(4): p. 278-87.
90. Barber, D.L., et al., *Restoring function in exhausted CD8 T cells during chronic viral infection.* Nature, 2006. **439**(7077): p. 682-7.

91. Lonning, S., J. Mannick, and J.M. McPherson, *Antibody targeting of TGF-beta in cancer patients.* Curr Pharm Biotechnol, 2011. **12**(12): p. 2176-89.
92. Suntharalingam, G., et al., *Cytokine storm in a phase 1 trial of the anti-CD28 monoclonal antibody TGN1412.* N Engl J Med, 2006. **355**(10): p. 1018-28.
93. Boyum, A., *Isolation of mononuclear cells and granulocytes from human blood. Isolation of monuclear cells by one centrifugation, and of granulocytes by combining centrifugation and sedimentation at 1 g.* Scand J Clin Lab Invest Suppl, 1968. **97**: p. 77-89.
94. Mamalaki, C., et al., *Positive and negative selection in transgenic mice expressing a T-cell receptor specific for influenza nucleoprotein and endogenous superantigen.* Dev Immunol, 1993. **3**(3): p. 159-74.
95. Ball, C., et al., *Antibody C region influences TGN1412-like functional activity in vitro.* J Immunol, 2012. **189**(12): p. 5831-40.
96. Gray, J.C., P.W. Johnson, and M.J. Glennie, *Therapeutic potential of immunostimulatory monoclonal antibodies.* Clin Sci (Lond), 2006. **111**(2): p. 93-106.
97. Stebbings, R., et al., *"Cytokine storm" in the phase I trial of monoclonal antibody TGN1412: better understanding the causes to improve preclinical testing of immunotherapeutics.* J Immunol, 2007. **179**(5): p. 3325-31.
98. Jin, H.T., R. Ahmed, and T. Okazaki, *Role of PD-1 in regulating T-cell immunity.* Curr Top Microbiol Immunol, 2011. **350**: p. 17-37.
99. Wei, F., et al., *Strength of PD-1 signaling differentially affects T-cell effector functions.* Proc Natl Acad Sci U S A, 2013. **110**(27): p. E2480-9.
100. Eastwood, D., et al., *Monoclonal antibody TGN1412 trial failure explained by species differences in CD28 expression on CD4+ effector memory T-cells.* Br J Pharmacol, 2010. **161**(3): p. 512-26.
101. Romer, P.S., et al., *Preculture of PBMCs at high cell density increases sensitivity of T-cell responses, revealing cytokine release by CD28 superagonist TGN1412.* Blood, 2011. **118**(26): p. 6772-82.
102. San Jose, E., et al., *Triggering the TCR complex causes the downregulation of nonengaged receptors by a signal transduction-dependent mechanism.* Immunity, 2000. **12**(2): p. 161-70.
103. Hedfors, I.A. and J.E. Brinchmann, *Long-term proliferation and survival of in vitro-activated T cells is dependent on Interleukin-2 receptor signalling but not on the high-affinity IL-2R.* Scand J Immunol, 2003. **58**(5): p. 522-32.
104. Eastwood, D., et al., *Severity of the TGN1412 trial disaster cytokine storm correlated with IL-2 release.* Br J Clin Pharmacol, 2013. **76**(2): p. 299-315.
105. Le-Carlson, M., et al., *Markers of antigen presentation and activation on eosinophils and T cells in the esophageal tissue of patients with eosinophilic esophagitis.* J Pediatr Gastroenterol Nutr, 2013. **56**(3): p. 257-62.
106. Marelli-Berg, F.M., K. Okkenhaug, and V. Mirenda, *A two-signal model for T cell trafficking.* Trends Immunol, 2007. **28**(6): p. 267-73.
107. Smith, A., et al., *LFA-1-induced T cell migration on ICAM-1 involves regulation of MLCK-mediated attachment and ROCK-dependent detachment.* J Cell Sci, 2003. **116**(Pt 15): p. 3123-33.
108. Oak, J.S. and D.A. Fruman, *Role of phosphoinositide 3-kinase signaling in autoimmunity.* Autoimmunity, 2007. **40**(6): p. 433-41.
109. Leslie, N.R., *PTEN: an intercellular peacekeeper?* Sci Signal, 2012. **5**(250): p. pe50.
110. Gourley, T.S. and C.H. Chang, *Cutting edge: the class II transactivator prevents activation-induced cell death by inhibiting Fas ligand gene expression.* J Immunol, 2001. **166**(5): p. 2917-21.
111. Kochli, C., et al., *CD80 and CD86 costimulatory molecules on circulating T cells of HIV infected individuals.* Immunol Lett, 1999. **65**(3): p. 197-201.

112. Sabzevari, H., et al., *Acquisition of CD80 (B7-1) by T cells.* J Immunol, 2001. **166**(4): p. 2505-13.
113. Nickoloff, B.J., et al., *Discordant expression of CD28 ligands, BB-1, and B7 on keratinocytes in vitro and psoriatic cells in vivo.* Am J Pathol, 1993. **142**(4): p. 1029-40.
114. Zhang, X., et al., *Tissue trafficking patterns of effector memory CD4+ T cells in rheumatoid arthritis.* Arthritis Rheum, 2005. **52**(12): p. 3839-49.
115. Sandilands, G.P., et al., *Were monocytes responsible for initiating the cytokine storm in the TGN1412 clinical trial tragedy?* Clin Exp Immunol, 2010. **162**(3): p. 516-27.
116. Iliopoulos, D., et al., *The negative costimulatory molecule PD-1 modulates the balance between immunity and tolerance via miR-21.* Eur J Immunol, 2011. **41**(6): p. 1754-63.
117. Pentcheva-Hoang, T., et al., *Programmed death-1 concentration at the immunological synapse is determined by ligand affinity and availability.* Proc Natl Acad Sci U S A, 2007. **104**(45): p. 17765-70.
118. Medina-Tato, D.A., S.G. Ward, and M.L. Watson, *Phosphoinositide 3-kinase signalling in lung disease: leucocytes and beyond.* Immunology, 2007. **121**(4): p. 448-61.
119. Tabares, P., et al., *Human regulatory T cells are selectively activated by low-dose application of the CD28 superagonist TGN1412/TAB08.* Eur J Immunol, 2014. **44**(4): p. 1225-36.
120. Mirenda, V., et al., *Physiologic and aberrant regulation of memory T-cell trafficking by the costimulatory molecule CD28.* Blood, 2007. **109**(7): p. 2968-77.
121. Thaventhiran, T., et al., *Failure to upregulate cell surface PD-1 is associated with dysregulated stimulation of T cells by TGN1412-like CD28 superagonist.* mAbs 2014. **6**(5): p. 1-10.
122. O'Sullivan, D., et al., *Memory CD8(+) T cells use cell-intrinsic lipolysis to support the metabolic programming necessary for development.* Immunity, 2014. **41**(1): p. 75-88.
123. Michalek, R.D., et al., *Cutting edge: distinct glycolytic and lipid oxidative metabolic programs are essential for effector and regulatory CD4+ T cell subsets.* J Immunol, 2011. **186**(6): p. 3299-303.
124. Beyersdorf, N., et al., *Superagonistic anti-CD28 antibodies: potent activators of regulatory T cells for the therapy of autoimmune diseases.* Ann Rheum Dis, 2005. **64 Suppl 4**: p. iv91-5.
125. Pfeiffer, T., S. Schuster, and S. Bonhoeffer, *Cooperation and competition in the evolution of ATP-producing pathways.* Science, 2001. **292**(5516): p. 504-7.
126. Karlsson, H. and L. Nassberger, *In vitro metabolic inhibition of the human lymphocyte: influence on the expression of interleukin-2 receptors.* Immunol Cell Biol, 1992. **70 (Pt 5)**: p. 309-13.
127. Kadenbach, B., *Introduction to mitochondrial oxidative phosphorylation.* Adv Exp Med Biol, 2012. **748**: p. 1-11.
128. Murphy, M.P., *How mitochondria produce reactive oxygen species.* Biochem J, 2009. **417**(1): p. 1-13.
129. Sirover, M.A., *Subcellular dynamics of multifunctional protein regulation: mechanisms of GAPDH intracellular translocation.* J Cell Biochem, 2012. **113**(7): p. 2193-200.
130. Berry, M.D. and A.A. Boulton, *Glyceraldehyde-3-phosphate dehydrogenase and apoptosis.* J Neurosci Res, 2000. **60**(2): p. 150-4.

131. Zheng, L., R.G. Roeder, and Y. Luo, *S phase activation of the histone H2B promoter by OCA-S, a coactivator complex that contains GAPDH as a key component.* Cell, 2003. **114**(2): p. 255-66.
132. Macintyre, A.N., et al., *The glucose transporter Glut1 is selectively essential for CD4 T cell activation and effector function.* Cell Metab, 2014. **20**(1): p. 61-72.
133. Zhang, J., et al., *Measuring energy metabolism in cultured cells, including human pluripotent stem cells and differentiated cells.* Nat Protoc, 2012. **7**(6): p. 1068-85.
134. Cai, L. and B.P. Tu, *On acetyl-CoA as a gauge of cellular metabolic state.* Cold Spring Harb Symp Quant Biol, 2011. **76**: p. 195-202.
135. van der Windt, G.J., et al., *Mitochondrial respiratory capacity is a critical regulator of CD8+ T cell memory development.* Immunity, 2012. **36**(1): p. 68-78.
136. Srere, P.A., *The enzymology of the formation and breakdown of citrate.* Adv Enzymol Relat Areas Mol Biol, 1975. **43**: p. 57-101.
137. Srere, P.A., *The citrate cleavage enzyme. I. Distribution and purification.* J Biol Chem, 1959. **234**: p. 2544-7.
138. Ramakrishna, S., D.L. Pucci, and W.B. Benjamin, *Dependence of ATP-citrate lyase kinase activity on the phosphorylation of ATP-citrate lyase by cyclic AMP-dependent protein kinase.* J Biol Chem, 1983. **258**(8): p. 4950-6.
139. Ramakrishna, S. and W.B. Benjamin, *Phosphorylation of different sites of acetyl CoA carboxylase by ATP-citrate lyase kinase and cyclic AMP-dependent protein kinase.* Biochem Biophys Res Commun, 1983. **117**(2): p. 435-43.
140. Abdel-Halim, M.N. and S.I. Farah, *Short-term regulation of acetyl CoA carboxylase: is the key enzyme in long-chain fatty acid synthesis regulated by an existing physiological mechanism?* Comp Biochem Physiol B, 1985. **81**(1): p. 9-19.
141. Bauer, D.E., et al., *ATP citrate lyase is an important component of cell growth and transformation.* Oncogene, 2005. **24**(41): p. 6314-22.
142. Pearce, J., *Fatty acid synthesis in liver and adipose tissue.* Proc Nutr Soc, 1983. **42**(2): p. 263-71.
143. Fendt, S.M., et al., *Reductive glutamine metabolism is a function of the alpha-ketoglutarate to citrate ratio in cells.* Nat Commun, 2013. **4**: p. 2236.
144. Fritz, V. and L. Fajas, *Metabolism and proliferation share common regulatory pathways in cancer cells.* Oncogene, 2010. **29**(31): p. 4369-77.
145. Yecies, J.L. and B.D. Manning, *Chewing the fat on tumor cell metabolism.* Cell, 2010. **140**(1): p. 28-30.
146. Warburg, O., *On the origin of cancer cells.* Science, 1956. **123**(3191): p. 309-14.
147. Menendez, J.A. and R. Lupu, *Fatty acid synthase and the lipogenic phenotype in cancer pathogenesis.* Nat Rev Cancer, 2007. **7**(10): p. 763-77.
148. Gatenby, R.A. and R.J. Gillies, *Why do cancers have high aerobic glycolysis?* Nat Rev Cancer, 2004. **4**(11): p. 891-9.
149. Hatzivassiliou, G., et al., *ATP citrate lyase inhibition can suppress tumor cell growth.* Cancer Cell, 2005. **8**(4): p. 311-21.
150. Yang, Z.J., et al., *The role of autophagy in cancer: therapeutic implications.* Mol Cancer Ther, 2011. **10**(9): p. 1533-41.
151. Li, X., et al., *Targeting mitochondrial reactive oxygen species as novel therapy for inflammatory diseases and cancers.* J Hematol Oncol, 2013. **6**: p. 19.
152. St-Pierre, J., et al., *Suppression of reactive oxygen species and neurodegeneration by the PGC-1 transcriptional coactivators.* Cell, 2006. **127**(2): p. 397-408.
153. Lee, S., et al., *Cell cycle-dependent mitochondrial biogenesis and dynamics in mammalian cells.* Biochem Biophys Res Commun, 2007. **357**(1): p. 111-7.
154. Wenz, T., *PGC-1alpha activation as a therapeutic approach in mitochondrial disease.* IUBMB Life, 2009. **61**(11): p. 1051-62.

155. Bastin, J., et al., *Activation of peroxisome proliferator-activated receptor pathway stimulates the mitochondrial respiratory chain and can correct deficiencies in patients' cells lacking its components.* J Clin Endocrinol Metab, 2008. **93**(4): p. 1433-41.
156. Diebold, R.J., et al., *Early-onset multifocal inflammation in the transforming growth factor beta 1-null mouse is lymphocyte mediated.* Proc Natl Acad Sci U S A, 1995. **92**(26): p. 12215-9.
157. Yoon, Y.S., et al., *TGF beta1 induces prolonged mitochondrial ROS generation through decreased complex IV activity with senescent arrest in Mv1Lu cells.* Oncogene, 2005. **24**(11): p. 1895-903.
158. Casalena, G., I. Daehn, and E. Bottinger, *Transforming growth factor-beta, bioenergetics, and mitochondria in renal disease.* Semin Nephrol, 2012. **32**(3): p. 295-303.
159. Naik, E. and V.M. Dixit, *Mitochondrial reactive oxygen species drive proinflammatory cytokine production.* J Exp Med, 2011. **208**(3): p. 417-20.
160. Kesarwani, P., et al., *Redox regulation of T-cell function: from molecular mechanisms to significance in human health and disease.* Antioxid Redox Signal, 2013. **18**(12): p. 1497-534.
161. Takahashi, A., et al., *Preferential cell death of CD8+ effector memory (CCR7-CD45RA-) T cells by hydrogen peroxide-induced oxidative stress.* J Immunol, 2005. **174**(10): p. 6080-7.
162. Kaminski, M.M., et al., *Mitochondrial reactive oxygen species control T cell activation by regulating IL-2 and IL-4 expression: mechanism of ciprofloxacin-mediated immunosuppression.* J Immunol, 2010. **184**(9): p. 4827-41.
163. Sieve, A.N., et al., *A novel immunoregulatory function for IL-23: Inhibition of IL-12-dependent IFN-gamma production.* Eur J Immunol, 2010. **40**(8): p. 2236-47.
164. Sena, L.A., et al., *Mitochondria are required for antigen-specific T cell activation through reactive oxygen species signaling.* Immunity, 2013. **38**(2): p. 225-36.
165. Farrar, W.L., H.M. Johnson, and J.J. Farrar, *Regulation of the production of immune interferon and cytotoxic T lymphocytes by interleukin 2.* J Immunol, 1981. **126**(3): p. 1120-5.
166. Sena, L.A. and N.S. Chandel, *Physiological roles of mitochondrial reactive oxygen species.* Mol Cell, 2012. **48**(2): p. 158-67.
167. Grayson, J.M., et al., *Mitochondrial potential and reactive oxygen intermediates in antigen-specific CD8+ T cells during viral infection.* J Immunol, 2003. **170**(9): p. 4745-51.
168. Jain, M., et al., *Mitochondrial reactive oxygen species regulate transforming growth factor-beta signaling.* J Biol Chem, 2013. **288**(2): p. 770-7.
169. Laniewski, N.G. and J.M. Grayson, *Antioxidant treatment reduces expansion and contraction of antigen-specific CD8+ T cells during primary but not secondary viral infection.* J Virol, 2004. **78**(20): p. 11246-57.
170. Oyewole, A.O., et al., *Comparing the effects of mitochondrial targeted and localized antioxidants with cellular antioxidants in human skin cells exposed to UVA and hydrogen peroxide.* FASEB J, 2014. **28**(1): p. 485-94.
171. Chong, S.J., I.C. Low, and S. Pervaiz, *Mitochondrial ROS and involvement of Bcl-2 as a mitochondrial ROS regulator.* Mitochondrion, 2014.
172. Wallace, D.C., *Mitochondria and cancer: Warburg addressed.* Cold Spring Harb Symp Quant Biol, 2005. **70**: p. 363-74.
173. Holling, T.M., E. Schooten, and P.J. van Den Elsen, *Function and regulation of MHC class II molecules in T-lymphocytes: of mice and men.* Hum Immunol, 2004. **65**(4): p. 282-90.

174. Tsang, J.Y., J.G. Chai, and R. Lechler, *Antigen presentation by mouse CD4+ T cells involving acquired MHC class II:peptide complexes: another mechanism to limit clonal expansion?* Blood, 2003. **101**(7): p. 2704-10.